National Library of Canada
Bibliothèque nationale du Canada

Canadian Theses Service
Service des thèses canadiennes

Ottawa, Canada
K1A 0N4

NOTICE

The quality of this microform is heavily dependent upon the quality of the original thesis submitted for microfilming. Every effort has been made to ensure the highest quality of reproduction possible.

If pages are missing, contact the university which granted the degree.

Some pages may have indistinct print especially if the original pages were typed with a poor typewriter ribbon or if the university sent us an inferior photocopy.

Reproduction in full or in part of this microform is governed by the Canadian Copyright Act, R.S.C. 1970, c. C-30, and subsequent amendments.

AVIS

La qualité de cette microforme dépend grandement de la qualité de la thèse soumise au microfilmage. Nous avons tout fait pour assurer une qualité supérieure de reproduction.

S'il manque des pages, veuillez communiquer avec l'université qui a conféré le grade.

La qualité d'impression de certaines pages peut laisser à désirer, surtout si les pages originales ont été dactylographiées à l'aide d'un ruban usé ou si l'université nous a fait parvenir une photocopie de qualité inférieure.

La reproduction, même partielle, de cette microforme est soumise à la Loi canadienne sur le droit d'auteur, SRC 1970, c. C-30, et ses amendements subséquents.

NL-339 (r. 88/04) c

Canada

UNIVERSITY OF ALBERTA

RESERVOIR LIMIT TESTING FOR GAS WELLS IN RECTANGULAR RESERVOIRS

BY

MURRAY W. BROWN

A thesis submitted to the Faculty of Graduate Studies and Research in partial fulfillment of the requirements for the degree of

MASTER OF SCIENCE

IN

PETROLEUM ENGINEERING

DEPARTMENT OF MINING, METALLURGICAL AND PETROLEUM ENGINEERING

EDMONTON, ALBERTA

SPRING, 1992

National Library of Canada
Bibliothèque nationale du Canada

Canadian Theses Service
Service des thèses canadiennes

Ottawa, Canada
K1A 0N4

The author has granted an irrevocable non-exclusive licence allowing the National Library of Canada to reproduce, loan, distribute or sell copies of his/her thesis by any means and in any form or format, making this thesis available to interested persons.

L'auteur a accordé une licence irrévocable et non exclusive permettant à la Bibliothèque nationale du Canada de reproduire, prêter, distribuer ou vendre des copies de sa thèse de quelque manière et sous quelque forme que ce soit pour mettre des exemplaires de cette thèse à la disposition des personnes intéressées.

The author retains ownership of the copyright in his/her thesis. Neither the thesis nor substantial extracts from it may be printed or otherwise reproduced without his/her permission.

L'auteur conserve la propriété du droit d'auteur qui protège sa thèse. Ni la thèse ni des extraits substantiels de celle-ci ne doivent être imprimés ou autrement reproduits sans son autorisation.

ISBN 0-315-73154-0

Canada

UNIVERSITY OF ALBERTA

RELEASE FORM

NAME OF AUTHOR: Murray William Brown

TITLE OF THESIS: Reservoir Limit Testing for Gas Wells in Rectangular Reservoirs

DEGREE FOR WHICH THESIS WAS PRESENTED: MASTER OF SCIENCE

YEAR THE DEGREE WAS GRANTED: SPRING, 1992

Permission is hereby granted to the University of Alberta Library to reproduce single copies of this thesis and to lend or sell such copies for private, scholarly or scientific research purposes only.

The author reserves other publication rights, and neither the thesis nor extensive extracts from it may be printed or otherwise reproduced without the author's written permission.

(SIGNED) 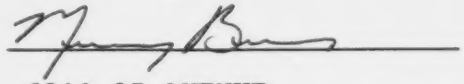

PERMANENT ADDRESS: 6211 87 AVENUE
EDMONTON, ALBERTA
CANADA

DATED: April 19, 1992

UNIVERSITY OF ALBERTA

FACULTY OF GRADUATE STUDIES AND RESEARCH

The undersigned certify that they have read, and recommended to the Faculty of Graduate Studies and Research for acceptance, a thesis entitled "RESERVOIR LIMIT TESTING FOR GAS WELLS IN RECTANGULAR RESERVOIRS" submitted by Murray W. Brown in partial fulfillment of the requirements for the degree of MASTER OF SCIENCE in PETROLEUM ENGINEERING.

A. K. Ambastha (Supervisor)

J. M. Whiting

R. G. Bentsen

S. M. Kresta

DATED: February 27, 1992

ABSTRACT

Analysis of drawdown pseudosteady-state flow period data is known as Limit Test analysis. A proper Limit Test analysis can provide an accurate estimation of reservoir drainage volume. In this study, the pseudosteady-state Cartesian method of Limit Test analysis is applied to gas reservoirs.

The drawdown pseudopressure response for square and rectangular reservoirs was considered for gas wells. The effects of pressure-dependent gas viscosity and gas compressibility on the drawdown response were considered for late-time pseudosteady-state data. A numerical solution to the non-linear partial differential equation describing gas flow was obtained for various flowrates. Rectangular reservoirs with aspects ratios of 1:1, 2:1, 4:1 and 10:1 were considered with well positions of (0.50,0.50), (0.75,0.50) and (0.75,0.75). Various initial reservoir conditions were considered as well as examples with gas contaminants. The late-time pseudopressure numerical results obtained were compared to the late-time liquid analytical drawdown solution.

The results focussed on the deviation of the gas pseudopressure response during the pseudosteady-state flow regime from the corresponding liquid pressure response. The

amount of deviation varied with respect to the flowrate, reservoir initial conditions, reservoir geometry and well position.

Gas well Limit Test data during the pseudosteady-state flow period will be in error due to the pressure-dependent gas viscosity-compressibility product. The pseudopressure response can be corrected by a time-averaging of the average gas viscosity-compressibility product during pseudosteady-state flow. The time-corrected pseudopressure response will correlate with the liquid pressure solution. Using the time-corrected pseudopressure response, the accuracy of Limit Test analysis can be significantly improved.

ACKNOWLEDGMENTS

The author expresses his sincere gratitude to Dr. Anil K. Ambastha for his guidance and assistance throughout this study. The author feels he has gained invaluable knowledge by the dedication and support Dr. Ambastha has provided. The importance of this research topic was first pointed out to Dr. Ambastha by Dr. Henry J. Ramey Jr. of Stanford University.

The author would like to thank Amoco Canada Petroleum Company Ltd. for a graduate scholarship. Financial support was also provided by NSERC and the Petroleum Graduate Research Program (formerly known as Petroleum Aid to Education Program).

The author appreciates the co-operation of Mr. Prasit Kosarussawadee toward the development of the two-dimensional, single-phase gas simulator used in this study.

The author is thankful for the computing services and support of the Department of Mining, Metallurgical and Petroleum Engineering at the University of Alberta.

The author would also like to thank Barbara and Ryan for their patience, understanding and support.

TABLE OF CONTENTS

Page

ABSTRACT..... iv

ACKNOWLEDGMENTS..... vi

TABLE OF CONTENTS..... vii

LIST OF TABLES..... ix

LIST OF FIGURES..... x

NOMENCLATURE..... xiii

1. INTRODUCTION..... 1

2. LITERATURE REVIEW..... 4

3. THEORY..... 12

4. COMPUTER MODEL DEVELOPMENT..... 24

5. VALIDITY OF COMPUTER MODEL..... 30

6. RESULTS AND DISCUSSION..... 38

6.1 INTRODUCTION..... 43

6.2 RESERVOIR GRIDDING..... 52

6.3 RESERVOIR CONDITIONS..... 57

6.3.1 EFFECT OF RESERVOIR ASPECT RATIO AND WELL LOCATION..... 57

6.3.2 EFFECT OF GAS CONTAMINANTS..... 63

6.3.3 EFFECT OF CHANGING TEMPERATURE..... 65

6.3.4 EFFECT OF VARYING PERMEABILITY..... 65

6.4 EFFECT OF FLOWRATE..... 68

6.5 LIMIT TEST ANALYSIS..... 77

7. CONCLUSIONS AND RECOMMENDATIONS..... 84

8. REFERENCES..... 87

APPENDIX A: COMPUTER PROGRAMS..... 90

LIST OF TABLES

Page

TABLE 6.1 - Reservoir initial conditions. 39

TABLE 6.2 - Well locations for Reservoirs A, B and C. 41

TABLE 6.3 - Contaminant concentrations for Reservoirs A, B and C. 41

TABLE 6.4 - Grid inputs for Grid 1 and Grid 2. 54

TABLE 6.5 - Grid inputs for reservoir aspect ratios. 54

TABLE 6.6 - Deviation t_{DA} values for Reservoir B with aspect ratio of 4:1. 59

TABLE 6.7 - 1% Deviations for Reservoir A. 59

TABLE 6.8 - 1% Deviations for wells at (0.50,0.50) and q_D =0.05. 60

TABLE 6.9 - Sour Gas Example, 1% Deviation for wells at (0.50,0.50) and q_D =0.05. 63

TABLE 6.10 - t_{DA} values for 1% deviation of m_{wD} from p_{wD} 70

TABLE 6.11 - Analysis results for limit test data for 2:1 Reservoir with well at (0.50,0.50). 79

LIST OF FIGURES

Page

Figure 4.1 - Reservoir gridding areas. 25

Figure 4.2 - Reservoir grid wellblock Area 1. 25

Figure 5.1 - Numerical m_{wD} and analytical p_{wD} response for a square. 33

Figure 5.2 - Numerical m_{wD} and analytical p_{wD} response and Reynolds et al.[18] data for a circle. 33

Figure 5.3 - Comparison of Wattenbarger[13] data and simulation data for various flowrates. 36

Figure 5.4 - Comparison of average pressure calculation method. 36

Figure 6.1 - 2:1 Reservoir grid dimensions, well at (0.75,0.75). 39

Figure 6.2 - Effect of initial conditions on 1:1 Reservoir well at (0.50,0.50). 44

Figure 6.3 - Cartesian plot of response for 1:1 Reservoir well at (0.50,0.50). 44

Figure 6.4 - μc_g variation with pressure. 46

Figure 6.5 - μ variation with pressure. 46

Figure 6.6 - Deviation data for 1:1 Reservoir with well at (0.50,0.50). 48

Figure 6.7 - Deviation data for 1:1 Reservoir with well at (0.50,0.50), expanded scale. . 48

Figure 6.8 - Late-time data slopes for 1:1 Reservoir with well at (0.50,0.50). .. 50

Figure 6.9 - Time-corrected response for 1:1 Reservoir A with well at (0.50,0.50). 50

Figure 6.10 - Response for Reservoir A grids 1 and 2. 55

Figure 6.11 - Grids 1 and 2 time-corrected results. 55

Figure 6.12 - Grids 1 and 2 average pressure error. 56

Figure 6.13 - Effect of well location on response for 4:1 Reservoir B. 61

Figure 6.14 - Well location deviation data for Reservoir B. 61

Figure 6.15 - Time-corrected well location response for 4:1 Reservoir B. 62

Figure 6.16 - Response for 2:1 Reservoir A with gas contaminants. 64

Figure 6.17 - Time-corrected response for 2:1 Reservoir A with gas contaminants. ... 64

Figure 6.18 - Effect of temperature on response for 2:1 Reservoir B. 66

Figure 6.19 - Time-corrected temperature response for 2:1 Reservoir B. 66

Figure 6.20 - Effects of permeability on response for 4:1 Reservoir C. 67

Figure 6.21 - Time-corrected permeability response for 4:1 Reservoir C. 67

Figure 6.22 - Response for 4:1 Reservoir A, $q_D = 0.10$. 71

Figure 6.23 - Effect of flowrate on response for 4:1 Reservoir A with well at (0.50,0.50). 71

Figure 6.24 - Effect of flowrate on deviation for 4:1 Reservoir A with well at (0.50,0.50). 72

Figure 6.25 - Flowrate deviation versus $\overline{p}/\overline{z}$ for 4:1 Reservoir A with well at (0.50,0.50). 72

Figure 6.26 - Effect of flowrate on response for 1:1 Reservoir A with well at (0.50,0.50). 75

Figure 6.27 - Deviation data for Reservoir A wells. 75

Figure 6.28 - Flowrate deviation versus $\overline{p}/\overline{z}$ for Reservoir A well locations. 76

Figure 6.29 - Response for 2:1 Reservoir A with well at (0.50,0.50), q_D =0.02. 82

Figure 6.30 - Response for 2:1 Reservoir A with well at (0.50,0.50), q_D =0.05. 82

Figure 6.31 - Response for 2:1 Reservoir C with well at (0.50,0.50), q_D =0.05. 83

Figure 6.32 - Response for 2:1 Reservoir A with well at (0.50,0.50), q_D =0.05 and 25% depleted. 83

NOMENCLATURE

∇ = grad

$\nabla\cdot$ = divergence

∇^2 = Laplacian operator

A = area, $x_1\ y_1$, ft^2

a_i = distance from producing well to ith image well, ft

a_{iD} = dimensionless distance from producing well to ith image well, $a_{iD} = a_i/\sqrt{A}$

AREA 1 = simulation grid area around producing well, ft^2

AREA 1A = interior subdivided AREA 1 grid, ft^2

AREA 2 = median simulation grid area, ft^2

AREA 3 = exterior simulation grid area, ft^2

B = formation volume factor, ft^3/scf

C_A = shape factor

c_t = total system compressibility, psi^{-1}

$c_g(p)$ = gas compressibility, psi^{-1}

$\overline{c_g}$ = average gas compressibility, psi^{-1}

Ei = exponential integral

e = constant, 2.7182818

h = formation thickness, ft

k = permeability, md

ln = natural logarithm to the base e

M = molecular weight

m = slope, psi/hour

MB = material balance ratio

$m(p)$ = real gas pseudopressure, Equation (3.9), psi^2/cp

m_D = dimensionless real gas pseudopressure, Equation (3.13)

m_{wD} = dimensionless wellbore pseudopressure, Equation (3.14)

m_{wD}' = dimensionless wellbore semi-ln pseudopressure derivative, Equation (6.1)

$m(\bar{p})$ = real gas average pseudopressure, psi^2/cp

N_x = number of grid blocks

p = pressure, psi

p_{pc} = pseudocritical pressure, psia

$\bar{p}$ = average pressure, psi

p_D = dimensionless pressure, Equation (3.19)

p_{int} = intercept of p_{wf} vs t Cartesian plot, psi

p_{pr} = pseudoreduced pressure, p/p_{pc}

p_r = reference pressure, psia

p_{wD} = dimensionless wellbore pressure, Equation (3.20)

p_{wD}' = dimensionless wellbore semi-ln pressure derivative, Equation (6.2)

q = surface flowrate, Mscf/day for gas, STB/day for liquid

q_D = dimensionless flowrate, Equation (3.21)

q_i = wellblock flowrate, Mscf/day

r = radial distance, ft

r_D = dimensionless radial distance, r/r_w

r_o = equivalent radius of a square wellblock, ft

r_w = wellbore radius, ft

R = Universal gas constant

s = skin factor

T = reservoir temperature, °F

T_{pc} = pseudocritical temperature, °R

T_{pr} = pseudoreduced temperature, T/T_{pc}

t = time, hours

Δt = time step increment, hours

t_D = dimensionless time, Equation (3.12) for gases, Equation (3.18) for liquid

t_{DA} = dimensionless time based on area A, Equation (3.24)

V_i = reservoir grid block volume, ft^3

v = velocity, ft/sec

x = x-axis producing well position, ft

x_D = dimensionless x-axis distance, x/x_1

x_i = x-axis distance from producing well to ith image well, ft

x_1 = reservoir length in x-direction, ft

Δx = grid block length in x-direction, ft

XMULT = grid block x-axis length multiplier

XWB1 = AREA 1 grid block x-axis length, ft

XWB2 = AREA 2 grid block x-axis length, ft

XWB3 = AREA 3 grid block x-axis length, ft

XY RATIO = reservoir aspect ratio, x_1/y_1

y = y-axis producing well position, ft

y_D = dimensionless y-axis distance, y/y_1

y_i = y-axis distance from producing well to ith image well, ft

y_1 = reservoir length in y-direction, ft

Δy = grid block length in y-direction, ft

YMULT = grid block y-axis length multiplier

YWB1 = AREA 1 grid block y-axis length, ft

YWB2 = AREA 2 grid block y-axis length, ft

YWB3 = AREA 3 grid block y-axis length, ft

z(p) = real gas deviation factor

$\bar{z}$ = average real gas deviation factor

GREEK SYMBOLS

Δ = increment

$\mu(p)$ = viscosity, cp

$(\mu z)_{avg}$ = average viscosity-gas deviation factor product, Equation (3.22), cp

$\bar{\mu}$ = average viscosity, cp

$\overline{\overline{\mu c_g}}$ = time-averaged viscosity-compressibility product, cp psi^{-1}

ϕ = porosity, fraction

π = pi, 3.141593

ρ = density, gm/cm^3

SUBSCRIPTS

A = area

D = dimensionless

i = initial or well index

(i,j) = wellblock (x,y) subscript

l = length

sc = standard conditions

w = internal boundary, the well

wf = well flowing

SUPERSCRIPTS

N = current time level

N+1 = next time level

N+1/2 = time increment average

1. INTRODUCTION

A reservoir limit test is an extended drawdown test used to estimate the reservoir volume in communication with the well. The estimated drainage volume calculated from a limit test can serve to locate reservoir boundaries. A limit test is particularly useful early in the life of the reservoir. Accurate information regarding reservoir extent is critical for any additional drilling activity.

An analysis of a reservoir limit test uses the pseudosteady state portion of the drawdown data. The effect of reservoir boundaries is to cause the drawdown response to deviate from the semilog straight line corresponding to infinite-acting radial flow. When all boundaries of a closed reservoir start affecting the pressure transient response, a Cartesian plot of bottom-hole pressure as a function of time yields a straight line whose slope is inversely proportional to reservoir drainage volume. This analysis method using a Cartesian graph is referred to as "pseudosteady state analysis". If pressure data are available during both the infinite-acting and pseudosteady state periods, the system shape factor may also be estimated, determining the reservoir configuration being drained by the well.

The pseudosteady state analysis is accurate for oil well tests. When pseudosteady state analysis for gas wells was introduced, its analysis method was assumed to be similar to the analysis method for oil wells. The pressure-dependent gas viscosity and compressibility, and non-ideal gas behavior may affect the accuracy of the estimated drainage volume using limit test data. Studies have been conducted, on circular reservoirs, indicating that there is a period of time when the gas flow solution in terms of real gas pseudo-pressure correlates with the liquid solution over a range of late times. Under those conditions, pseudosteady state analysis applies. However, for reservoir configurations other than a circle, information regarding the time period during which pseudosteady state analysis applies is not available.

In this study, reservoir limit testing for rectangular reservoirs was considered. Gas reservoirs with no-flow outer boundaries were considered. Transient gas flow has been simulated using a two-dimensional, single-phase gas reservoir simulator. The accuracy and applicability of pseudosteady state analysis has been determined by comparing the late-time gas pseudo-pressure response with the late-time liquid pressure solution. The time period for accurate pseudosteady state analysis has been investigated. The effects of reservoir aspect ratio, well location, gas composition, and production

rates on limit tests were also considered for a rectangular reservoir.

2. LITERATURE REVIEW

Analysis of reservoir limit tests was introduced by P. Jones[1] in 1956. As stated by Jones[1], a reservoir limit test is a test of a new well which consists of measuring the rate of change of bottom- hole pressure at a constant production rate. Jones[1] discussed limit test analysis for closed, or no-flow outer boundary, oil and gas reservoirs.

As defined by Jones[1], the noise or tone of a well is the rate of pressure change per unit production rate. The tone of a well prevails when the constant producing rate is the only cause of decreasing bottom-hole flowing pressure. Both the transient and pseudosteady state tones were plotted on a log-log scale. The transient flow period tone was represented by a unit slope straight line. The pseudosteady state flow period tone was represented by a horizontal line, with a transition period between the two flow periods. During pseudosteady state flow, the rate of pressure decline at the well, at external boundaries, and at all points in between, is constant. The constant value of tone during pseudosteady state is used to compute the gas in place, given the gas formation volume factor and compressibility at initial reservoir pressure. No attention was given to the non-linear behavior of gases.

Previous to the work of Jones[1], Bruce et al.[2] had developed a stable numerical procedure for solving the gas flow equation for production of gas at a constant rate from linear and radial systems. The equation was solved using a finite-difference implicit numerical model. Ideal gas behavior was assumed and gas viscosity assumed constant. The compressibility of the gas was assumed to be constant over the range of pressures considered, and its value inversely proportional to well-block pressure. Bruce et al.'s[2] analysis was for transient flow.

Aronofsky and Jenkins[3] also presented a numerical solution of the gas flow equation, similar to that presented by Bruce et al[2]. The results obtained for transient radial gas flow compared well with the liquid flow solution of van Everdingen and Hurst[4]. Aronofsky and Jenkins[3] also correlated Bruce et al.'s[2] data in terms of the radius of drainage.

L. Jones[5] developed a method of calculation which duplicated the transient radial gas flow results of Bruce et al.[2], and Aronofsky and Jenkins[3]. Jones[5] assumed non-ideal gas flow behavior. It was stated that the gas deviation factor and viscosity should be evaluated at the volumetric average pressure, but, at that time there were no rules regarding this procedure. Using the radius of drainage concept, a method for

determining reservoir extent, or minimum reservoir volume, was presented for radial flow.

P. Jones[6] discussed reservoir limit testing for gas wells, in 1962. Again an analysis method was presented similar to the liquid solution method for oil wells. Jones[6] discussed the effects of faults, anisotropic permeability, gas-water contact and multiple wells for circular reservoirs.

Also in 1962, Carter[7] presented a numerical solution for transient radial gas flow. The finite-difference solution accounted for the variation of viscosity and gas deviation factor with pressure. It was also mentioned that a more general correlation, similar to the pseudopressure integral, would account for variations of the product of gas viscosity and deviation factor. Carter[7] presented results which correlated well with the liquid flow solution when gas viscosity, compressibility and deviation factor were computed based on instantaneous average pressure. One solution was also presented with the gas viscosity, compressibility and deviation factor evaluated at a constant average pressure. This solution deviated significantly below the liquid flow solution. The gas compressibility was evaluated as the reciprocal of the average pressure for all cases.

In 1963, L. Jones[8] commented on the validity of the method of

determining gas reserves based on solutions to liquid flow equations. Jones[8] discussed the potential problems of turbulent flow and well damage. The effects of these terms, both a function of flowrate, were dismissed due to a constant flowrate and data analysis in differential form. Jones'[8] solution for transient and pseudosteady state flow related well pressure and cumulative production for gas wells flowing at a constant rate as developed in Reference 5. The analysis procedure consisted of a Cartesian plot of flowing well pressure versus production, and reserves determined from the straight line. It was noted by Jones[8] that there were no field data available at that time to check results. Therefore, numerical data were generated. His analysis results compared favorably with the numerical data.

In 1964, Root et al.[9] discussed the then current methods of determining gas reserves. It was stated that the principal error for reservoir limit testing is in the determination of the minimum field radius proved by the test. Gas results were illustrated for a linearization of the gas flow equation, similar to the liquid solution, and for a succession of steady states, or gas properties evaluated at instantaneous average pressures, as suggested by Jones[8]. The slope of the Cartesian plot of pseudosteady state data, similar to Jones[8], was used to determine the size of the reservoir. Root et al.[9] also stated that, for an accurate estimation of reserves, a

considerable portion of pseudosteady state data is required.

Eilerts et al.[10] illustrated a method for computing the availability or reserve of gas in a formation. An implicit finite-difference numerical model was used with pressure-dependent permeability, viscosity, compressibility, and gas deviation factor. Lean and rich fluid properties were used to evaluate different constant rate recoveries. Gas recovery was shown to be a function of flowrate, permeability and fluid properties.

Al-Hussainy et al.[11] defined the pseudopressure integral in an attempt to linearize the gas flow equation. The linearized real gas pseudopressure equation is similar to the ideal gas equation solution and does not involve as many simplifying assumptions. Using the Eilerts et al.[10] form of the gas flow numerical solution plotted in terms of pseudopressure, Al-Hussainy et al.[11] compared liquid, gas, and condensate radial flow. All data compared very well during the transient flow period on a semi-log scale. This was noted to be a severe test of the linearization of the gas flow equation. A Cartesian plot of pseudosteady state data revealed that the correlation with liquid flow was not as good for late-time analysis. The use of the pseudopressure integral, however, made it possible to correlate finite-difference real gas solutions to liquid and ideal gas solutions during transient flow.

Al-Hussainy and Ramey[12] applied pseudopressure, or real gas flow theory, to well testing and deliverability forecasting. Drawdown test interpretation results using pseudopressure were more accurate than both the liquid and the ideal gas method of analysis. Al-Hussainy and Ramey[12] also stated that, when using pseudopressure, the gas physical properties do not appear in the engineering equations.

Wattenbarger[13] stated that the pseudopressure linearization of real gas flow was effective for transient solutions, but not for boundary-dominated pseudosteady state flow. The real gas pseudopressure response for radial flow deviated below the liquid case. The amount of departure increased with cumulative production. Wattenbarger[13] considered the application of pseudopressure for gas well testing with effects of formation damage, wellbore storage, turbulent flow and vertical fractures.

Zana and Thomas[14] considered the effects of contaminants on real gas flow. Gas well transient tests were analyzed using a corrected viscosity and gas deviation factor. They found that failing to correct for contaminants resulted in an underestimation of the formation flow capacity. The calculations of skin and average reservoir pressure were not as severely affected.

Earlougher[15] showed how to use pressure drawdown data to estimate both the size and geometry of reservoirs. The procedure required both transient and pseudosteady state drawdown data. The calculated shape factor, representing the reservoir geometry, can be used to estimate the time to pseudosteady state flow.

Aziz et al.[16] commented on the use of pseudopressure when analyzing gas well transient drawdown tests. The pseudopressure, pressure and pressure-squared methods were compared when calculating flowing well pressure response. The pseudopressure response yielded the most acceptable results when fluid properties were assumed to be constant at initial reservoir conditions.

Earlougher[17] stated that Cartesian pseudosteady state analysis appears to be the simplest and least prone to error, as compared to other techniques.

The more recent work of Reynolds et al.[18] indicated that there is a period of time when the pseudopressure response correlates with the liquid solution. This limited time period was for circular reservoirs. A correction for the gas viscosity-compressibility product based on the volumetric average reservoir pressure was also suggested. The corrected response resulted in a very good correlation of gas and liquid

solutions at late time for circular reservoirs.

The literature review summarizes the development of the solution to the gas flow equation. For this study, the late-time gas flow solution will be applied to limit test analysis of gas reservoirs. The Cartesian method of analysis, as first suggested by Jones[8], will be applied to rectangular gas reservoirs. The gas flow equation will be solved in terms of pseudopressure as defined by Al-Hussainy et al[11]. The significance of a correction for the gas viscosity-compressibility product, as suggested by Reynolds et al[18] will also be considered.

3. THEORY

Fluid flow through porous media is dependent on the physical properties of the matrix, geometry of the flow model, P-V-T properties of the flowing fluid, and pressure distribution within the flow system[11]. For the real gas flow equation under consideration, the following assumptions were made:

1) the matrix is homogeneous and isotropic.

2) the reservoir has only a single-phase gas.

3) the gas is of constant composition.

4) the flow is laminar or Darcy, turbulent or non-Darcy flow will not be considered.

5) isothermal conditions prevail.

6) gravity effects are negligible.

Reservoir fluid velocity, under laminar or Darcy flow, can be expressed as:

$$\vec{v} = - \frac{k}{\mu(p)} \nabla p \qquad \ldots\ldots\ldots\

$$\nabla \cdot [\rho \vec{v}] = - \phi \frac{\partial \rho}{\partial t} \qquad \ldots\ldots\ldots\ldots\ldots\ldots\ldots\ldots\ldots\ldots\ldots\ldots (3.2)$$

The density of a real gas, expressed in terms of the gas deviation factor, z(p), is written as:

$$\rho = \frac{M}{RT} \left[\frac{p}{z(p)} \right] \qquad \ldots\ldots\ldots\ldots\ldots\ldots\ldots\ldots\ldots\ldots\ldots\ldots (3.3)$$

where z(p) is a function of pressure, temperature, and gas composition. Substituting for velocity and density in the continuity equation results in:

$$\nabla \cdot \left[\frac{pM}{z(p)RT} \frac{k}{\mu(p)} \nabla p \right] = \phi \frac{\partial}{\partial t} \left[\frac{pM}{z(p)RT} \right] \qquad \ldots\ldots\ldots\ldots\ldots (3.4)$$

For isothermal gas flow, this equation can be reduced to:

$$\nabla \cdot \left[\frac{p}{z(p)\mu(p)} \nabla p \right] = \frac{\phi}{k} \frac{\partial}{\partial t} \left[\frac{p}{z(p)} \right] \qquad \ldots\ldots\ldots\ldots\ldots\ldots (3.5)$$

There has been extensive research conducted in expanding Equation (3.5). Using the definition of isothermal compressibility of real gas:

$$c_g = \frac{1}{\rho} \frac{\partial \rho}{\partial p} = \frac{z(p)}{p} \frac{d}{dp} \left(\frac{p}{z(p)} \right) = \frac{1}{p} - \frac{1}{z(p)} \frac{dz(p)}{dp} \qquad \ldots\ldots (3.6)$$

and substituting in Equation (3.5), the equation, in terms of field units, becomes:

$$\nabla^2 p^2 - \frac{d[\ln(\mu(p)\, z(p))]}{dp^2} (\nabla p^2)^2 = \frac{\phi\mu(p) c_g(p)}{0.0002637k} \frac{\partial p^2}{\partial t} \quad (3.7)$$

In past research, assumptions have been made to simplify this expression. It has been assumed that, if the gas $\mu(p)z(p)$ product changed slowly with pressure, the pressure differential of $\ln(\mu(p)z(p))$ becomes negligible. It has also been assumed that, if pressure gradients were small in the reservoir, the ∇p^2 term would become negligible. Using either of these assumptions, Equation (3.7) can be simplified to become:

$$\nabla^2 p^2 = \frac{\phi\mu(p) c_g(p)}{0.0002637k} \frac{\partial p^2}{\partial t} \quad \ldots\ldots\ldots\ldots\ldots\ldots\ldots\ldots (3.8)$$

These assumptions are not valid under all reservoir conditions.

Al-Hussainy et al.[11] defined the gas pseudopressure [m(p)] to be:

$$m(p) = 2 \int_{pr}^{p} \frac{p}{\mu(p) z(p)} dp \quad \ldots\ldots\ldots\ldots\ldots\ldots\ldots\ldots (3.9)$$

When substituting this expression in Equation (3.5), the resulting equation is of similar form to that of Equation

(3.8) obtained when the simplifying assumptions were used. In terms of m(p), Equation (3.5) becomes:

$$\nabla^2 m(p) = \frac{\phi\mu(p)c_g(p)}{0.0002637k} \frac{\partial m(p)}{\partial t} \quad \text{.....(3.10)}$$

This equation is still nonlinear, as $\mu(p)$ and $c_g(p)$ are functions of pressure.

For radial flow, Equation (3.10) becomes:

$$\frac{\partial^2 m(p)}{\partial r^2} + \frac{1}{r} \frac{\partial m(p)}{\partial r} = \frac{\phi\mu(p)c_g(p)}{0.0002637k} \frac{\partial m(p)}{\partial t} \quad \text{.....(3.11)}$$

Al-Hussainy et al.[11] defined the following dimensionless parameters:

$$t_D = \frac{0.0002637kt}{\phi(\mu c_g)_i r_w^2} \quad \text{.....(3.12)}$$

$$m_D = \frac{(m(p_i) - m(p))\, khT_{sc}}{50,300 q_{sc} p_{sc} T} \quad \text{.....(3.13)}$$

Similarly, the dimensionless pseudopressure drop at the wellbore is defined as:

$$m_{wD} = \frac{(m(p_i) - m(p_{wf}))\, khT_{sc}}{50,300 q_{sc} p_{sc} T} \quad \text{.....(3.14)}$$

$$r_D = \frac{r}{r_w} \quad \text{.....(3.15)}$$

Substituting the definitions of dimensionless variables given by Equations (3.12), (3.13) and (3.15) into Equation (3.11) yields:

$$\frac{\partial^2 m_D}{\partial r_D^2} + \frac{1}{r_D}\frac{\partial m_D}{\partial r_D} = \frac{\partial m_D}{\partial t_D} \qquad \text{.....(3.16)}$$

This form of the real gas diffusivity equation in terms of m_D is similar to the liquid flow diffusivity equation stated in dimensionless form as:

$$\frac{\partial^2 p_D}{\partial r_D^2} + \frac{1}{r_D}\frac{\partial p_D}{\partial r_D} = \frac{\partial p_D}{\partial t_D} \qquad \text{.....(3.17)}$$

where:

$$t_D = \frac{0.0002637\,kt}{\phi\mu c_t r_w^2} \qquad \text{.....(3.18)}$$

and:

$$p_D = \frac{(p_i - p)\,kh}{141.2\,q\mu B} \qquad \text{.....(3.19)}$$

Similarly, the dimensionless pressure drop at the wellbore is defined as:

$$p_{wD} = \frac{(p_i - p_{wf})\,kh}{141.2\,q\mu B} \qquad \text{.....(3.20)}$$

Thus, the real gas m_{wD} response should correlate with the

liquid p_{wD} response.

The dimensionless flowrate for gases, q_D, can be defined as:

$$q_D = \frac{1423\ q\ T}{kh\ m(p_i)} \qquad \ldots\ldots\ldots\

resulted in all three methods yielding similar acceptable results when predicting p_{wf}. However, when the gas properties were evaluated at initial conditions, the m(p) method of analysis was superior. The m(p) solutions were the most accurate for the examples with extremely high drawdown.

Reservoir limit test analysis makes use of the pseudosteady state portion of the drawdown data, as first introduced by Jones[1]. The dimensionless pressure drop, p_{wD}, can be calculated as a linear function of time from:

$$p_{wD} = 2\pi t_{DA} + \frac{1}{2}\ln\left(\frac{A}{r_w^2}\right) + \frac{1}{2}\ln\left(\frac{2.2458}{C_A}\right) \quad \ldots\ldots\ldots\ldots (3.23)$$

where:

$$t_{DA} = t_D\left(\frac{r_w^2}{A}\right) \quad \ldots\ldots\ldots\ldots\ldots\ldots\ldots\ldots\ldots\ldots\ldots\ldots (3.24)$$

The fluid properties expressed in t_{DA} were based on initial reservoir pressure. When expressing Equation (3.23) in the form:

$$p_{wf} = mt + p_{int} \quad \ldots\ldots\ldots\ldots\ldots\ldots\ldots\ldots\ldots\ldots\ldots\ldots (3.25)$$

and plotting p_{wf} versus t on Cartesian co-ordinates, the

reservoir volume can be calculated from:

$$\phi hA = \frac{-0.23395\ qB}{c_t m} \qquad \text{.....(3.26)}$$

The reservoir shape factor, C_A, can then be calculated from Equation (3.23), or from analysis of the transient and pseudosteady state data. Thus, the area and the shape of the reservoir can be determined from pseudosteady state analysis.

Analysis of gas pseudosteady state m(p) data was first discussed by Al-Hussainy et al.[11]. Al-Hussainy et al.[11] compared the results of Eilerts et al.[10] to that of the liquid flow solution. Production was at a constant rate from a closed circular reservoir. Both semi-log and Cartesian plots were illustrated for m_{wD} vs t_{DA} with fluid properties evaluated at initial conditions. The liquid p_{wD} response and gas m_{wD} data computed from Eilerts et al.[10] solution for radial flow of real gases compared very well during transient flow, as illustrated by the semi-log plot. The data considered from Eilerts et al.[10] work covered a wide range of pressures and flowrates.

As stated by Al-Hussainy et al.[11], there was considerable difference between p_{wD} and m_{wD} responses at late time. The ideal gas solution of Aronofsky and Jenkins[3] was also

presented on the Cartesian plot. The pseudosteady state drawdown data illustrated that both the real and ideal gas solutions produced a dimensionless pressure drop lower than that of the liquid solution. Also, the ideal gas dimensionless pressure drop was lower than the real gas solution and therefore reached a limiting production pressure earlier than the real gas. Thus, it was stated by Al-Hussainy et al.[11] that the production forecasts based on ideal gas flow will be conservative when compared to real gas flow.

Al-Hussainy et al.[11] also stated that the deviation of the gas data from the liquid solution was dependent on flowrate. At higher flowrates, there was a larger deviation of real gas m_{wD} from the liquid p_{wD} response. As stated by Wattenbarger[13], the resulting pressure drop is not as much a function of flowrate as average reservoir pressure. The higher flowrate represents a higher cumulative production than a lower flowrate and hence a higher departure of average reservoir pressure from initial pressure.

The deviation of gas data was also dependent on the type of reservoir gas produced. From Eilerts et al.[10] data, Al-Hussainy et al.[11] compared natural gas and gas-condensate results at an equal flowrate. The condensate case deviated much further below the liquid solution line than the natural gas. It was, therefore, concluded by Al-Hussainy et al.[11]

that for long producing times, there would be no one single set of m_{wD} correlations for all gases.

Reynolds et al.[18] discussed the analysis of gas well drawdown and buildup data using the pseudopressure response for radial gas flow. The transient drawdown results indicated that semilog analysis should be based on actual flowing time with the gas $\mu(p)c_g(p)$ product evaluated at initial conditions. The analysis based on actual flowing time was superior to that based on pseudotime or normalized time. Reynolds et al.[18] stated that semilog analysis should be based on the actual flowing time because the $\mu(p)c_g(p)$ product at the radius of investigation is approximately equal to $(\mu c_g)_i$ at any time during transient flow.

When the drawdown response is influenced by an outer boundary, it was indicated by Reynolds et al.[18] that if the pseudopressure response correlated with the liquid solution, the pseudopressure would be given by Equation (3.23).

The results of Al-Hussainy et al.[11], Wattenbarger[13] and Reynolds et al.[18] all indicated that at late time the m(p) solution is not accurate for gas reservoirs.

Reynolds et al.[18] defined a dimensionless time period for circular reservoirs for which Equation (3.23) is accurate for

gas well pseudopressure response. From the numerical results, it was found that the pseudopressure response was within 1% of the liquid solution for t_{DA} values between 0.07 and 0.30. During this time period the reservoir pore volume can be accurately determined by limit test analysis, provided there is sufficient pseudosteady state data.

Reynolds et al.[18] stated that for a circular reservoir, at $t_{DA}>0.10$, pressures in the reservoir fall below p_i. Therefore, a graph of m_{wD} vs t_{DA} falls below the liquid solution. To correct the m_{wD} response at late times, the μc_g product in the t_{DA} expression must be modified, or averaged over time and space as:

$$\overline{\overline{\mu c_g}} = \frac{1}{\frac{1}{t}\int_0^t \frac{dt}{\overline{\mu}\,\overline{c_g}}} \qquad \text{.....(3.27)}$$

with $\overline{\mu}\,\overline{c_g}$ evaluated at the instantaneous average reservoir pressure.

Now, t_{DA} becomes an average t_{DA}, expressed as:

$$\overline{t_{DA}} = \frac{0.0002637\ kt}{\phi\overline{\overline{\mu c_g}}A} \qquad \text{.....(3.28)}$$

A graph of m_{wD} vs $\overline{t_{DA}}$ was shown to correlate with the liquid solution for all times.

In this study, the time correction method used by Reynolds et al.[18] will be applied to gas wells within rectangular reservoirs. The m_{wD} response, computed from a numerical simulator, will be compared to the analytical liquid solution p_{wD} response for analysis of pseudosteady state drawdown data.

4. COMPUTER MODEL DEVELOPMENT

The differential equation governing gas flow through porous media is given by Equation (3.10). Equation (3.10) can be expressed in Cartesian co-ordinates as:

$$\frac{\partial^2 m(p)}{\partial x^2} + \frac{\partial^2 m(p)}{\partial y^2} = \frac{\phi \mu(p) c_g(p)}{0.0002637k} \frac{\partial m(p)}{\partial t} \qquad \text{.....(4.1)}$$

Equation (3.27) will be numerically solved for pseudopressure distribution for gas flow in square or rectangular reservoirs. The reservoir thickness will be set at a constant of 1 foot. The reservoir porosity and permeability will also be set at a constant over the entire reservoir grid area. The wellblock is defined as the grid block containing the producing well.

As illustrated in Figure 4.1, there are 3 reservoir grid areas for the X- and Y-axes. Areas 2 and 3 each represent 40% of the reservoir area, with Area 1 occupying 20%. The shaded portion of Area 1, centered at the well, contains square grid blocks surrounding the well with length and width XWB1. As shown in Figure 4.2, this shaded wellblock Area 1 can be further divided into a smaller area of square grid blocks, Area 1A, with length and width XWB1A. The fraction of AREA 1 to be subdivided into Area 1A was defined to be the input XWB1F.

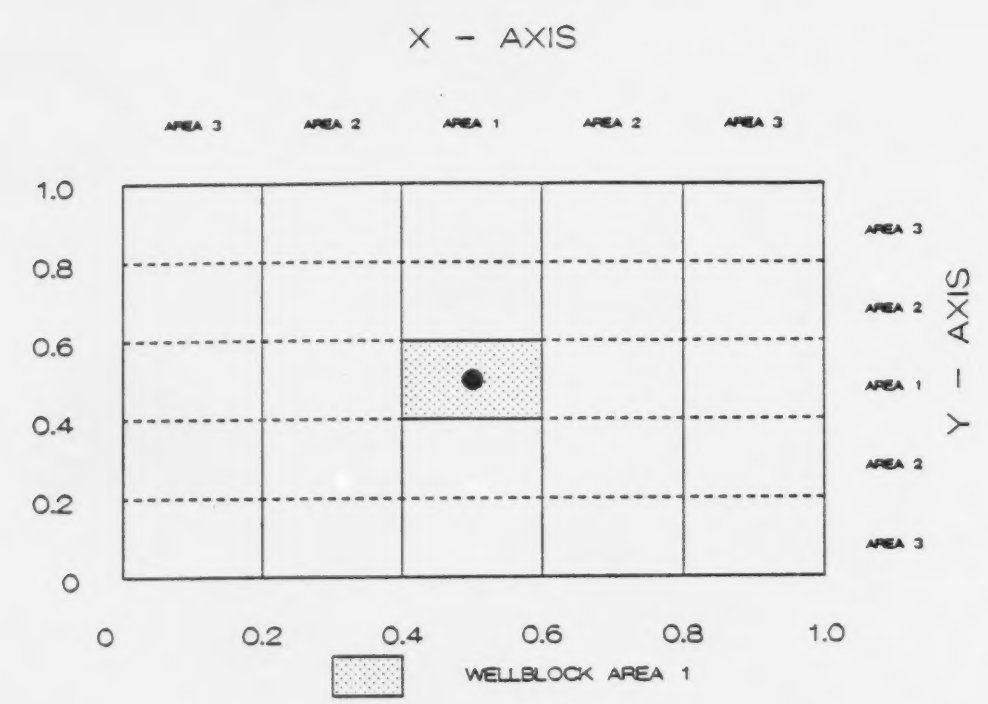

Figure 4.1 - Reservoir gridding areas.

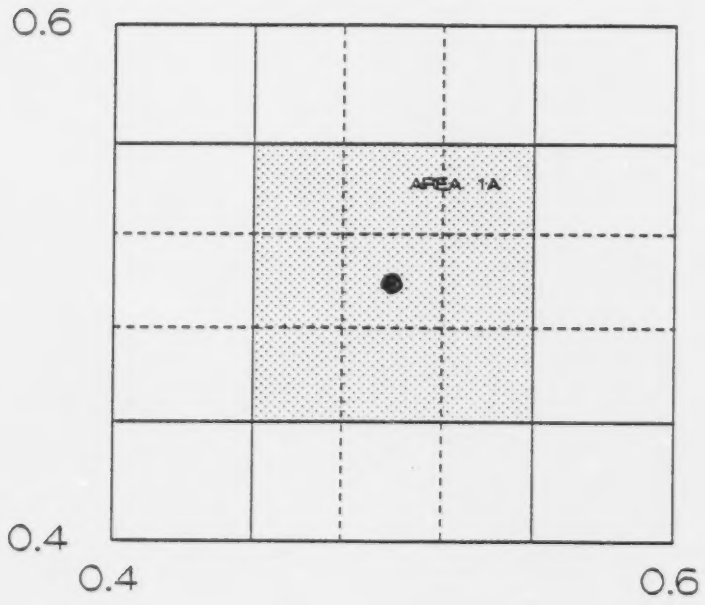

Figure 4.2 - Reservoir grid wellblock Area 1.

This refined Area 1 gridding may be necessary to minimize any numerical wellbore storage effect.

The grid block dimensions for Areas 2 and 3 are the product of Area 1 block size and the X- and Y-axis multiplier. If there is a defined AREA 1A, the dimensions for AREA 1 block are the product of AREA 1A block size and the X- and Y-axis multiplier. The X-axis multiplier is input by the program user and the Y-axis multiplier determined relative to the reservoir aspect ratio as:

$$\text{YMULT} = \text{XMULT} / \text{XY RATIO}$$

If YMULT is computed to be less than 1, it will be set at 1 and the grid block length along the Y-axis remains constant over the entire reservoir grid. For Areas 2 and 3, the X-axis block sizes are computed as follows:

$$\text{AREA 2 X-AXIS BLOCK SIZE} = (\text{AREA 1 BLOCK SIZE} \times \text{XMULT})$$

$$\text{AREA 3 X-AXIS BLOCK SIZE} = (\text{AREA 2 X-AXIS BLOCK SIZE} \times \text{XMULT})$$

The Y-axis block sizes are computed similarly using the YMULT value, when YMULT does not equal 1. The grid block size remains constant over the specified Area 1, 2 or 3. For wells off-center, Area 3 will be extended to the reservoir boundary along the longer axis. The shorter axis may be within AREA 1 or AREA 2. The grid flexibility options are necessary to

determine the best block arrangement for late-time analysis.

Equation (4.1) was arranged in a finite-difference form using a central-difference approximation in space and forward-difference in time. The resulting finite-difference approximation for block (i,j) at time N+1 becomes:

$$\frac{m(p)^{N+1}_{(i-1,j)} - 2m(p)^{N+1}_{(i,j)} + m(p)^{N+1}_{(i+1,j)}}{\Delta x^2} + \frac{m(p)^{N+1}_{(i,j-1)} - 2m(p)^{N+1}_{(i,j)} + m(p)^{N+1}_{(i,j+1)}}{\Delta y^2}$$

$$= \frac{\phi\mu(p)^{N+\frac{1}{2}} c_g(p)^{N+\frac{1}{2}}}{0.0002637k} \left(\frac{m(p)^{N+1}_{(i,j)} - m(p)^{N}_{(i,j)}}{\Delta t} \right) \qquad \text{.....(4.2)}$$

The gas flow differential equation is non-linear. Therefore, the finite-difference numerical solution is an iterative process. The finite-difference equation for each grid block within the reservoir can be combined to yield a penta-diagonal coefficient matrix. The system of grid block equations is simultaneously solved to obtain block m(p) at each time step. The non-linear gas properties $\mu(p)$ and $c_g(p)$ are calculated at an average of the previous block m(p) ($m(p)^N$) and the current calculated block m(p) ($m(p)^{N+1}$) value for each grid block for the time-step interval. Therefore, the current m(p) solution at each time-step is dependent on the m(p) solution at the previous time-step.

The matrix of equations is solved using a SPARSPAK[20] routine for large systems of linear equations. SPARSPAK[20] uses Gaussian elimination to solve for the m(p) values. The iterative process is continued until the consecutive m(p) values calculated vary by no more than 0.001%. The solution was considered to be sufficiently converged at that iteration level. The number of iterations was dependent on the gas volume removed from the reservoir over the time interval. The larger the gas volume removed, the greater the change in m(p) and hence, the larger number of iterations required to converge to the solution. The average number of iterations for the examples considered in this work was 4, with a maximum number of 10 iterations for larger produced volumes.

Once the solution converged, there was a check of the change in the pressure of the wellblock over the time interval. The maximum change in wellblock pressure was taken as 200 psi. This value of 200 psi was selected as an upper limit to minimize any error associated with averaging the $\mu(p)c_g(p)$ product from time-step to time-step. If this value was exceeded, the time interval was decreased and the iterative process restarted. The new time interval was calculated from:

$$\Delta t_{new} = \frac{\Delta t_{old}}{1.5} \frac{200.}{\Delta p_{max}} \qquad \text{.....(4.3)}$$

The wellblock m(p) was converted to flowing well pseudopressure $m(p_{wf})$, by determining the equivalent radius of a square wellblock, r_o, as developed by Peaceman[19]. For a Δx by Δx square:

$$r_o = 0.2\,\Delta x \qquad \ldots\ldots\ldots\

5. VALIDITY OF COMPUTER MODEL

The numerical simulation results were validated by the following methods:

1. comparing the m_{wD} with liquid p_{wD} results,
2. comparing square reservoir results with existing m_{wD} solution for circular reservoirs,
3. material balance check and checking block residuals,
4. computing reservoir volumetric average pressure from simulation data and compare with material balance average pressure.

Reynolds et al.[18] compared p_{wD} and m_{wD} data for circular reservoirs at both early time and late time. For circular reservoirs, the infinite-system solution response can be used for $t_{DA}<0.1$[17]. Early-time analysis will refer to data at $t_{DA}<0.1$, and late-time analysis will refer to data at $t_{DA}>0.1$. For square reservoirs, the infinite-system solution response can be used for $t_{DA}<0.09$. Transient data for circular and square reservoirs should correlate very well. The shape factors for bounded circular and square reservoirs are 31.62 and 30.88, respectively. Therefore, late-time data for both reservoir shapes, with similar drainage volumes, should also correlate very well.

Analytical p_D responses were generated for bounded rectangular reservoir configurations using the exponential-integral (Ei) solution, image wells and the principle of superposition in space. The p_D response at any point and at any time was calculated from:

$$p_D\,(x_D, y_D, t_{DA}) = -\frac{1}{2}\sum_{i=1}^{\infty} Ei\left(-\frac{a_{iD}^2}{4t_{DA}}\right) \qquad \text{.....(5.1)}$$

where:

$$a_{iD} = a_i/\sqrt{A} \qquad \text{.....(5.2)}$$

$$a_i = \sqrt{x_i^2 + y_i^2} \qquad \text{.....(5.3)}$$

The dimensions x_i and y_i represent the distance from the active (producing) well to each image well.

Program 2 in Appendix A is a printout of the analytical liquid simulator program.

Transient numerical m_{wD} data can be compared with the Ei solution p_{wD} data. However, the late-time pseudosteady state response may require analysis for the applicability of the time correction as presented by Reynolds et al.[18].

From Reynolds et al.[18] results, a semi-log plot of m_{wD} and p_{wD}

vs t_D was found to have the proper early-time slope of 1.151. The data correlated very well with the liquid solution transient response. Reynolds et al.[18] also observed that a Cartesian plot of m_{wD} and p_{wD} vs t_D illustrated the late-time deviation of the m_{wD} data from p_{wD} for a circular reservoir. The initial pressure, p_i=5000 psia, and flowrate, q_D=0.05, were used by Reynolds et al.[18]

Data were generated for a square reservoir with the same initial pressure, flowrate, drainage volume and with a well location in the center. The data for the square is shown in Figure 5.1. The transient m_{wD} and p_{wD} responses, plotted on a semi-log scale, vs t_{DA}, correlated well. The infinite-acting transient m_{wD} slope is within 1% of the liquid p_{wD} value of 1.151.

Figure 5.2 shows a Cartesian plot of late-time data for a well in the center of a square. There is a significant deviation of m_{wD} from p_{wD}. Reynolds et al.'s[18] numerical m_{wD} results for the circular reservoir showed less than 1% deviation from the p_{wD} solution up to $t_{DA}<0.3$. The m_{wD} results of Reynolds et al.[18] are also plotted in Figure 5.2. The numerical results for a square also indicated a less than 1% error for $t_{DA}<0.3$ for a reservoir at an initial pressure of 5,000 psia and produced with flowrate q_D = 0.05. Under these reservoir conditions, the numerical m_{wD} data for a square correlated very well with the

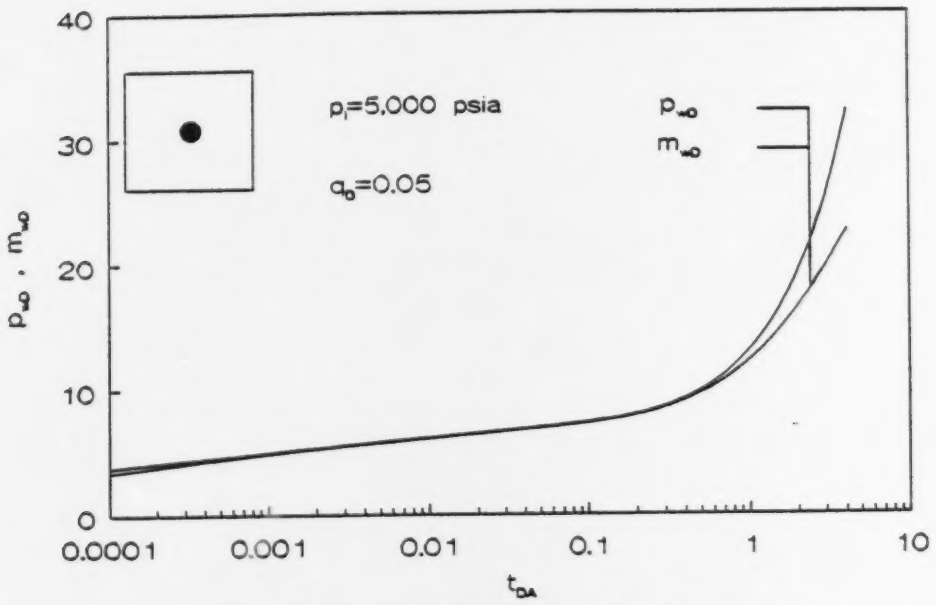

Figure 5.1 – Numerical m_{wD} and analytical p_{wD} response for a square.

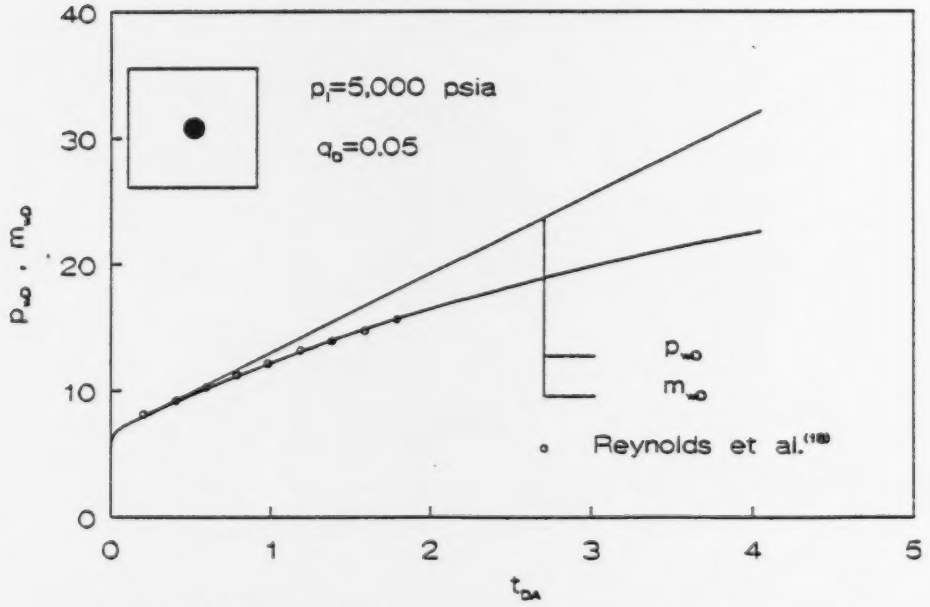

Figure 5.2 – Numerical m_{wD} and analytical p_{wD} response and Reynolds et al.[18] m_{wD} data for circle.

results of Reynolds et al.[18] for circular reservoirs.

The simulated drawdown m(p) response of a square was also compared to the results of Wattenbarger[13] for circular reservoirs. Results for Wattenbargers's[13] Well B, at an initial pressure of 5,000 psia, were computed using a square reservoir of the same drainage volume as the circular reservoir. The results plotted versus t_{DA} should correlate directly. For the three flowrates used, the results obtained by Wattenbarger[13] overlay the numerical results of the square reservoir as shown in Figure 5.3. Figure 5.3 also shows the liquid p_{wD} response.

A material balance calculation was performed on the grid block system when the constraints on converged m(p) and maximum value of wellblock pressure change were satisfied. The material balance check would insure that there were no serious errors in the numerical solution of the differential equations. The material balance was based on the equation:

$$MB = \frac{\sum_{i=1}^{N_x} \frac{T_{sc}\phi V_i}{p_{sc}T}\left(\frac{p_i^{N+1}}{z_i^{N+1}} - \frac{p_i^{N}}{z_i^{N}}\right)}{\sum_{i=1}^{N_x} q_i^{*}\Delta t} \qquad \text{.....(5.4)}$$

Equation (5.4) equates the summation of the ratio of the change in reservoir pressure to reservoir volume produced

during a specific time interval. The summation was over the entire reservoir grid. Two time periods were used. A local or incremental time interval was used, from time-step N to N+1.

Also, a global or cumulative time interval was used from the initial start of production.

The residual for each grid block was also calculated for each time step. The residual for each well block was the difference between the left-hand side and right-hand side of the finite-difference equation, similar to Equation (4.2). The maximum residual value over the entire grid was recorded for each time step.

The tolerance of the m(p) iterative calculation was viewed as the primary solution constraint. Once the m(p) tolerance of 0.001% was satisfied, the material balance and residual values were well within the .1% range.

The numerical data generated for Wattenbarger's[13] Well B, for flowrate $q_D = 0.010$, was analyzed with respect to material balance and block residuals. The maximum value of the material balance error was 1.8×10^{-08}. The local and global material balance values were similar. The maximum block residual value was 4.7×10^{-13}. These values are well within the acceptable tolerance necessary for adequate numerical results.

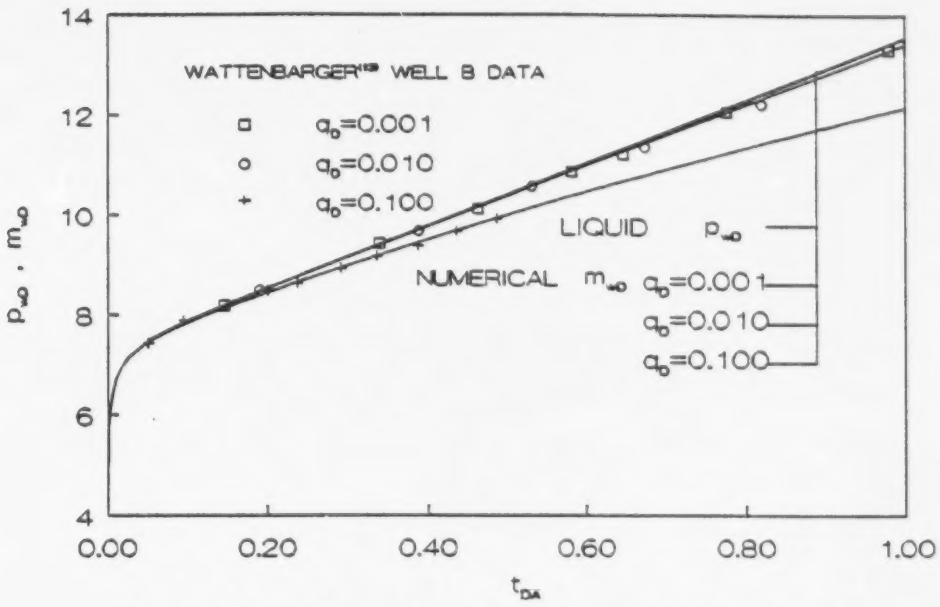

Figure 5.3 – Comparison of Wattenbarger[13] data and simulation data for various flowrates.

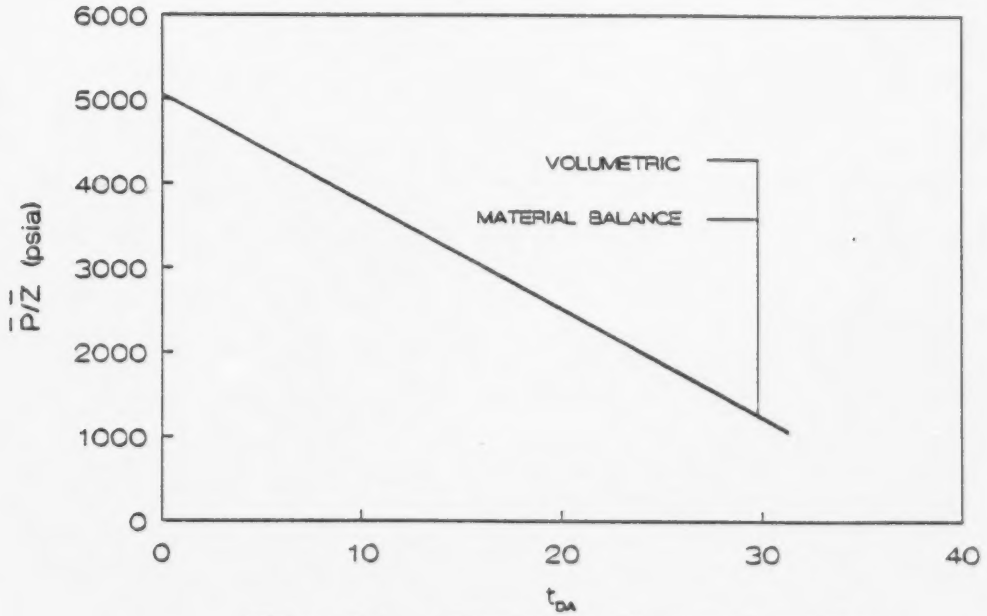

Figure 5.4 – Comparison of average pressure calculation methods.

From the numerical m(p) data, the volumetric average pressure and average z(p) factor ($\overline{p}/\overline{z}$) were calculated for each time interval. A material balance $\overline{p}/\overline{z}$ value was also calculated based on cumulative production from a volumetric reservoir. For Well B at p_i=5,000 psia and q_D=0.010, the volumetric and material balance $\overline{p}/\overline{z}$ values were compared. As shown in Figure 5.4, the average pressure values differed by less than 0.1% at t_{DA} = 0.3. At t_{DA} = 0.3, the 1% deviation of the numerical data from the liquid response is a valid finding (see Figure 5.2) as there is very little simulator error at that time. The maximum difference was about 3%, at $\overline{p}/\overline{z}$ = 1,050 psia and t_{DA} = 31.

6. RESULTS AND DISCUSSION

The simulation program was applied to analyze numerical m_{wD} drawdown data from rectangular reservoirs. Data was obtained from rectangular reservoirs with aspect ratios of 1:1, 2:1, 4:1 and 10:1. For reservoirs with aspect ratios of 1:1, 2:1 and 4:1, the single active well locations were chosen to be, in terms of dimensionless co-ordinates, at (0.50,0.50), (0.75,0.50) and (0.75,0.75). For the 10:1 rectangular reservoir, the only active well location analyzed was (0.50,0.50).

Figure 6.1 illustrates the active well location for a well at (0.75,0.75) within a 2:1 rectangular reservoir. For each reservoir configuration, the length (y-axis) was held at a constant 1,000 feet. The reservoir width (x-axis) varied depending on the aspect ratio. For the 2:1 reservoir the width was 2,000 feet, for a 4:1 reservoir the width was 4,000 feet and for a 10:1 reservoir the width was 10,000 feet.

The results of Aziz et al.[16] provided reservoir data for 24 typical gas wells in Alberta. From this data, 3 specific groups were chosen for initial reservoir conditions. Table 6.1 lists initial pressure, temperature, and gas specific gravity

TABLE 6.1 - Reservoir initial conditions.

RES.	p_i psia	T_i °F	GAS SPEC. GRAV.	p_{pc} psia	T_{pc} °R	p_{pr}	T_{pr}
A	5000	250	0.75	664.6	406.6	7.52	1.75
B	3000	200	0.70	666.9	391.2	4.50	1.69
C	1000	150	0.65	669.4	375.8	1.49	1.62

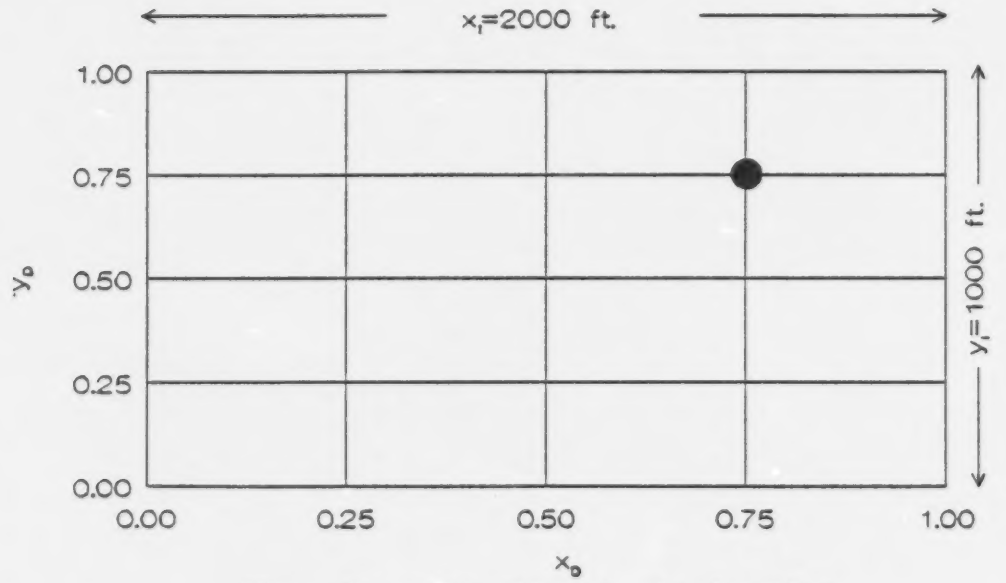

Figure 6.1 - 2:1 Reservoir grid dimensions, well at (0.75,0.75).

for Reservoirs A, B and C used for this study. For each reservoir, the permeability, porosity and zone thickness were held constant at 1 md, 20% and 1 foot, respectively. A well radius of 0.333 foot was also selected. A dimensionless flowrate (q_D) of 0.05 was used for preliminary analysis. The well locations chosen for each aspect ratio are summarized in Table 6.2.

The effects of gas contaminants, H_2S, CO_2 and N_2, on the m(p) response were also considered. The data of Aziz et al.[16] also included the mole fractions of any contaminants for each reservoir. Within Reservoirs A and B, from Table 6.1, at initial pressures of 5,000 and 3,000 psia, respectively, data were obtained for reservoirs with 3 different contaminant concentrations. The data provided by Aziz et al.[16] were used as a guide for the contaminant mole fractions. For a sour gas, data were obtained for one well location, (0.50,0.50), for each aspect ratio. Table 6.3 lists the contaminant mole fraction used for Reservoirs A and B. Reservoir C, at an initial pressure of 1,000 psia, had negligible contaminant levels. However, data were obtained for one set of contaminants as listed in Table 6.3.

The following topics will be discussed in subsections of this chapter:

1) Introduction - general results of a 1:1 rectangle with

TABLE 6.2 - Well locations for Reservoirs A, B and C.

ASPECT RATIOS	WELL LOCATIONS (x_D,y_D)
1:1	(0.50,0.50) , (0.75,0.50) , (0.75,0.75)
2:1	(0.50,0.50) , (0.75,0.50) , (0.75,0.75)
4:1	(0.50,0.50) , (0.75,0.50) , (0.75,0.75)
10:1	(0.50,0.50)

TABLE 6.3 - Contaminant concentrations for Reservoirs A, B and C.

RESERVOIR	p_i (psia)	Mole Fraction			ASPECT RATIOS [Well Located at (0.50,0.50)]
		N_2	H_2S	CO_2	
A	5000	0	0.20	0	1:1, 2:1, 4:1
		0.05	0.20	0.10	
		0	0.40	0	
B	3000	0	0.10	0	1:1, 2:1, 4:1
		0.05	0.10	0.05	
		0	0.20	0	
C	1000	0.05	0.10	0.05	2 : 1

analysis of the following:

i) changing $\mu(p)c_g(p)$ product and late-time data.

ii) late-time correction of Reynolds et al.[18].

2) Reservoir Gridding - effects of changing gridding configuration on late-time data and time corrected data.

3) Reservoir Conditions - reservoir conditions to be considered for analysis can be summarized as follows:

i) effects of reservoir aspect ratio and well location on Reservoirs A, B and C.

ii) effects of gas contaminants H_2S, CO_2 and N_2.

iii) effects of changing reservoir temperature.

iv) effects of varying reservoir permeability.

4) Flowrates - effects of changing flowrate on late-time data.

5) Limit Test Analysis.

The transient and pseudosteady state m(p) data will be analyzed with respect to:

i) deviation of gas m_{wD} from liquid p_{wD} solution.

ii) applicability of the time correction as proposed by Reynolds et al.[18]

iii) significance of semi-ln pressure derivative of drawdown data.

Also, the reservoir simulation volumetric average pressure will be compared with the material balance average pressure to check the simulation accuracy.

6.1 INTRODUCTION

The simulation m(p) results were obtained first for a 1:1 rectangle, or square reservoir. For q_D=0.05, the results for a well at (0.50,0.50) are presented in Figure 6.2 for Reservoirs A, B and C. The semi-log plot of Figure 6.2 illustrates the transient flow period infinite-acting semi-log straight line. The slope of the infinite-acting radial flow period data for each reservoir initial condition was within 1% of the liquid flow (p_{wD}) semi-log slope of 1.151. From the semi-log plot, at t_{DA}≈1.0 all solutions start to deviate from infinite-acting flow. The simulation volumetric average pressure error, compared to material balance, for q_D=0.05, is less than 0.1% during the transient period.

The Cartesian plot, Figure 6.3, illustrates the degree of deviation during the pseudosteady state flow period. At t_{DA}≈0.30 the m_{wD} solutions start to deviate from the liquid solution. When plotted versus t_{DA}, the reservoir with the higher initial pressure had the higher deviation from the liquid solution. This was a result of the larger variation of the $\mu(p)c_g(p)$ product within the reservoir. The larger the variation of $\mu(p)c_g(p)$, the greater the deviation of m_{wD} from p_{wD}.

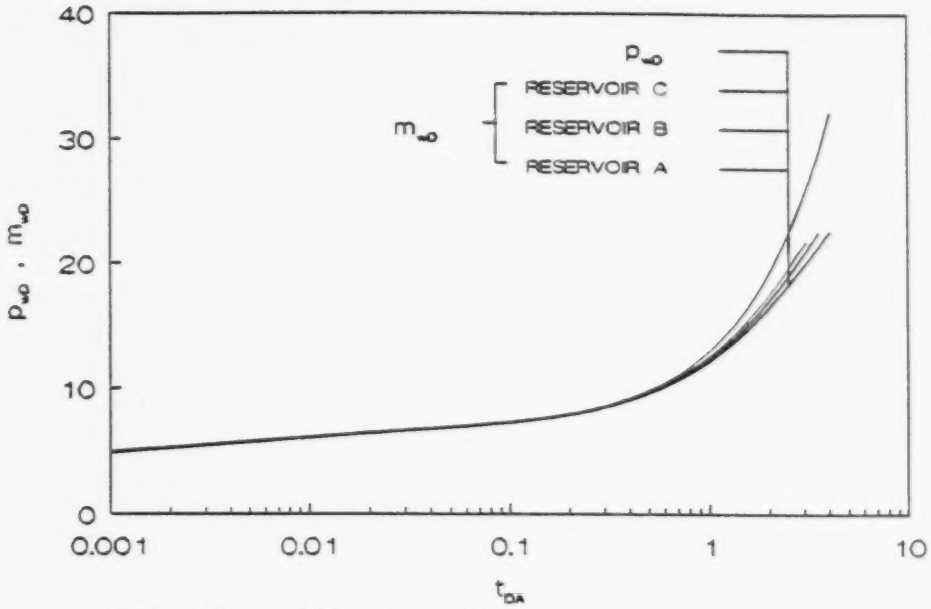

Figure 6.2 – Effect of initial conditions on 1:1 Reservoir well at (0.50,0.50).

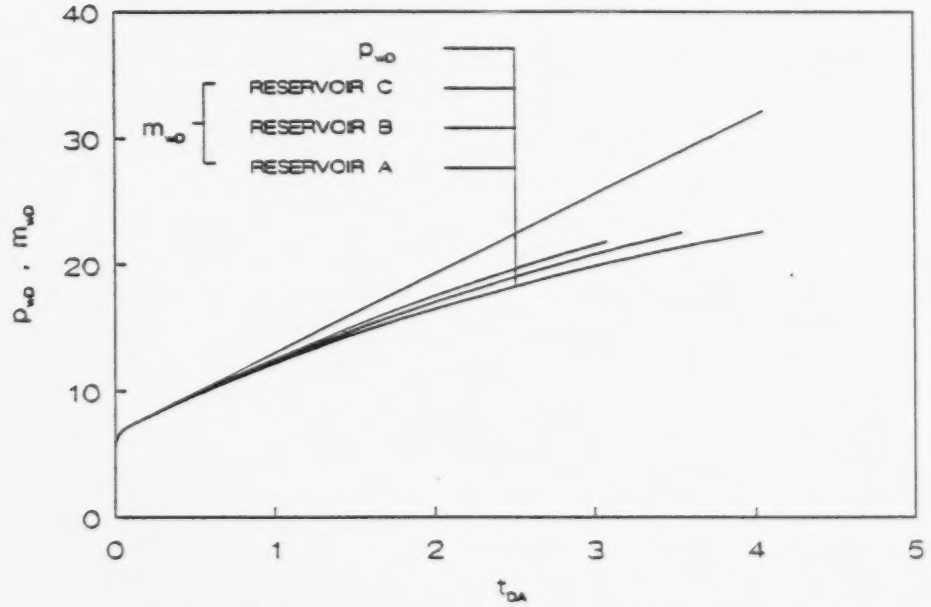

Figure 6.3 – Cartesian plot of response for 1:1 Reservoir well at (0.50,0.50).

Figure 6.4 shows the variation of $\mu(p)c_g(p)$ with pressure. For Reservoirs A, B and C, the change in the $\mu(p)c_g(p)$ product versus pressure is computed as a ratio of the initial conditions. From Figure 6.4, it is apparent that for similar changes in pressures, the change in the $\mu(p)c_g(p)$ product for Reservoir A is approximately double the change for Reservoir C. The response for Reservoir B lies between that of Reservoirs A and C.

Figure 6.5 illustrates the variation of $\mu(p)$ with pressure. The fluid mobility within the reservoir, $k/\mu(p)$, is affected only by the changing magnitude of $\mu(p)$. For Reservoir A, the gas viscosity decrease with a reduction in pressure is greater than that for Reservoirs B and C. As $\mu(p)$ decreases, the fluid mobility increases. For a higher fluid mobility, a higher $m(p_{wf})$ is obtained. The higher flowing $m(p_{wf})$ results in lower m_{wD} values and greater deviations from p_{wD}.

As listed in Table 6.1, the pseudoreduced temperature (T_{pr}) and specific gravity (SG) of Reservoir B gas is 1.69 and 0.70, respectively. The data points in Figures 6.4 and 6.5 are plotted for gas reservoir pressures of 5000 psia and 1000 psia with T_{pr}=1.69 and SG=0.70. The effect of pressure on gas $\mu(p)$ and $c_g(p)$ is illustrated by comparing the data points with the response of Reservoir B. The effects of temperature on gas $\mu(p)$ and $c_g(p)$ are illustrated by comparing the data

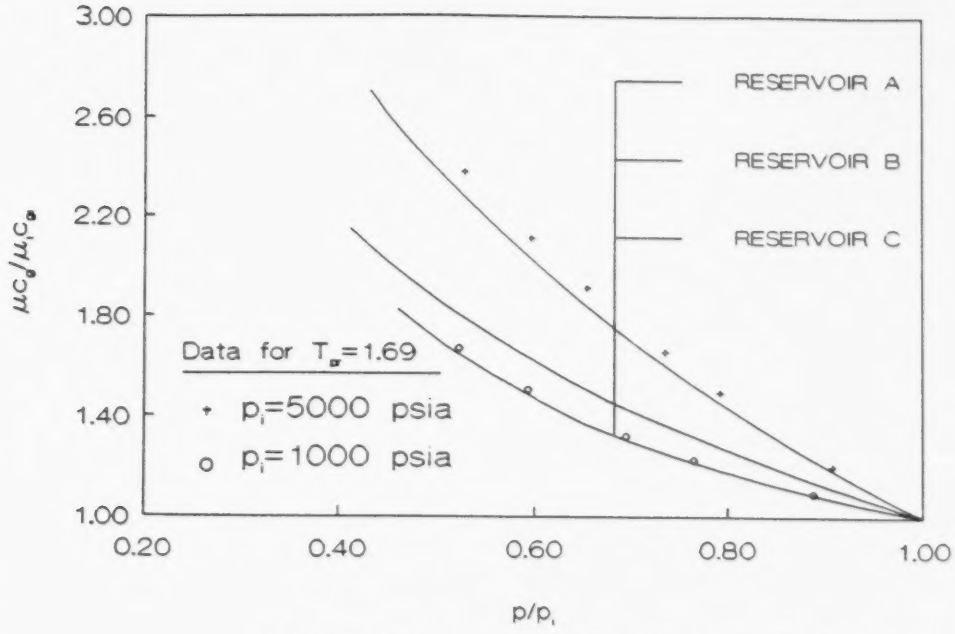

FIGURE 6.4 – μc_g variation with pressure.

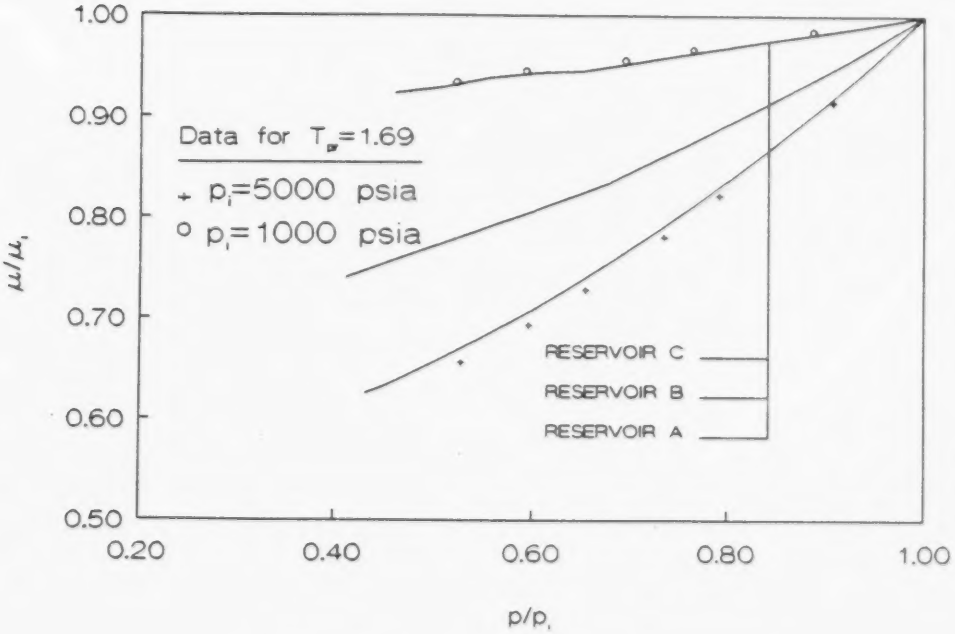

Figure 6.5 – μ variation with pressure.

points for 5000 psia and 1000 psia to the curves for Reservoirs A and C, respectively.

The combined effects of the increasing magnitude of the $\mu(p)c_g(p)$ product and decreasing magnitude of the gas viscosity with a decrease in pressure lead to deviations of m_{wD} from the p_{wD} solution. As illustrated in Figure 6.4, $(\mu c_g)_i$ is less than the $\mu(p)c_g(p)$ product at any pressure other than p_i. Therefore, when plotted versus t_{DA}, the m_{wD} data is displaced in the positive x-axis direction, as t_{DA} is inversely proportional to $(\mu c_g)_i$.

For a 1:1 rectangle and well at (0.50,0.50), the effect of varying the magnitude of the $\mu(p)c_g(p)$ product is illustrated in Figure 6.6. In Figure 6.6, the deviation of m_{wD} from p_{wD} is plotted versus t_{DA}. The deviation for each reservoir is very slight during the infinite-acting flow period. For values of $t_{DA}>0.3$, the deviation increases steadily. At equivalent values of t_{DA}, the deviation for Reservoir A is greater than that for Reservoirs B and C. For Reservoir A, at $t_{DA}\approx4.0$, the m_{wD} response deviates from the corresponding p_{wD} by approximately 30%.

Reynolds et al.[18] analyzed circular reservoirs with respect to the time to a 1% m_{wD} deviation from p_{wD}. For a 1:1 rectangle, Figure 6.7 illustrates the deviation data on an

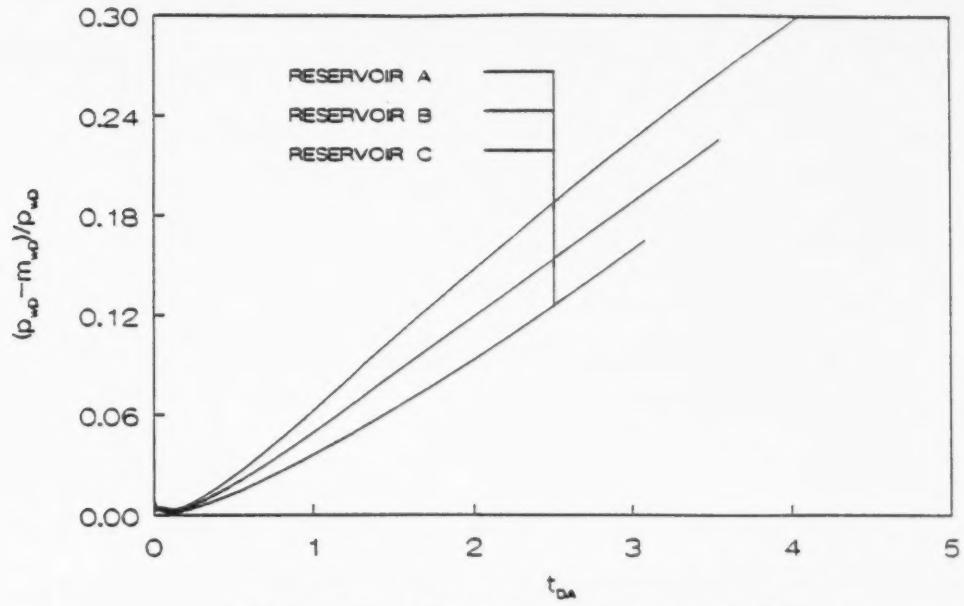

Figure 6.6 – Deviation data for 1:1 Reservoir with well at (0.50,0.50).

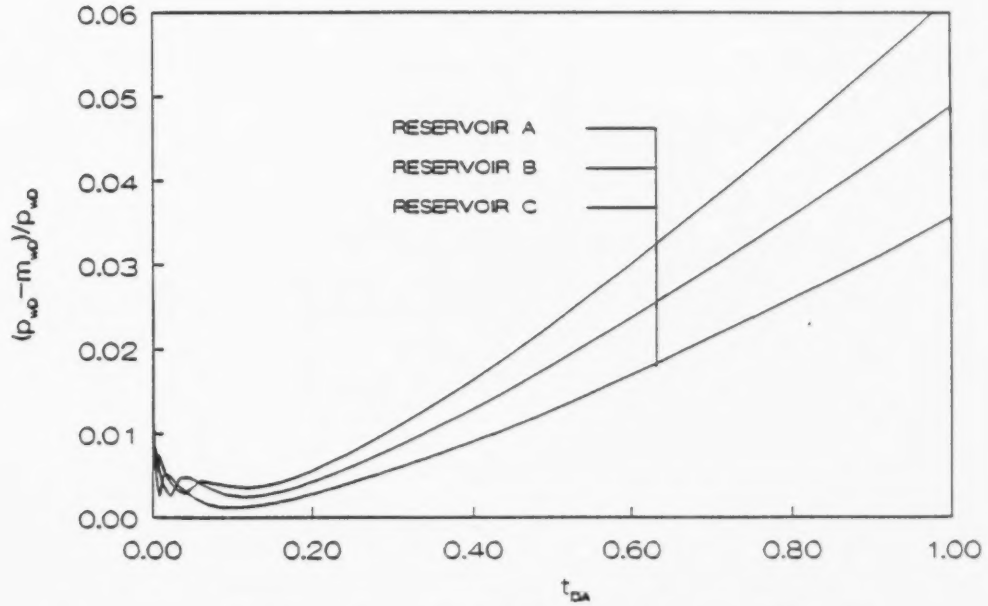

Figure 6.7 – Deviation data for 1:1 Reservoir with well at (0.50,0.50), expanded scale.

expanded scale to compare the time to 1% deviation for each reservoir with q_D=0.05. The t_{DA} values of the 1% deviation for Reservoirs A, B and C are 0.30, 0.34 and 0.44, respectively.

The m_{wD} deviation during psuedosteady state flow affects limit test analysis. In Figure 6.8, the straight lines were fitted through the latter m_{wD} data segments for each 1:1 reservoir with q_D=0.05. As noted on Figure 6.8, there is a considerable difference between the computed slopes. From Equation (3.26), the reservoir pore volume is inversely proportional to the Cartesian pseudosteady state data slope. Therefore, as the slope is decreasing with increasing deviation, the pore volume error will be increasing on the high side. Using this portion of the pseudosteady state data results in a gross overestimation of reservoir pore volume.

Figure 6.9 illustrates the use of the time corrected or averaged t_{DA} data, as described by Reynolds et al.[18]. The plot shows data for a 1:1 Reservoir A well at (0.50,0.50), p_i=5,000 psia and q_D=0.05. Also, Figure 6.9 contains semi-ln derivative data, m_{wD}' and p_{wD}', as well as the m_{wD} and m_{wD}' data without time correction. For gas, the semi-ln derivative is calculated from:

$$m'_{wD} = \frac{dm_{wD}}{d\ln(t_{DA})} = \frac{dm_{wD}}{dt_{DA}} \times t_{DA} \quad \ldots\ldots\ldots\ldots\ldots\ldots\ldots\ldots\ldots\ldots (6.1)$$

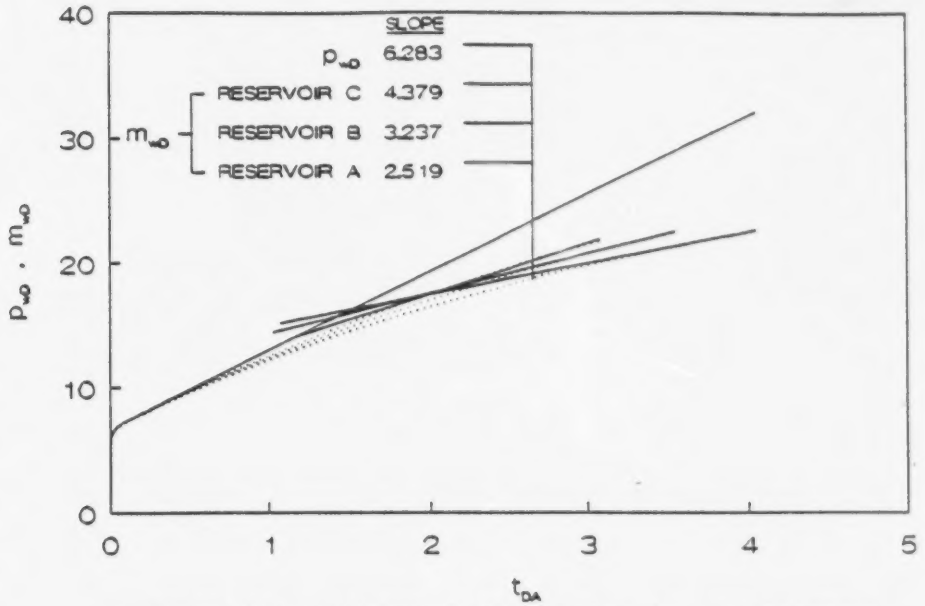

Figure 6.8 – Late–time data slopes for 1:1 Reservoir with well at (0.50,0.50).

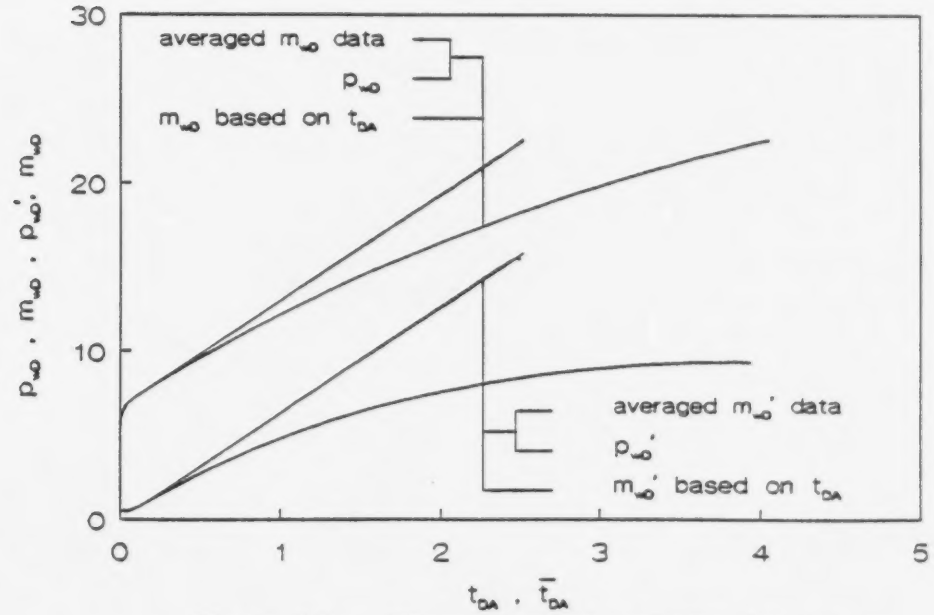

Figure 6.9 – Time–corrected response for 1:1 Reservoir A with well at (0.50,0.50).

For liquid, the semi-ln derivative is calculated analytically from:

$$p'_{wD} = \frac{1}{2} \sum_{i=1}^{\infty} e^{\frac{-a_{iD}^2}{4t_{DA}}} \qquad \text{.....(6.2)}$$

The averaging procedure corrects $\mu(p)c_g(p)$ using Equation (3.27). The replotting of the data versus $\overline{t_{DA}}$ resulted in a very good match between m_{wD} and p_{wD} data. This matching of time corrected m_{wD} data with p_{wD} was also evident for Reservoirs B and C. Limit test analysis of time corrected data would be far more accurate than that of the uncorrected or raw data.

The averaged semi-ln derivative data also correlated very well. The sensitivity of the derivative response is illustrated in Figure 6.9. The m_{wD}' curve shows an initial deviation earlier than that of the m_{wD} curve. Also, the degree of deviation of m_{wD}' is greater than that of m_{wD}. Therefore, the correction of the derivative response, based on averaging of the $\mu(p)c_g(p)$ product, was assumed to be a severe test of the averaging process. The nature of the derivative response would expose any potential problems of the procedure.

6.2 RESERVOIR GRIDDING

Chapter 4 included a discussion of the reservoir gridding. The gridding dimensions appear to affect the late-time data more than the early-time data. Figure 6.10 illustrates the p_{wD} and m_{wD} data for a 1:1 Reservoir A well at (0.50,0.50) and q_D=0.02, plotted versus t_{DA}. The m_{wD} results were generated from simulations using two reservoir grids. The block data for Reservoir Grids 1 and 2 are listed in Table 6.4. As XWB1F=1 for Grid 2, there is no Grid Area 1A. Therefore, no entry is shown in Table 6.4 for XWB1A for Grid 2. From Figure 6.10, on an absolute scale, there is little difference between the two m_{wd} curves. The late-time m_{wD} results for Grid 2 are slightly closer to the p_{wD} curve than the m_{wD} curve obtained from Grid 1. The time of 1% deviation of m_{wD} from p_{wD} is the same for both data sets.

In Figure 6.11, the p_{wD} and m_{wD} data are plotted versus $\overline{t_{DA}}$. When plotted on the time corrected scale, the relative difference between the p_{wD} and m_{wD} data for Grids 1 and 2 becomes significant. The late-time data for Grid 2 correlated much better with the p_{wD} curve than the late-time Grid 1 data. At $\overline{t_{DA}} \sim 5$, the m_{wD} errors with respect to p_{wD} for Grids 1 and 2 are 2% and 0.5%, respectively.

The errors of the simulation average pressure for Grids 1 and 2 are plotted versus $\bar{p}/\bar{z}$ in Figure 6.12. The error of the time corrected m_{wD} data of Figure 6.11 is directly proportional to the accuracy of the simulation volumetric average pressure when compared to the material balance average pressure. The calculated $\bar{p}/\bar{z}$ error of Grid 2 is less than that of Grid 1. The 1% $\bar{p}/\bar{z}$ error of Grid 2 at $\bar{p}/\bar{z}$ = 2,800 psia corresponded to the 0.5% time corrected error of Figure 6.11.

For the 1:1 reservoir, to minimize the simulation error, Grid 2 was selected for the numerical m_{wD} results. Grid analysis was also undertaken for the other reservoir aspect ratios. The gridding inputs for each reservoir are presented in Table 6.5. The Grid Area 1 fraction, XWB1F, was set to equal 1.0 for each aspect ratio. Thus, there was no Grid Area 1A. This explains why there are no entries for XWB1A in Table 6.5. For the minimum $\bar{p}/\bar{z}$ error, the reservoir grid arrangement used had minimal block size variation. That is, with XWB1F = 1.0 and with low XGM and YGM values, the block size does not vary excessively within the reservoir. The more consistent the block size, the more accurate the late-time pressure data. The improved late-time data results in an improved time corrected solution as illustrated in Figure 6.11. All results presented have similar grid configurations as listed in Table 6.5.

TABLE 6.4 - Grid inputs for Grid 1 and Grid 2.

1:1 RESERVOIR (1000' x 1000')		
GRID INPUTS	GRID 1	GRID 2
XWB1A (FEET)	10.	-
XWB1F (fraction)	0.5	1.0
XWB1 (FEET)	20.	25.
XGM	2.	1.
YGM	2.	1.

TABLE 6.5 - Grid inputs for reservoir aspect ratios.

GRID INPUTS	RESERVOIR ASPECT RATIOS 1:1	2:1	4:1	10:1
XWB1A (FEET)	-	-	-	-
XWB1F (fraction)	1.0	1.0	1.0	1.0
XWB1 (FEET)	25.	25.	25.	40.
XGM	1.0	2.0	4.0	5.0
YGM	1.0	1.0	1.0	1.0

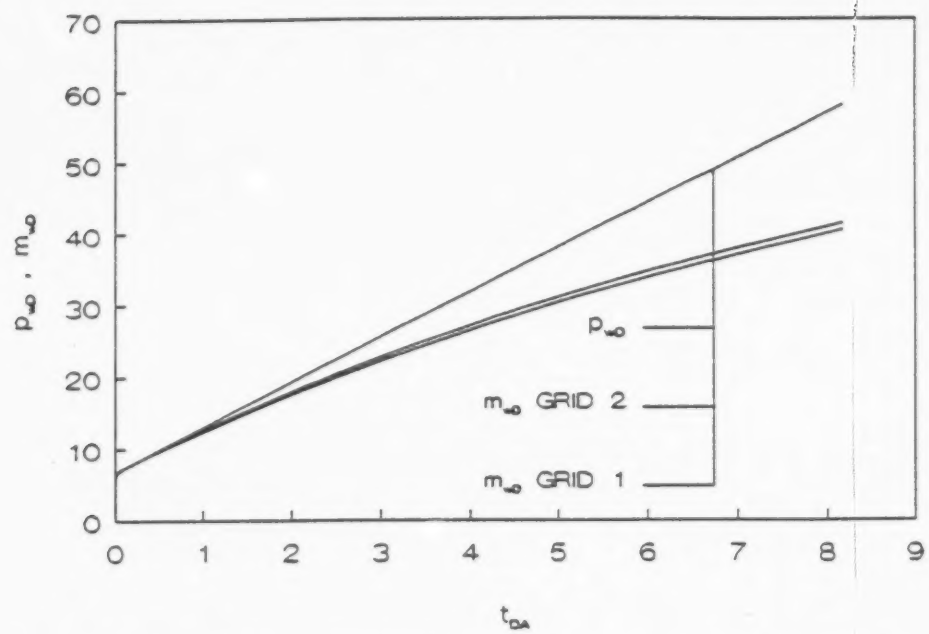

Figure 6.10 – Response for Reservoir A grids 1 and 2.

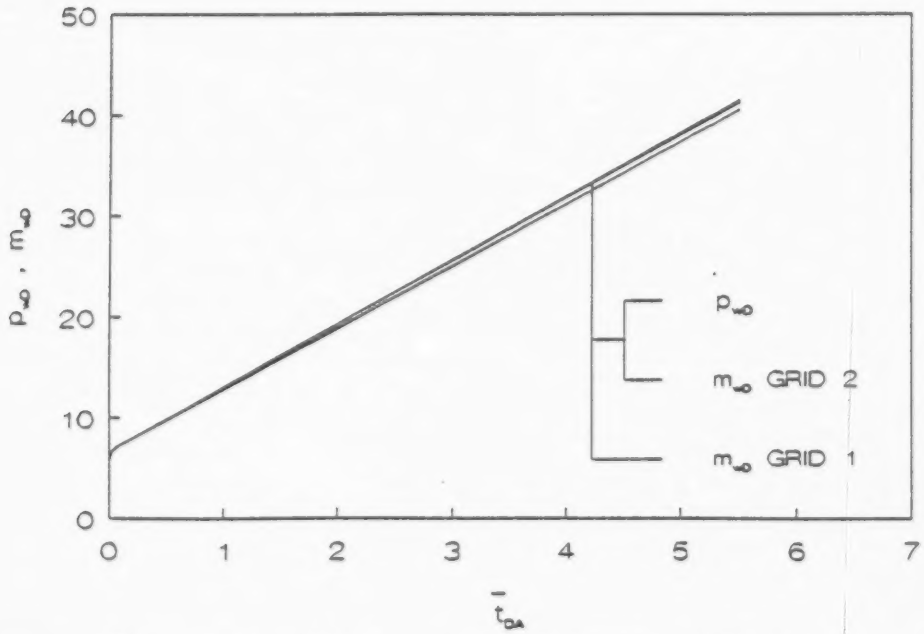

Figure 6.11 – Grids 1 and 2 time-corrected results.

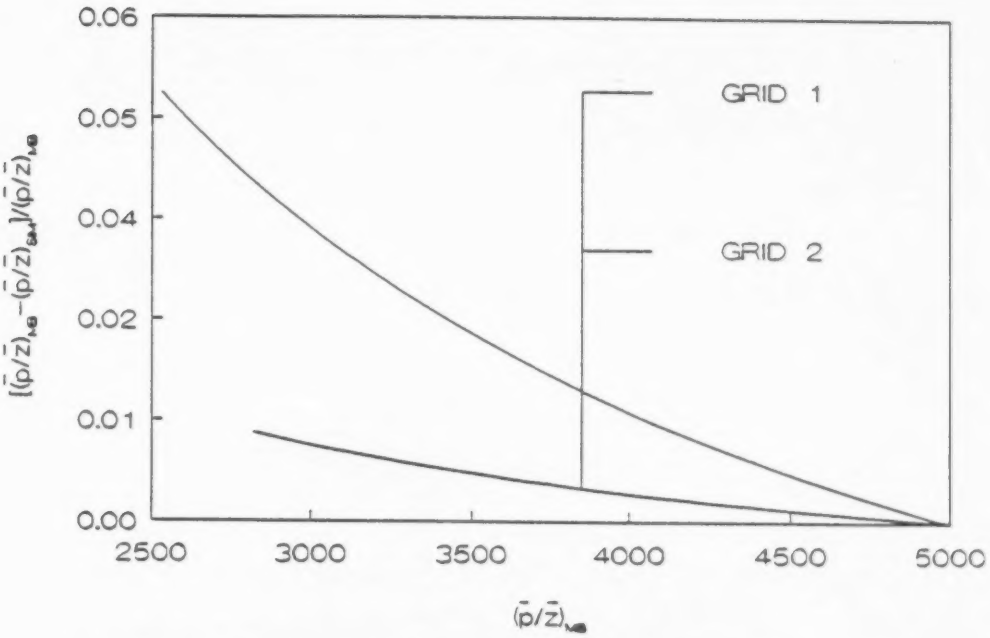

Figure 6.12 – Grids 1 and 2 average pressure error.

6.3 RESERVOIR CONDITIONS

Results discussed up to this point have been for 1:1 or square reservoirs, with a well in the center, and q_D=0.05. The applicability of the time correction of Reynolds et al.[18] has been confirmed for the reservoirs considered. The effects of the varying $\mu(p)c_g(p)$ product have been discussed. The simulation gridding configurations have been determined for the aspect ratios used in the study to minimize the material balance $\overline{p}/\overline{z}$ errors. The following example discussions use a variety of reservoir initial conditions (A, B or C), well positions and aspect ratios. Data have been tabulated to summarize results obtained for the particular section.

6.3.1 EFFECT OF RESERVOIR ASPECT RATIO AND WELL LOCATION

As summarized in Table 6.2, results were obtained for various well locations and aspect ratios. Figure 6.13 shows the p_{wD} and m_{wD} responses for Reservoir B with a 4:1 aspect ratio. The higher p_{wD} and m_{wD} values are for the off-centered well locations. The late-time deviation is similar for each well location. The late-time response for the (0.50,0.50) well location is similar to that of Reservoir B in Figure 6.3 for a 1:1 reservoir. That is, the deviation of m_{wD} from p_{wD} is similar for the corresponding t_{DA} values. The error of the

limit tests for each aspect ratio and well location for Reservoir B is similar. This conclusion is also extended to Reservoirs A and C. The late-time deviation between m_{wD} and p_{wD} is not greatly affected by well location or aspect ratio, as illustrated in Figure 6.14. Figure 6.14 shows the deviation results for two wells located in Reservoir B, one for a 1:1 reservoir at location (0.50,0.50) and the other for a 4:1 reservoir at (0.75,0.75). The late-time deviations for both cases are similar when plotted in terms of t_{DA}.

The time to 1% deviation of m_{wD} from p_{wD} for the results of Figure 6.13 are listed in Table 6.6. The t_{DA} values for 1% deviation of m_{wD} from p_{wD} do change considerably with the varying well position and aspect ratio. For wells located in Reservoir B, at p_i=3,000 psia, the value of t_{DA} for a 1:1 reservoir with a well at (0.50,0.50) for 1% deviation is 0.34. This value is significantly higher than the values listed in Table 6.6. For non-square reservoirs, the time (t_{DA}) to the end of infinite-acting radial flow is less than that of square reservoirs. The earlier time to the transition flow period creates a greater variance of m(p) within the reservoir area. This leads to earlier deviations of m_{wD} from p_{wD}. However, during pseudosteady state flow there is a more uniform m(p) decline within the reservoir as the pressure transient has reached all boundaries. Thus, there is a more consistent m_{wD} departure from p_{wD}. Results for the t_{DA} values for 1% deviation

for Reservoir A are listed in Table 6.7. The 1% deviation results for Reservoirs A, B and C with well location (0.50,0.50) are listed in Table 6.8.

TABLE 6.6 - Deviation t_{DA} values for Reservoir B with an aspect ratio of 4:1.

WELL LOCATION	(0.50,0.50)	(0.75,0.50)	(0.75,0.75)
t_{DA} FOR 1% DEVIATION	0.22	0.20	0.16

TABLE 6.7 - 1% Deviations for Reservoir A.

ASPECT RATIO	RESERVOIR A - q_D=0.05 t_{DA} FOR 1% DEVIATION AT SPECIFIC WELL LOCATIONS		
	(0.50,0.50)	(0.75,0.50)	(0.75,0.75)
1:1	0.30	0.20	0.10
2:1	0.28	0.17	0.12
4:1	0.15	0.14	0.12
10:1	0.081	-	-

TABLE 6.8 - 1% Deviations for wells at (0.50,0.50) and q_D=0.05.

RESERVOIR	t_{DA} FOR 1% DEVIATION WITH WELL LOCATED AT (0.50,0.50) FOR SPECIFIED ASPECT RATIOS			
	1:1	2:1	4:1	10:1
A	0.30	0.28	0.15	0.081
B	0.34	0.34	0.22	0.11
C	0.44	0.44	0.37	0.21

The time correction of Reynolds et al.[18] was applied to the data of Figure 6.13 and replotted in Figure 6.15. Once the $\mu(p)c_g(p)$ product was corrected, the m_{wD} data for each well location correlated very well with the p_{wD} data. Any late-time data analysis would be accurate under these conditions, provided corrected data is used.

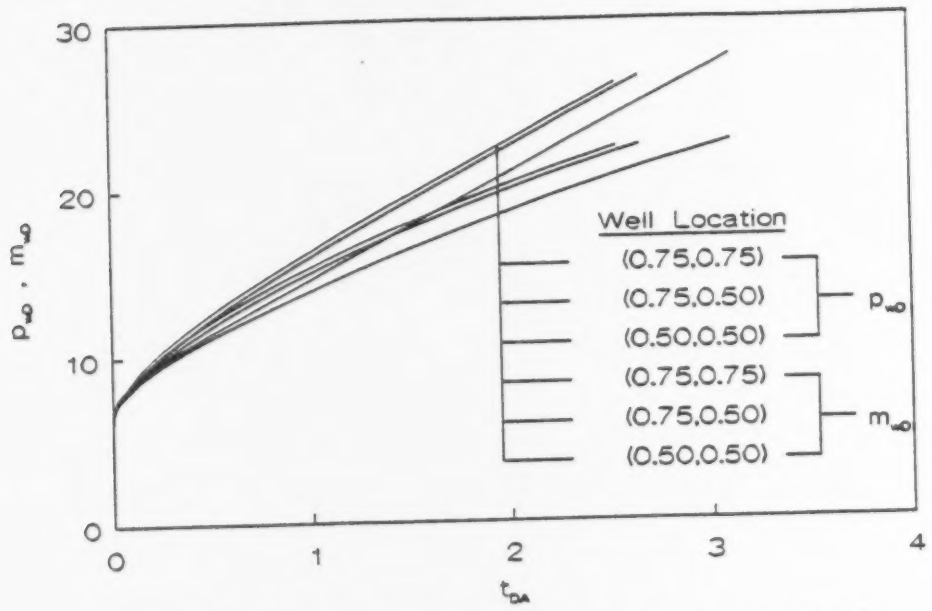

Figure 6.13 – Effect of well location on response for 4:1 Reservoir B.

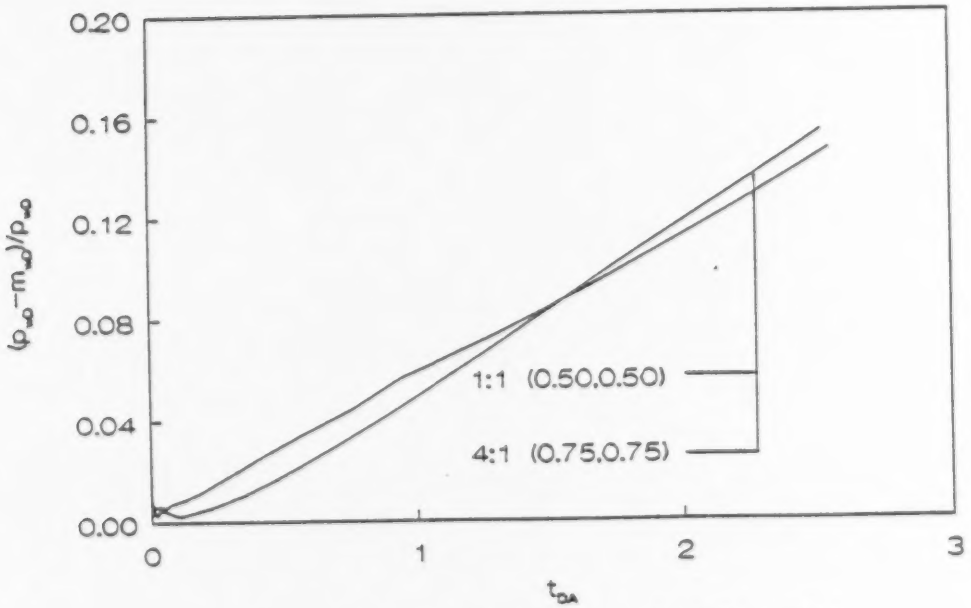

Figure 6.14 – Well location deviation data for Reservoir B.

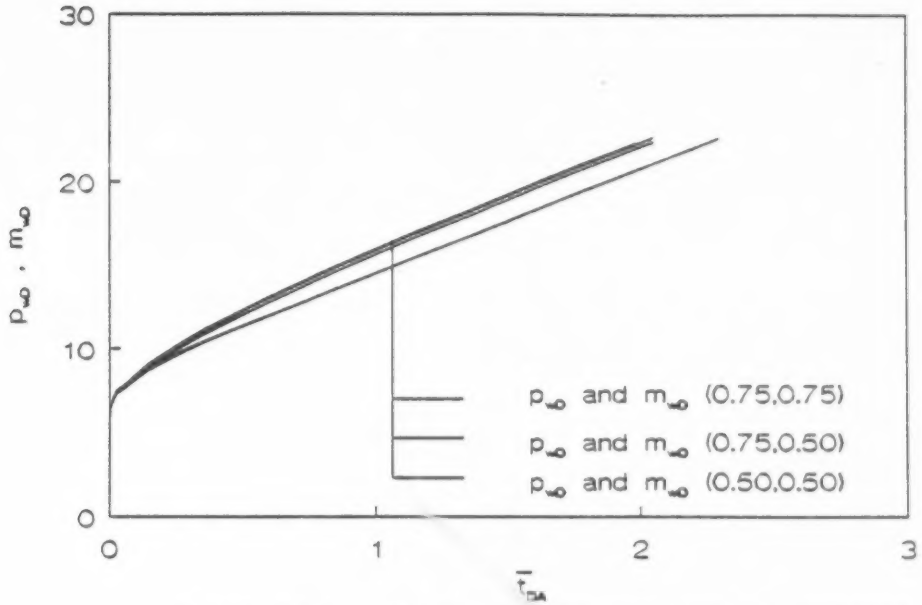

Figure 6.15 – Time-corrected well location response for 4:1 Reservoir B.

6.3.2 EFFECT OF GAS CONTAMINANTS

The gas contaminant concentration for each reservoir group is listed in Table 6.2. For a 2:1 Reservoir A with a well at (0.50,0.05), q_D=0.05 and p_i=5,000 psia, the m_{wD} response with contaminants is plotted in Figure 6.16. The m_{wD} values are very similar for each contaminant concentration. The m_{wD} response for sweet gas is also presented and lies slightly below the m_{wD} response for sour gas. The m_{wD} results for sour gases at Reservoirs B and C conditions also correlated very well with each other. The time correction of Reynolds et al.[18] was also applied and results again correlated very well with p_{wD}, as illustrated in Figure 6.17.

The time to 1% deviation for an example sour gas run for each aspect ratio is presented in Table 6.9. When compared to Table 6.8, the t_{DA} values of Table 6.9 do not differ significantly.

TABLE 6.9 - Sour Gas Example, 1% Deviations for wells at (0.50,0.50) and q_D=0.05.

RESERVOIR	t_{DA} FOR 1% DEVIATION WITH WELL LOCATED AT (0.50,0.50) FOR SPECIFIED ASPECT RATIOS		
	1:1	2:1	4:1
A + 40% H_2S	0.31	0.30	0.16
B + 20% H_2S	0.35	0.34	0.19
C + 10% H_2S	-	0.44	-

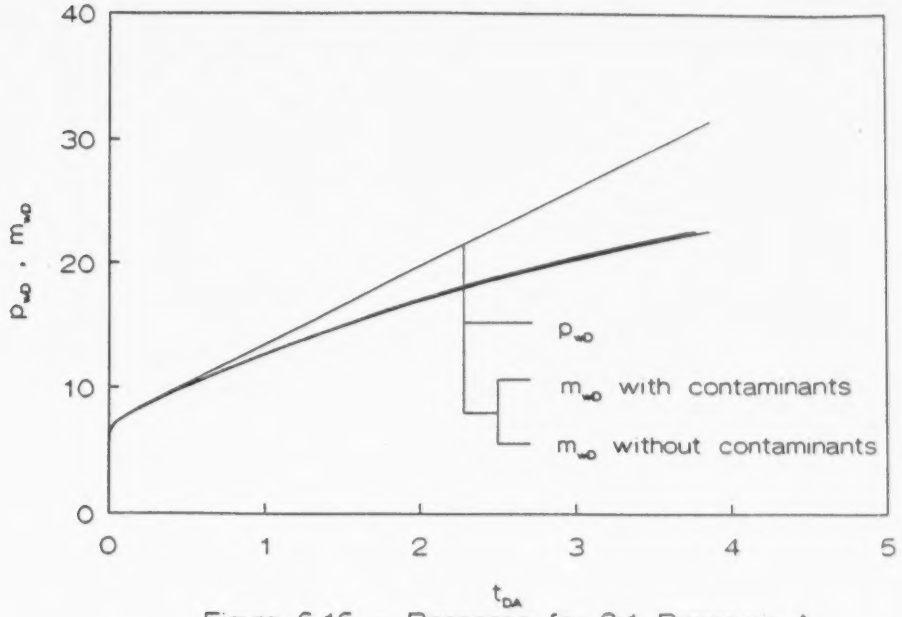

Figure 6.16 – Response for 2:1 Reservoir A with gas contaminants.

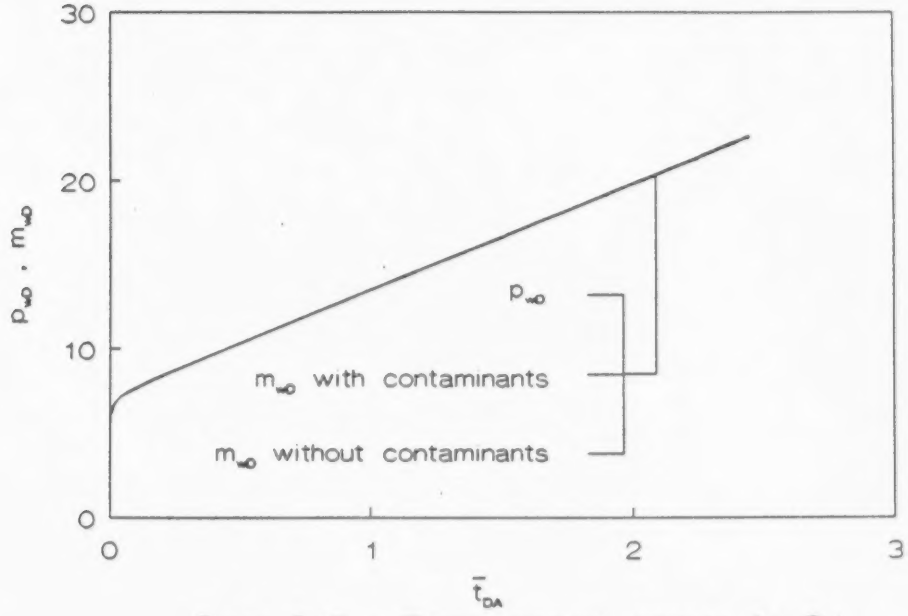

Figure 6.17 – Time-corrected response for 2:1 Reservoir A with gas contaminants.

6.3.3 EFFECT OF CHANGING TEMPERATURE

Figure 6.3 compared the m_{wD} response for reservoir gas with varying initial pressure, temperature and specific gravity. Considered here is the effect of varying temperature with constant initial pressure and specific gravity. For a 2:1 Reservoir B with a well at (0.50,0.50), q_D=0.05 and at p_i=3,000 psia, Figure 6.18 illustrates the m_{wD} response for reservoir temperatures of 150, 200 and 250°F. The m_{wD} response for each temperature is similar with the data at 150°F slightly below the other temperatures. The effects of the varying $\mu(p)c_g(p)$ product must be comparable for each temperature.

Figure 6.19 shows the results for the Reynolds et al.[18] time correction. For each temperature, the m_{wD} response correlated with the p_{wD} data.

6.3.4 EFFECT OF VARYING PERMEABILITY

The effects of a changing permeability on m_{wD} data were considered using data from a 4:1 Reservoir C with a well at (0.50,0.50) and q_D=0.05. Permeabilities used were 1 and 2 millidarcies. As shown in Figure 6.20, the m_{wD} results were the same for both permeabilities used for equivalent flowrate, q_D=0.05. The time corrected m_{wD} data[18] of Figure 6.21 also

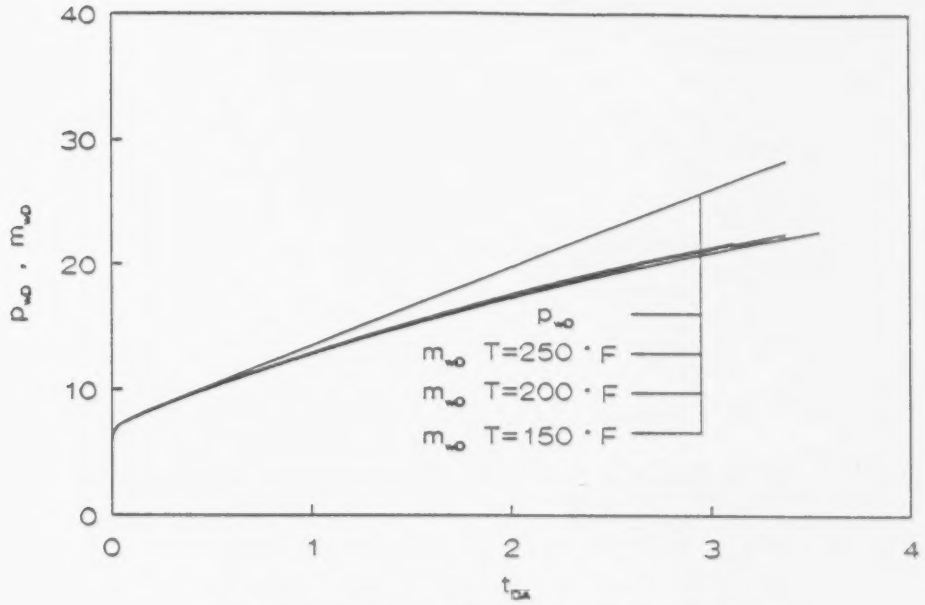

Figure 6.18 – Effect of temperature on response for 2:1 Reservoir B.

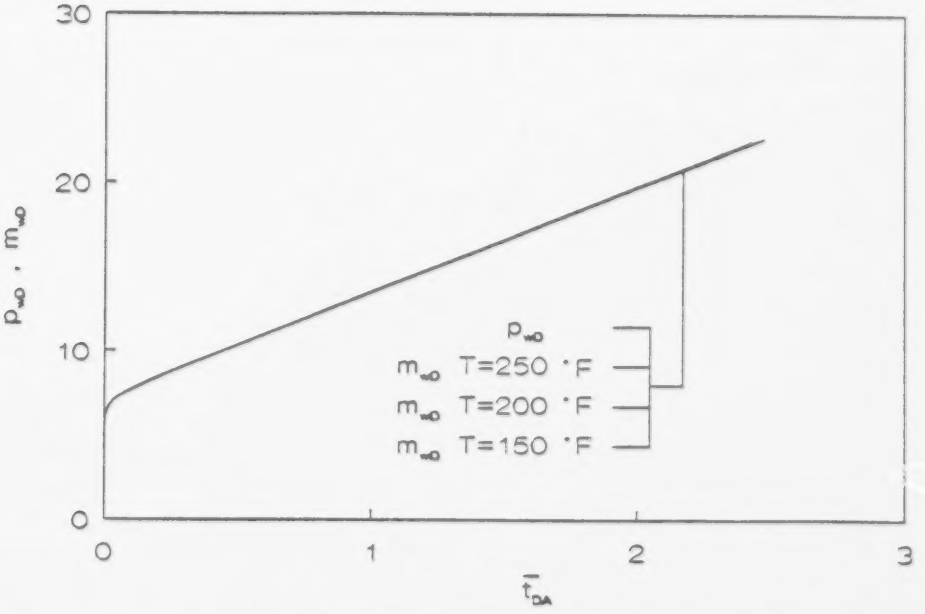

Figure 6.19 – Time-corrected temperature response for 2:1 Reservoir B.

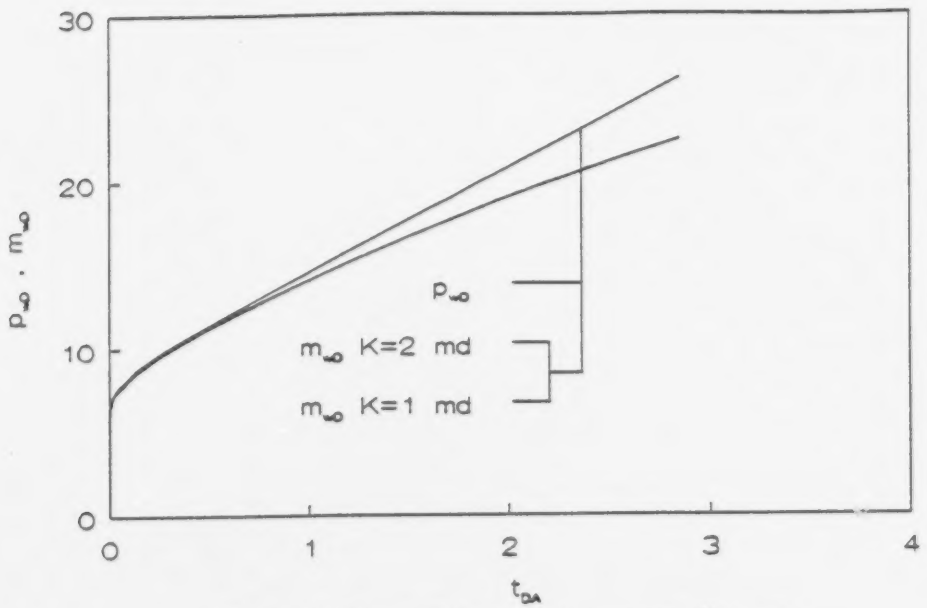

Figure 6.20 – Effects of permeability on response for 4:1 Reservoir C.

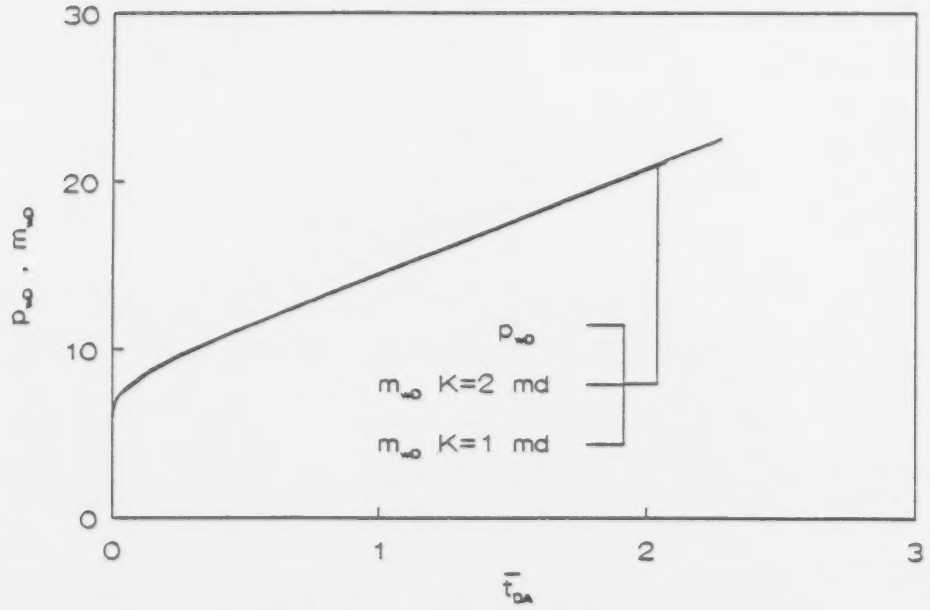

Figure 6.21 – Time-corrected permeability response for 4:1 Reservoir C.

correlated with the p_{wD} data.

6.4 EFFECT OF FLOWRATE

The data of Al-Hussainy et al.[11] included pseudosteady state drawdown results for q_D values of 0.05 and 0.10. The effects of flowrate on deviation of real gas m_{wD} from liquid p_{wD} was discussed by Wattenbarger[13]. Wattenbarger[13] stated that for different flowrates, the m_{wD} deviation from p_{wD} should be the same at equivalent values of $\overline{p}/\overline{z}$.

For rectangular reservoirs, the Reservoir A m_{wD} response has been evaluated for q_D=0.02, q_D=0.05 and q_D=0.10. The effects of flowrate on m_{wD} deviation from p_{wD} have been studied for 1:1, 2:1 and 4:1 reservoirs. Well positions at (0.50,0.50), (0.75,0.50) and (0.75,0.75) have been considered. The effects of changing flowrate have been discussed with respect to m_{wD} deviation and late-time Limit Test data.

Figure 6.22 illustrates the p_{wD} and m_{wD} response for a 4:1 Reservoir A wells with q_D=0.10. The m_{wD} curves for the three well locations all deviate from the p_{wD} solutions. During the late-time period, the amount of deviation is fairly similar for each well location. Therefore, the results are focussed on one well location, (0.50,0.50).

Figure 6.13 illustrates the same data for Reservoir B with q_D=0.05. For equivalent t_{DA} values, the deviation of Reservoir A of Figure 6.22 at q_D=0.10 is much greater than that of Figure 6.13. Table 6.10 lists the t_{DA} values for 1% deviation of m_{wD} from p_{wD} for each reservoir, flowrate and well location.

The p_{wD} and m_{wD} responses for Reservoir A with a well at (0.50,0.50) are shown in Figure 6.23. The effects of flowrate on m_{wD} deviation are clearly illustrated. For q_D=0.10, there is a significant deviation at t_{DA}=1. For q_D=0.02, there is only slight deviation at t_{DA}=1.

The deviation values for each flowrate presented in Figure 6.23 are plotted versus t_{DA} in Figure 6.24. As expected, the higher the flowrate, the greater the deviation when plotted in terms of t_{DA}. The maximum deviation for q_D of 0.10, 0.05 and 0.02 was 10%, 24% and 32%, respectively. For a 4:1 Reservoir A with well at (0.50,0.50), as listed in Table 6.10, the values of t_{DA} at 1% deviation for q_D of 0.10, 0.05 and 0.02 are 0.075, 0.15 and 0.35, respectively.

In Figure 6.25, the m_{wD} deviations are plotted versus $\overline{p}/\overline{z}$. Now, at equal values of $\overline{p}/\overline{z}$, or when equal volumes have been produced from the reservoir, the deviations are lower for the higher flowrates. This condition existed for all reservoir

TABLE 6.10 - t_{DA} values for 1% deviation of m_{wD} from p_{wD}.

p_i (psia)	ASPECT RATIO	WELL LOCATION	q_D=0.02	q_D=0.05	q_D=0.10
5,000	1:1	(0.50,0.50)	0.47	0.30	0.19
		(0.75,0.50)	0.42	0.20	0.10
		(0.75,0.75)	0.29	0.10	0.05
	2:1	(0.50,0.50)	0.47	0.28	0.11
		(0.75,0.50)	0.26	0.17	0.10
		(0.75,0.75)	0.20	0.12	0.03
	4:1	(0.50,0.50)	0.35	0.15	0.08
		(0.75,0.50)	0.25	0.14	0.07
		(0.75,0.75)	0.20	0.12	0.02
3,000	1:1	(0.50,0.50)	-	0.34	-
	2:1	(0.50,0.50)	-	0.34	-
	4:1	(0.50,0.50)	-	0.22	-
1,000	1:1	(0.50,0.50)	-	0.44	-
	2:1	(0.50,0.50)	-	0.44	-
	4:1	(0.50,0.50)	-	0.37	-

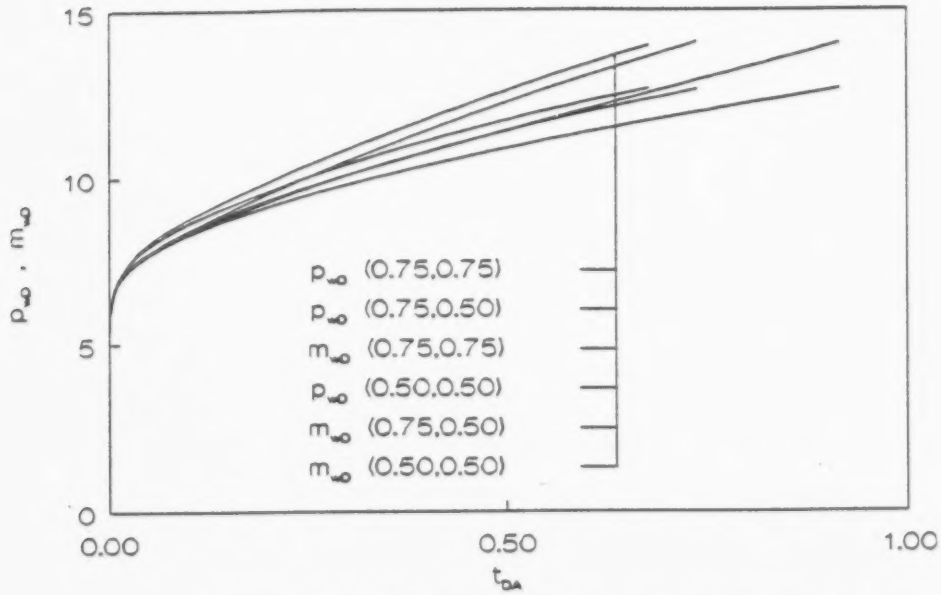

Figure 6.22 – Response for 4:1 Reservoir A q_D=0.10.

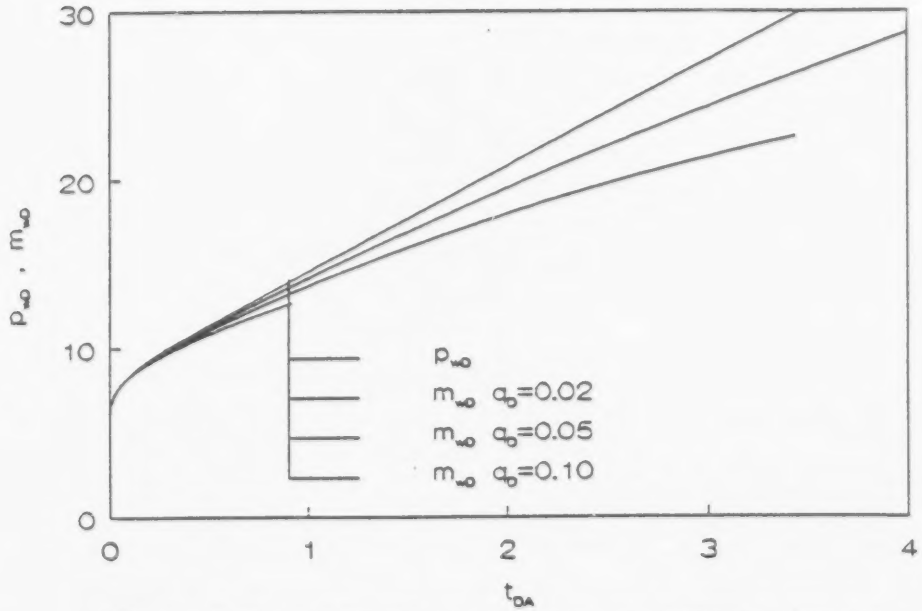

Figure 6.23 – Effects of flowrate on response for 4:1 Reservoir A with well at (0.50,0.50).

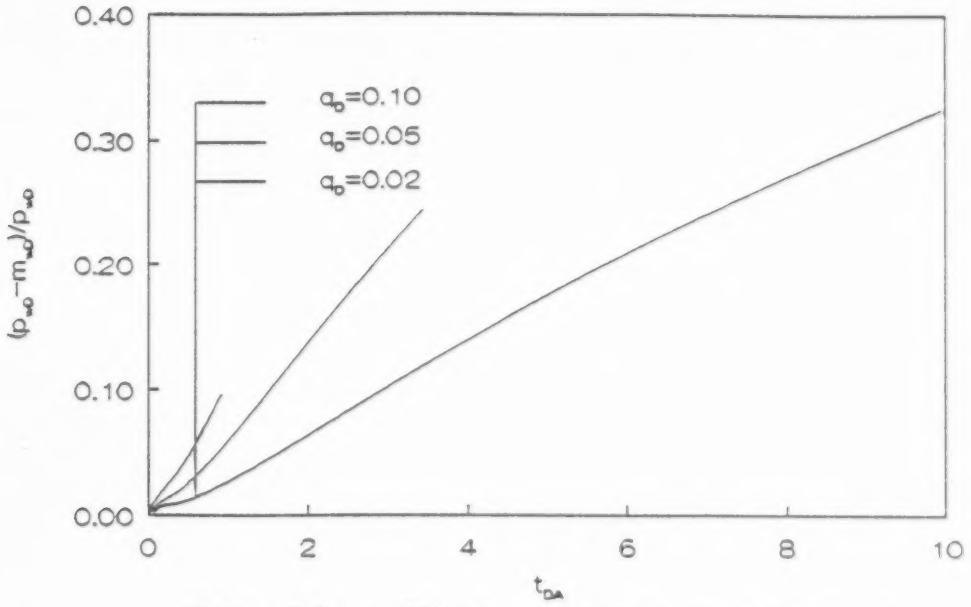

Figure 6.24 – Effects of flowrate on deviation for 4:1 Reservoir A with well at (0.50,0.50).

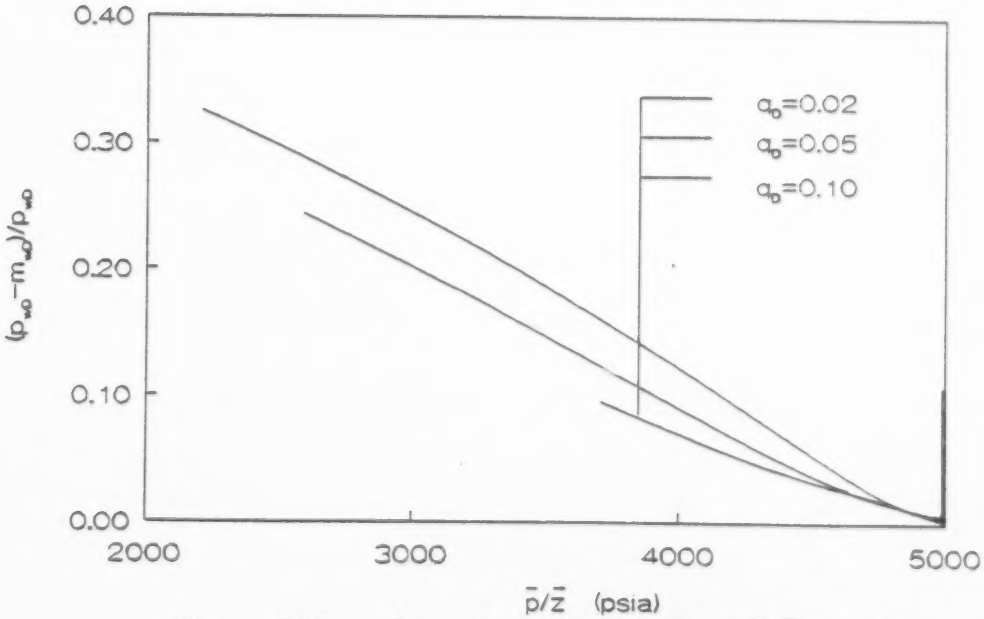

Figure 6.25 – Flowrate deviation versus $\bar{p}/\bar{z}$ for 4:1 Reservoir A with well at (0.50,0.50).

cases considered. The decrease in deviation for a higher flowrate can be a result of the reservoir pressure profile associated with the production rate. This observation is in contradiction to Wattenbarger's[13] statement of similar deviations of m_{wD} from p_{wD} responses at equivalent values of $\overline{p}/\overline{z}$ for different flowrates.

When production rate is high, there is a large pressure profile within the reservoir. The difference between the wellbore and boundary pressure is high compared to that difference for a lower flowrate. For two reservoirs starting at similar initial conditions with an equal produced volume, the average pressures are equal. However, the reservoir with the higher flowrate has a portion of reservoir space (close to the reservoir boundary) at pressures closer to initial conditions. Therefore, this reservoir will behave more similar to the liquid p_{wD} case with μ and c_g evaluated at initial conditions, as deviation does not occur until all points within the reservoir space are below p_i.

Summarizing, in terms of t_{DA}, the m_{wD} response for the higher flowrate case deviates earlier and at greater magnitude than was the case for the lower flowrates. However, in terms of $\overline{p}/\overline{z}$, m_{wD} deviation from p_{wD} is less for the higher flowrates.

The m_{wD} and p_{wD} responses for 1:1 Reservoir A with well at

(0.50,0.50) are plotted in Figure 6.26. A comparison of the m_{wD} deviation for the two Reservoir A aspect ratios (m_{wD} results are shown in Figure 6.23 and 6.26), is illustrated in Figure 6.27. When plotted versus t_{DA}, the deviations for the two situations corresponding to Figures 6.23 and 6.26 are close to one another for any given flowrate.

Figure 6.28 shows the data of Figure 6.27 plotted versus $\overline{p}/\overline{z}$. Again the higher flowrate produced the lower deviation. For each flowrate, the deviation data for the 4:1 reservoir with a well at (0.75,0.75) did not vary as much as that for the 2:1 reservoir with a well at (0.50,0.50). The skewed position of the (0.75,0.75) well position creates a further influence on the pressure profile within the reservoir. This influence diminishes the potential effects of the varying flowrate.

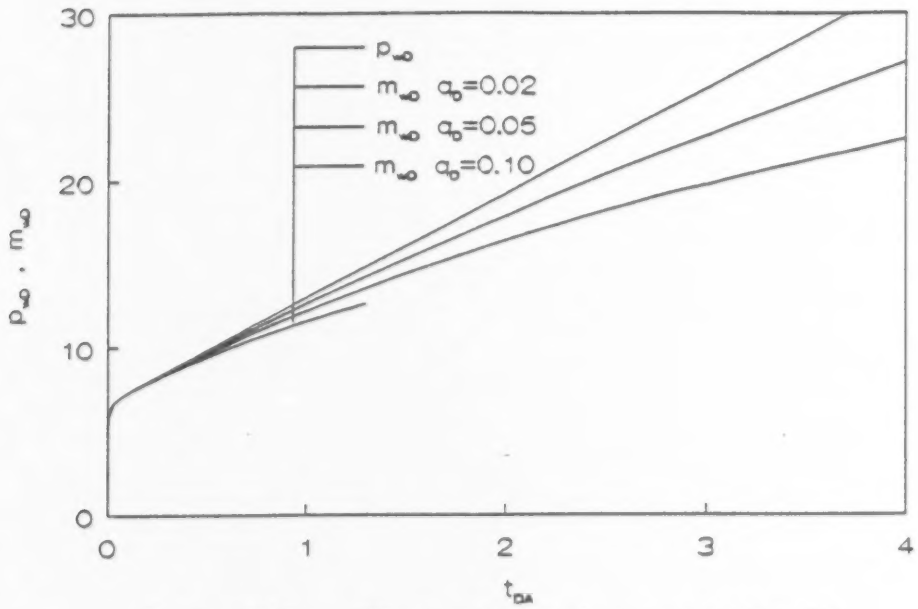

Figure 6.26 – Effect of flowrate on response for 1:1 Reservoir A with well at (0.50,0.50).

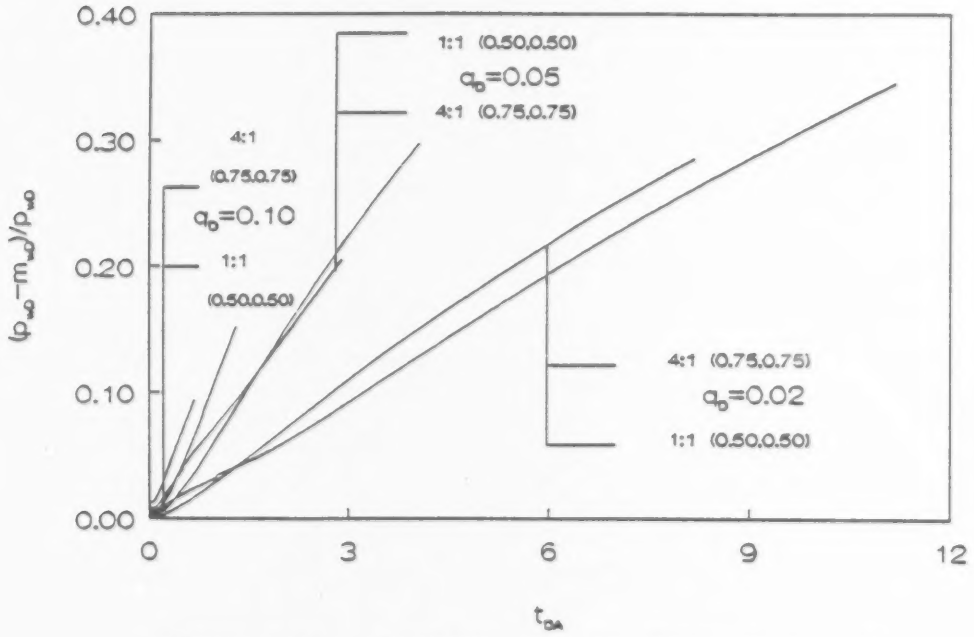

Figure 6.27 – Deviation data for Reservoir A wells.

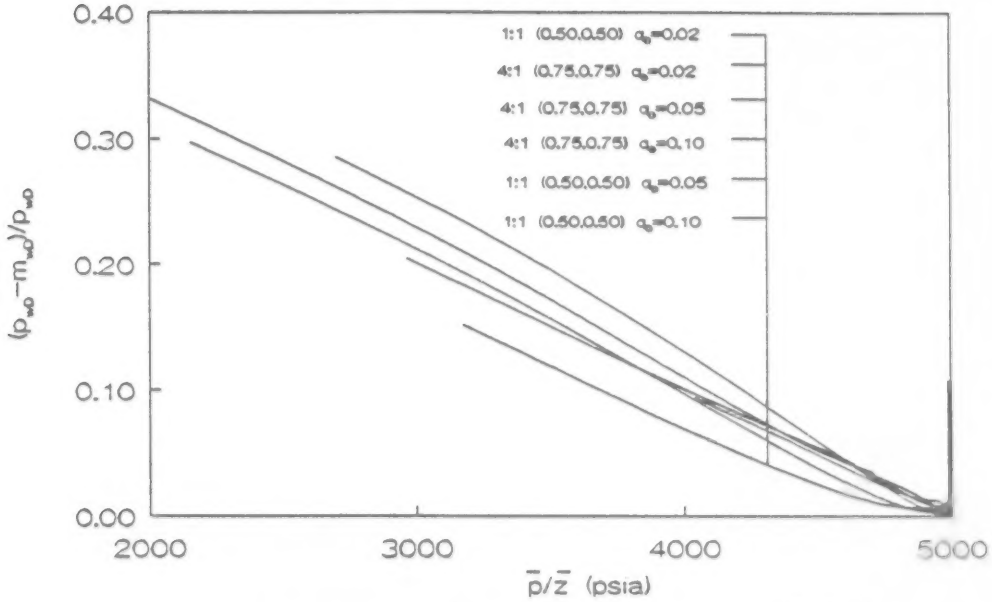

Figure 6.28 – Flowrate deviation versus $\bar{p}/\bar{z}$ for Reservoir A well locations.

6.5 LIMIT TEST ANALYSIS

The m_{wD} data for Limit Test analysis is affected by varying the flowrate. Also, as shown previously in Figure 6.8, the reservoir initial pressure affects Limit Test m_{wD} data. The effects of flowrate and initial pressure are considered for Limit Test Analysis. The method of time correction, as presented by Reynolds et al.[18], is applied and Limit Test slopes calculated. Results are compared and practical aspects of the method discussed.

Figure 6.29 illustrates m_{wD} and p_{wD} responses for 2:1 Reservoir A with a well at (0.50,0.50) and q_D=0.02. The data is plotted versus t_{DA}, meaning that the reservoir area is known. Reservoir area is not known for conditions of a Limit Test analysis. But the value of t_{DA} is proportional to real time and, therefore, any analysis of late-time Limit Test slopes versus t_{DA} is proportional to slopes calculated versus real time. For convenience, the method of analysis is restricted to plotting data versus t_{DA}.

The practical aspects of the analysis method require an estimate of the reservoir average pseudopressure. It is assumed that the reservoir $m(p_{avg})$ can be estimated within ±10%. Using the $m(p_{avg})$+10% and $m(p_{avg})$-10% reservoir pressures,

the value of the $\mu(p)c_g(p)$ product is calculated and averaged using Equation (3.27). The corresponding averaged t_{DA} is then calculated using Equation (3.28). The m_{wD} results are plotted versus $\overline{t_{DA}}$ and compared to the m_{wD} data plotted versus the uncorrected t_{DA}. Limit Test slopes are computed for the late-time uncorrected data.

For a 2:1 Reservoir A with well at (0.50,0.50), the m_{wD} and p_{wD} data are plotted versus tDA and $\overline{t_{DA}}$ in Figure 6.29, for q_D=0.02. The x-axis scale for t_{DA} and $\overline{t_{DA}}$ is the same. The time corrected m_{wD}, p_{wD} and $m_{wD}\pm10\%$ data are plotted versus $\overline{t_{DA}}$. The uncorrected m_{wD} data is plotted versus t_{DA}. The Limit Test slope is calculated from a linear regression of the latter segment of the uncorrected m_{wD} versus t_{DA} data. For this example, the average reservoir pressure has decreased to about 60% of initial pressure.

From Figure 6.29, the m_{wD} and $m_{wD}\pm10\%$ data correlated well with the p_{wD} data when plotted versus $\overline{t_{DA}}$. The Cartesian slopes of the $m_{wD}\pm10\%$ data are within 5% of the p_{wD} late-time slope. The data m_{wD}-10% is overcorrected and lies above the p_{wD} data. The Limit Test slope of the straight line through the latter data segment of m_{wD} versus t_{DA} is 2.45. This slope of 2.45 is 61% less than the p_{wD} versus t_{DA} slope of 6.283 (or 2π). As can be seen from Equation (26), the reservoir drainage volume is inversely proportional to the late-time drawdown slope.

Therefore, the result would be to calculate a drainage volume from the Limit Test data about 2.5 times the actual volume. If $m(p_{avg})$ can be estimated within 10%, the method of time correction can give adequate results for Limit Test analysis. Table 6.11 lists the Limit Test slope error when compared to the Limit Test slope of 6.283 for p_{wD} versus t_{DA} data.

TABLE 6.11 - Analysis results for limit test data for 2:1 Reservoir with well at (0.50,0.50).

p_i psia	q_D	% DECREASE IN RESERVOIR PRESSURE	LIMIT TEST SLOPE ERRORS (%) - m_{wD} VERSUS p_{wD} [Limit Test Slope Errors of m_{wD} data versus p_{wD} for specified dimensionless time]			
			$\overline{t_{DA}}$	$\overline{t_{DA_{m(p_{avg})-10\%}}}$	$\overline{t_{DA_{m(p_{avg})+10\%}}}$	t_{DA}
5,000	0.02	60	-0.3	-4.9	3.7	61
	0.05	50	-0.2	-4.9	4.0	58
	0.10	35	1.1	-4.9	5.1	43
	0.05	25	-0.7	-4.0	5.9	29
3,000	0.05	50	-0.6	-4.7	3.0	46
1,000	0.05	50	-1.5	-5.8	2.1	40

Figure 6.30 results are for Reservoir A with a well at (0.50,0.50) and q_D=0.05. Again, there is improvement using the time correction method for m_{wD}±10% and the slopes are within 5% of the p_{wD} late-time slope. Figure 6.30 can be compared directly to Figure 6.31. Figure 6.31 results are for Reservoir C with a well at (0.50,0.50) and q_D=0.05. The average reservoir pressure has decreased to about 50% of the initial pressure for both Figures 6.30 and 6.31. As listed in Table 6.11, the errors for the m_{wD} versus t_{DA} late-time data for Figures 6.30 and 6.31 are 58% and 42%, respectively. The error for the lower initial pressure (Reservoir C) is less than the error for the higher initial pressure (Reservoir A). This was previously indicated in Figure 6.8.

Figure 6.32 results are for Reservoir A with a well at (0.50,0.50) and q_D=0.05. For this example, the average reservoir pressure has decreased to about 25% of initial pressure. As listed in Table 6.11, the Limit Test slope error for m_{wD} versus t_{DA} late-time data is 29%. From a comparison of columns 3 and 7 of Table 6.11, the Limit Test slope error can be approximated by assuming the error to be equal to the decrease in reservoir average pressure.

Using the method of time correction, as proposed by Reynolds et al.[18], with a reasonable estimate of reservoir average pressure (±10%), the corrected Limit Test slope was within an

acceptable range (±5%) to accurately predict drainage volume.

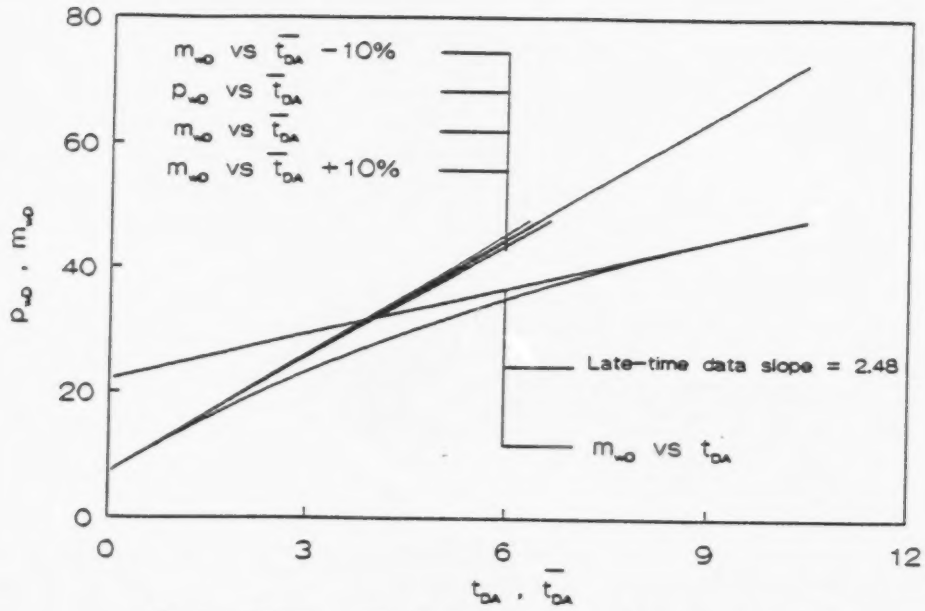

Figure 6.29 – Response for 2:1 Reservoir A with well at (0.50,0.50), q_D=0.02.

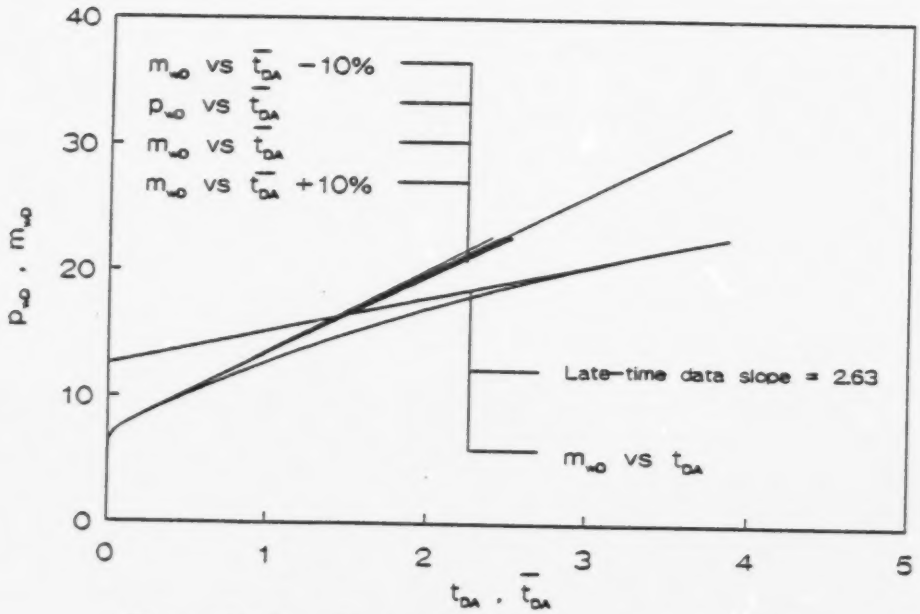

Figure 6.30 – Response for 2:1 Reservoir A with well at (0.50,0.50), q_D=0.05.

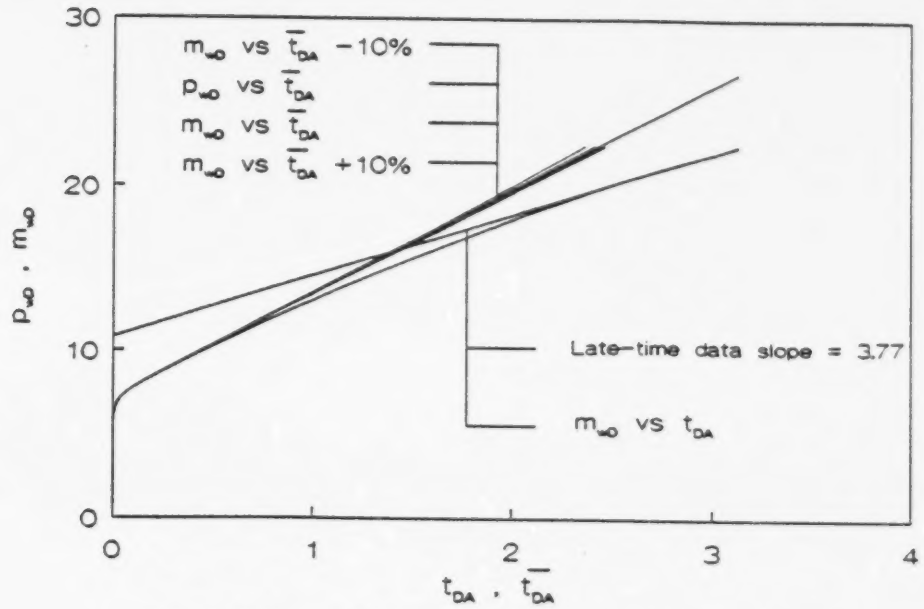

Figure 6.31 – Response for 2:1 Reservoir C with well at (0.50,0.50), q_D=0.05.

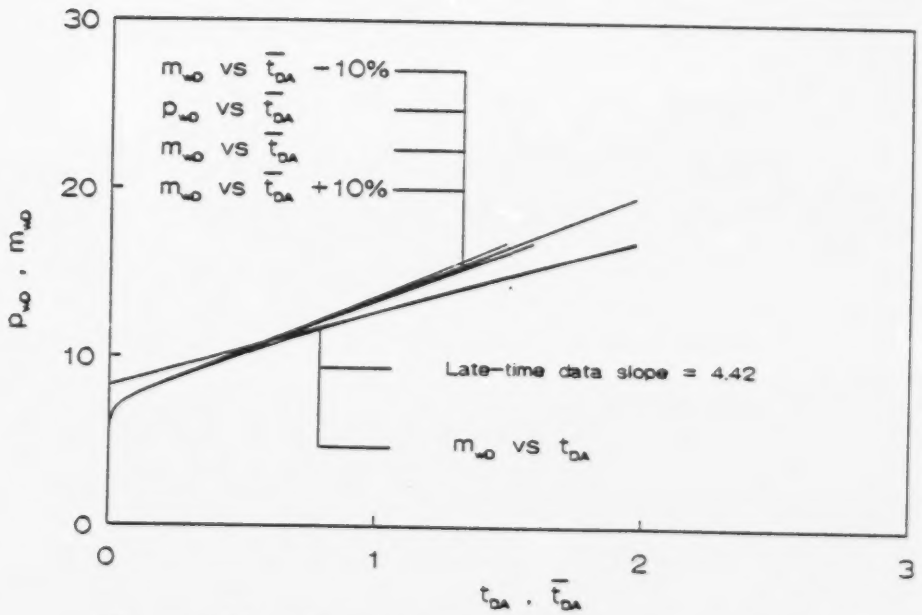

Figure 6.32 – Response for 2:1 Reservoir A with well at (0.50,0.50), q_D=0.05 and 25% depleted.

7. CONCLUSIONS AND RECOMMENDATIONS

The following conclusions have resulted from this study:

1. The m_{wD} response for a gas reservoir is affected by the initial reservoir conditions. The m_{wD} response is a function of the pressure dependent gas viscosity compressibility product variation with average reservoir pressure. For higher reservoir pressures, the $\mu(p)c_g(p)$ product has a greater range. The deviation of $\mu(p)c_g(p)$ from initial conditions is greater at higher pressures. The result is a greater deviation of m_{wD} from p_{wD}.

2. The time correction of Reynolds et al.[18] using the average $\mu(p)c_g(p)$ values enabled the computation of a proper dimensionless time for modifying the m_{wD} data to correspond to the p_{wD} data. The time correction was appropriate for the square and rectangular reservoir shapes used.

3. The numerical simulation gridding affected the late-time gas well data. More accurate time-corrected solutions were obtained when consistent block sizes were used throughout the grid.

4. The effect of changing reservoir well locations and aspect ratios was not as significant to the m_{wD} response as the effect of changing initial conditions. For similar reservoir initial conditions, the deviation of m_{wD} from p_{wD} was comparable for each well location and aspect ratio.

5. For reservoirs at similar initial conditions, there was little change in the m_{wD} response for variations of gas contaminants, temperature, and permeability.

6. The m_{wD} response is dependent on the flowrate. The higher the flowrate, the lower the m_{wD} deviation from p_{wD} when plotted versus reservoir average pressure. This conclusion is in contradiction to the findings of Wattenbarger[13], although the previous works of Wattenbarger[13] and Reynolds et al.[18] had not considered the late-time results to the degree considered in this study.

7. The time corrected Limit Test data analysis method, with a reasonable estimation of average reservoir pressure, can provide more accurate results than that of uncorrected data. Using uncorrected m_{wD} data, the Limit Test analysis slope can result in serious error when estimating the drainage volume.

The following recommendations are made for future

investigations:

1. Further work can be done to analyze the m_{wD} response for various flowrates. Correlations can be attempted to quantify m_{wD} deviation from p_{wD} when considering reservoir initial conditions, flowrate and depletion.

2. The work considered for this study was for closed square or rectangular reservoirs. The late-time m_{wD} data can be extended to evaluate the steady-state response of combinations of closed and constant-pressure outer boundaries.

3. The drawdown m_{wD} response can be combined with the buildup m_{wD} response. The drawdown and buildup data can be evaluated for a complete well test analysis.

8. REFERENCES

1. Jones, P.: "Reservoir Limit Test," *Oil and Gas Journal* (June 18, 1956) 184-196.
2. Bruce, G.H., Peaceman, D.W., Rachford, H.H., Jr., and Rice, J.D.: "Calculations of Unsteady-State Gas Flow Through Porous Media," *Trans.*, AIME (1953) **198**, 79.
3. Aronofsky, J.S., and Jenkins, R.: "A Simplified Analysis of Unsteady Radial Gas Flow," *Trans.*, AIME (1954) **201**, 149.
4. van Everdingen, A.F., and Hurst, W.: "The Application of the Laplace Transformation to Flow Problems in Reservoirs,"*Trans.*,AIME (1949) **186**, 305.
5. Jones, L.G.: "An Approximate Method for Computing Nonsteady-State Flow of Gases in Porous Media," *Society of Petroleum Engineers Journal* (Dec. 1961) 264-276.
6. Jones, P.: "Reservoir Limit Test on Gas Wells," *Journal of Petroleum Technology* (May 1962) 613-619.
7. Carter, R.D.: "Solutions of Unsteady-State Radial Gas Flow,"*Journal of Petroleum Technology* (May 1962) 549-554.
8. Jones, L.G.: "Reservoir Reserve Tests," *Journal of Petroleum Technology* (March 1963) 333-337.
9. Root, P.J., Warren, J.E., and Hartsock, J.H.: "Implications of Transient Flow Theory: The Estimations of

Gas Reserves," *API Drilling and Production Practises* (1964) 141-156.

10. Eilerts, C.K., Sumner, E.F., and Potts, N.L.: "Integration of Partial Differential Equation for Transient Radial Flow of Gas-Condensate Fluids in Porous Structures," *Society of Petroleum Engineers Journal* (June 1965) 141-152.
11. Al-Hussainy, R., Ramey, H.J., Jr., and Crawford, P.B.: "The Flow of Real Gases Through Porous Media," *Journal of Petroleum Technology (May 1966) 624-636.*
12. *Al-Hussainy, R., and Ramey, H.J., Jr.: "Application of Real Gas Flow Theory to Well Testing and Deliverability Forecasting,"Journal of Petroleum Technology* (May 1966) 637-642.
13. Wattenbarger, R.A.: "Effects of Turbulence, Wellbore Damage, Wellbore Storage, and Vertical Fractures on Gas Well Testing,"Ph. D. Thesis, Stanford University, Stanford, California (1967).
14. Zana, E.T., and Thomas, G.W.: "Some Effects of Contaminants on Real Gas Flow," *Journal of Petroleum Technology* (Sept. 1970) 1157-1168.
15. Earlougher, R.C., Jr.: "Estimating Drainage Shapes from Reservoir Limits Tests," *Journal of Petroleum Technology* (Oct. 1971) 1266-1268.
16. Aziz, K., Mattar, L., Ko, S., and Brar, G.S.: "Use of Pressure, Pressure-Squared or Pseudo-Pressure in the Analysis of Transient Pressure Drawdown Data from Gas

Wells," *Journal of Canadian Petroleum Technology* (April-June 1976) 58-65.

17. Earlougher, R.C., Jr.: *Advances in Well Test Analysis*, Monograph 5, SPE of AIME, Dallas, Texas (1977) 203.
18. Reynolds, R.C., Bratvold, R.B., and Ding, W.: "Semilog Analysis of Gas Well Drawdown and Buildup Data," *SPE Formation Evaluation* (Dec. 1987) 657-670.
19. Peaceman, D.W.: "Interpretation of Well-Block Pressures in Numerical Reservoir Simulation," *Society of Petroleum Engineers Journal* (June 1978) 183-194.
20. "SPARSPAK: Waterloo Sparse Linear Equations Package," Department of Computer Science, University of Waterloo, Waterloo, Ontario, Canada.

APPENDIX A

PROGRAM 1 - Numerical Real Gas Simulator

PROGRAM 2 - Analytical Liquid Simulator

```
C          PROGRAM 1 - NUMERICAL REAL GAS SIMULATOR
C
C        PROGRAM GSRECT
C
C        DECLARATION
C
         IMPLICIT REAL*8 (A-H,O-Z)
         PARAMETER (MAX=100,MAXMAX=10000,MAXTAB=200,
     A              TOLEMB=1.D-3,TOLEPP=1.D-5,DELPMX=2.D2,
     B              C1=5.1169126531327D11,
     C              C2=8.0857805766753D13,
     D              C3=1.9405873384021D15,
     E              PSC=14.7D0, TSC=519.7D0,
     F              TEMRAK=459.7D0 )
         DIMENSION TABP(0:MAXTAB),TABMP(0:MAXTAB),S(6*MAXMAX),
     A             IR(5),VISCGN(MAXMAX),
     B             VISCGO(MAXMAX),PPRESO(MAXMAX),
     B             PPRESI(MAXMAX),
     C             PPRESN(MAXMAX),ACOEF(MAXMAX,5),
     D             XG(MAX),YG(MAX),DX(MAX),DY(MAX),
     E             VALUES(5),BVEC(MAXMAX),TEMPO(4)
         LOGICAL FTDEL,FBUP
         CHARACTER*8 OUTFIL
         COMMON /SPKUSR/MSGLVL,IERR,MAXS,NEQNS
C
C
C        INITIALIZING
C
C        CALL SUBROUTINE FOR READING INPUT FILES
C
         CALL INPUT(PC,TC,PERM,PINIT,TEM,RW,POROS,TEMPO,
     A        PDEL,OUTFIL,MAXX,MAXY,IWELL,JWELL,XG,YG,
     B        FBUP,TFDD,TSLD,TCONS,TSI,TFBU,TSLB,QINPT)
         SPG=TEMPO(1)
C
C        CONVERSION TO MOLE PERCENT
                NTDEL=1
C
         CNCN2=TEMPO(2)*1.D2
         CNCH2S=TEMPO(3)*1.D2
         CNCCO2=TEMPO(4)*1.D2
         LWELL=(IWELL-1)*MAXY+JWELL
         FTDEL=.FALSE.
C
C        CALCULATE P,M(P) TABLE (ARRAYS TABP & TABMP)
         PRSMAX=PINIT+4.D0*PDEL
         CALL PSUDOP(PRSMAX,PDEL,TEM,SPG,TC,PC,CNCH2S,CNCCO2,
     A   CNCN2,TABP,TABMP,NSTEP)
C
C        DETERMINE M(P) INITIAL & CALCULATE VIS*COM @ P INITIAL
C
C         OUTPUT FILE FOR M(PAVG) DATA
C
          OPEN(UNIT=13,FILE='AVDAT')
          WRITE(13,*)TEMRAK,TEM,TC,PINIT,PC,PRSMAX,PDEL,SPG,
     A               CNCN2,CNCH2S,CNCCO2
C
         CALL TABSEQ(PINIT,TABP,TABMP,NSTEP,PP)
         CALL VISCY((TEM+TEMRAK)/TC,PINIT/PC,SPG,TEM,CNCH2S,
     A   CNCCO2,CNCN2,VISGR,VISG,JERR)
```

```
      CALL ZANDC(TEM,TC,PINIT,PC,CNCH2S,CNCCO2,ZED,CMPG,JERR)
      DO 20 I=1,MAXX*MAXY
         PPRESN(I)=PP
         PPRESI(I)=PP
         PPRESO(I)=PP
         VISCGO(I)=VISG*CMPG
         VISCGN(I)=VISCGO(I)
        VISCGIN=VISG*CMPG
        VISIN=VISG
        CGIN=CMPG
        ZIN=ZED
        PPRESIN=PP
20    CONTINUE
C
C     CALCULATE DX AND DY FOR BLOCK SIZING
C
      XCUM=0.D0
      DO 22 I=1,MAXX
          DX(I)=2.D0*(XG(I)-XCUM)
          XCUM=XCUM+DX(I)
22    CONTINUE
      YCUM=0.D0
      DO 24 J=1,MAXY
          DY(J)=2.D0*(YG(J)-YCUM)
          YCUM=YCUM+DY(J)
24    CONTINUE
      SUMINT=PINIT/ZED
      SUMOLD=SUMINT
C
C     INITIALIZE SPARSPAK
C
      CALL SPRSPK
      MAXS=6*MAXMAX
C     MSGLVL=0
C
C     SAVE STRUCTURE OF MATRIX A
C
      CALL IJBEGN
C
C     GIVING LOCATION OF NON-ZERO ELEMENTS
C     MATRIX A OBTAINED BY SCROLLING THROUGH ALL RESERVOIR
C     GRID BLOCKS. FIXING I AND FIRST VARING J.
C
      DO 10 I=1,MAXX
         DO 15 J=1,MAXY
            NORD=(I-1)*MAXY+J
            NIR=1
            IR(NIR)=NORD
            IF(I.GT.1) THEN
               NIR=NIR+1
               IR(NIR)=NORD-MAXY
            ENDIF
            IF(I.LT.MAXX) THEN
               NIR=NIR+1
               IR(NIR)=NORD+MAXY
            ENDIF
            IF(J.GT.1) THEN
               NIR=NIR+1
               IR(NIR)=NORD-1
            ENDIF
```

```
                IF(J.LT.MAXY) THEN
                   NIR=NIR+1
                   IR(NIR)=NORD+1
                ENDIF
                CALL INROW(NORD,NIR,IR,S)
15           CONTINUE
10        CONTINUE
C
C         FINISH GIVING LOCATION OF NON-ZEROS
C
          CALL IJEND(S)
C
C         GIVE ORDERING FOR A
          CALL ORDRA4(S)
C
C         CONSTRUCTION OF MATRIX ACOEFF(MAXX*MAXY,5)
C
          DO 100 I=1,MAXX
             DO 110 J=1,MAXY
               NORD=(I-1)*MAXY+J
               IF(I.NE.1.AND.I.NE.MAXX) THEN
                  CDELX=XG(I+1)-XG(I)
                  SDELX=XG(I)-XG(I-1)
                  ACOEF(NORD,1)=1.0D0/(SDELX*(SDELX+CDELX))
                  ACOEF(NORD,3)=-1.0D0/(SDELX*CDELX)
                  ACOEF(NORD,5)=1.0D0/(CDELX*(SDELX+CDELX))
               ELSE
                  IF(I.EQ.1) THEN
                     CDELX=XG(I+1)-XG(I)
                     ACOEF(NORD,1)=0.0D0
                     ACOEF(NORD,3)=-0.5D0/(CDELX*CDELX)
                     ACOEF(NORD,5)=0.5D0/(CDELX*CDELX)
                  ELSE
C       I=MAXX
                     SDELX=XG(I)-XG(I-1)
                     ACOEF(NORD,1)=0.5D0/(SDELX*SDELX)
                     ACOEF(NORD,3)=-0.5D0/(SDELX*SDELX)
                     ACOEF(NORD,5)=0.0D0
                  ENDIF
               ENDIF
               IF(J.NE.1.AND.J.NE.MAXY) THEN
                 CDELY=YG(J+1)-YG(J)
                 SDELY=YG(J)-YG(J-1)
                 ACOEF(NORD,2)=1.0D0/(SDELY*(SDELY+CDELY))
                 ACOEF(NORD,3)=ACOEF(NORD,3)-1.0D0/(SDELY*CDELY)
                 ACOEF(NORD,4)=1.0D0/(CDELY*(SDELY+CDELY))
               ELSE
                 IF(J.EQ.1) THEN
                  CDELY=YG(J+1)-YG(J)
                  ACOEF(NORD,2)=0.0D0
                  ACOEF(NORD,3)=ACOEF(NORD,3)-0.5D0/(CDELY*CDELY)
                  ACOEF(NORD,4)=0.5D0/(CDELY*CDELY)
                 ELSE
C       J=MAXY
                  SDELY=YG(J)-YG(J-1)
                  ACOEF(NORD,2)=0.5D0/(SDELY*SDELY)
                  ACOEF(NORD,3)=ACOEF(NORD,3)-0.5D0/(SDELY*SDELY)
                  ACOEF(NORD,4)=0.0D0
                 ENDIF
               ENDIF
```

```
            DO 120 K=1,5
              ACOEF(NORD,K)=ACOEF(NORD,K)*C1/C3
120         CONTINUE
110       CONTINUE
100     CONTINUE
C       WRITE(6,*)'ACOEF CREATED'
C
C       CALCULATE Q (Q IS INPUT AS MSCF/D)
C
        CALL ZANDC(TSC,TC,PSC,PC,CNCH2S,CNCCO2,ZED,CMPG,
     A             JERR)
C       WRITE(6,*)'ABOUT TO CALCULATE QSOR'
        QSOR=(-QINPT)*1.D3*(TEM+TEMRAK)/PERM/ZED*C2/C3*
     A       PSC/TSC/(DX(IWELL)*DY(JWELL))
C
C       CALCULATE QSOR TO BE USED IN MB. CHECK
C
        QSORMB=(-QINPT)*1.D3*(TEM+TEMRAK)*PSC/ZED/TSC/24.D0
C       WRITE(6,*)'QSOR & QSORMB CALCULATED'
C
C       OPEN THE OUTPUT FILE AS UNIT 9,10,11
C
        OPEN(UNIT=9,FILE='R.'//OUTFIL,STATUS='NEW')
        OPEN(UNIT=10,FILE='A.'//OUTFIL,STATUS='NEW')
        OPEN(UNIT=11,FILE='M.'//OUTFIL,STATUS='NEW')
        OPEN(UNIT=12,FILE='T.'//OUTFIL,STATUS='NEW')
        OPEN(UNIT=13,FILE='P.'//OUTFIL,STATUS='NEW')
C
C       DETERMINATION OF delT & EXIT TIME
C
        TEXIT=TSI
        TCUM=0.D0
        TDEL=TFDD
        TSLE=TSLD
        GOTO 500
C
C       REENTRY POINT FOR SUBSEQUENT CALCULATIONS
C
600     IF(FTDEL) THEN
           TCUM=TCUM-TDEL
        ENDIF
        IF(TCUM.EQ.TEXIT) THEN
            IF( .NOT.FBUP) THEN
                WRITE(12,*)NTDEL
               STOP
            ELSE
               FBUP=.FALSE.
               TEXIT=TSLB
               TSLE=TSLB
               TDEL=TFBU
               TCUM=0.0D0
               QSOR=0.0D0
               GOTO 500
            ENDIF
        ENDIF
        IF(TCUM.LT.TSLE) THEN
            IPOWR=INT(DLOG10(TCUM))
            IF(IPOWR.LT.0) THEN
               IPOWR=IPOWR-1
            ELSE
```

```
                IF(IPOWR.EQ.0) THEN
                     IF(DLOG10(TCUM).LT.0.D0) THEN
                         IPOWR=-1
                     ELSE
                         IPOWR=0
                     ENDIF
                 ENDIF
               ENDIF
                 TDEL=0.5*((10.0D0)**IPOWR)
                 IF((TCUM+1.2*TDEL).GE.TSLE) THEN
                    TDEL=TSLE-TCUM
                 ENDIF
            ELSE
              TDEL=TCONS
              IF((TCUM+1.2*TDEL).GE.TEXIT) THEN
                 TDEL=TEXIT-TCUM
              ENDIF
            ENDIF
            IF (FTDEL) THEN
            TDEL=TDELS
               TCONS=TDELS
            ENDIF
500         TCUM=TCUM+TDEL
C
C           AFTER CONVERGENCE REPLACE VARIABLES AT OLD TIME
C           LEVEL WITH NEW TIME LEVEL IF FTDEL REMAINS FALSE
C           OTHERWISE DO BACK TRACKING BY SKIPPING THIS STEP
C           AND REASSIGN OLD VARIABLES TO NEW ONES
C
            IF(.NOT.FTDEL) THEN
               DO 30 I=1,MAXX*MAXY
                 PPRESO(I)=PPRESN(I)
                 PPRESI(I)=PPRESN(I)
                 VISCGO(I)=VISCGN(I)
30             CONTINUE
            ELSE
               FTDEL=.FALSE.
               DO 35 I=1,MAXX*MAXY
                 PPRESI(I)=PPRESO(I)
                 VISCGN(I)=VISCGO(I)
35             CONTINUE
            ENDIF
C
C           GIVE VALUES FOR MATRIX A & B
C
300         DO 40 I=1,MAXX
             DO 50 J=1,MAXY
               NORD=(I-1)*MAXY+J
               NIR=1
               IR(NIR)=NORD
               VALUES(NIR)=ACOEF(NORD,3)-POROS/PERM/TDEL*
     A                     (VISCGO(NORD)+VISCGN(NORD))/4.D0
               IF(I.GT.1) THEN
                 NIR=NIR+1
                 IR(NIR)=NORD-MAXY
                 VALUES(NIR)=ACOEF(NORD,1)
               ENDIF
               IF(I.LT.MAXX) THEN
                 NIR=NIR+1
                 IR(NIR)=NORD+MAXY
```

```
                VALUES(NIR)=ACOEF(NORD,5)
              ENDIF
              IF(J.GT.1) THEN
                NIR=NIR+1
                IR(NIR)=NORD-1
                VALUES(NIR)=ACOEF(NORD,2)
              ENDIF
              IF(J.LT.MAXY) THEN
                NIR=NIR+1
                IR(NIR)=NORD+1
                VALUES(NIR)=ACOEF(NORD,4)
              ENDIF
              CALL INROW4 (NORD,NIR,IR,VALUES,S)
50          CONTINUE
40          CONTINUE
C
C
C           FOR VECTOR B
C
            DO 60 I=1,MAXX*MAXY
              BVEC(I)=-POROS/PERM/TDEL/4.0D0*(VISCGO(I)+VISCGN(I))
     A                *PPRESO(I)
60          CONTINUE
            BVEC(LWELL)=BVEC(LWELL)-QSOR
            CALL INRHS(BVEC,S)
C
C           SOLVE FOR THE SOLUTION MATRIX
C
            CALL SOLVE4 (S)
C           CALL PSTATS
C
            DO 65 I=1,MAXX*MAXY
                PPRESN(I)=S(I)
                  PPRESNI=PPRESN(I)
               IF (I.EQ.LWELL) THEN
                 XLRWRAT=RW/0.2/DX(IWELL)
                  PPWFN=PPRESN(I)+((1.423D3*QINPT*(TEM+TEMRAK)/PERM)
     A           *DLOG(XLRWRAT))
                    PPDIM=PERM*(PPRESIN-PPWFN)/(1.423D3*QINPT*(TEM
     A                +TEMRAK))
                    TDIMA=2.637D-4*PERM*TCUM/(POROS*VISCGIN*XCUM*
     A            YCUM)
                      ARWRAT=(XCUM*YCUM)**.5/RW
C                  WRITE(6,*)I,PPRESN(I),PPWFN,PPDIM,TDIMA,ARWRAT
               ENDIF
65          CONTINUE
              OPEN(UNIT=14,FILE='PPSWB')
              WRITE(14,*)PERM,QINPT,XLRWRAT
C
C           TEST OF CONVERGENCE
C
C           MATERIAL BALANCE CHECK WILL BE PERFORMED
C           ON DRAWDOWN CALCULATION ONLY.
C
            ERRMAX=0.D0
            DO 62 I=1,MAXX*MAXY
                 DMP=DABS((PPRESN(I)-PPRESI(I))/PPRESN(I))
                 IF (DMP.GT.ERRMAX) THEN
                    ERRMAX=DMP
                 ENDIF
```

```
62      CONTINUE
        IF (ERRMAX.LT.TOLEPP)
     A  THEN
C
C       CHECK IF delPmax IS EXCEEDED
C
200     CALL TABSEQ(PPRESO(LWELL),TABMP,TABP,NSTEP,PO)
        CALL TABSEQ(PPRESN(LWELL),TABMP,TABP,NSTEP,PN)
        IF(DABS(PN-PO).GT.DELPMX) THEN
            FTDEL=.TRUE.
            TDELS=TDEL*DELPMX/1.5D0/DABS(PN-PO)
        ELSE
              RESMAX=0.D0
              RESINT=0.D0
              DO 42 I=1,MAXX
              DO 52 J=1,MAXY
               NORD=(I-1)*MAXY+J
               SMLHS=(ACOEF(NORD,3)-POROS/PERM/TDEL*
     A                (VISCGO(NORD)+VISCGN(NORD))/4.D0)
     B                 *PPRESN(NORD)
               IF(I.GT.1) THEN
               SMLHS=ACOEF(NORD,1)*PPRESN(NORD-MAXY)+SMLHS
               ENDIF
               IF(I.LT.MAXX) THEN
               SMLHS=ACOEF(NORD,5)*PPRESN(NORD+MAXY)+SMLHS
               ENDIF
               IF(J.GT.1) THEN
               SMLHS=ACOEF(NORD,2)*PPRESN(NORD-1)+SMLHS
               ENDIF
               IF(J.LT.MAXY) THEN
               SMLHS=ACOEF(NORD,4)*PPRESN(NORD+1)+SMLHS
               ENDIF
               RESINT=DABS((SMLHS-BVEC(NORD))/BVEC(NORD))
               IF (RESINT.GT.RESMAX) THEN
                   RESMAX=RESINT
                   IRESMX=I
                   JRESMX=J
               ENDIF
52            CONTINUE
42            CONTINUE
             IF(QSOR.NE.0.0D0) THEN
                SUM=0.0D0
                SUMP=0.D0
                SUMPZ=0.D0
                DO 70 I=1,MAXX
                    DO 72 J=1,MAXY
                      NORD=(I-1)*MAXY+J
                      SUM=SUM+(VISCGN(NORD)+VISCGO(NORD))*
     A                     (PPRESN(NORD)-PPRESO(NORD))*
     B                      DX(I)*DY(J)
                 CALL TABSEQ(PPRESN(NORD),TABMP,TABP,NSTEP,P)
               CALL ZANDC(TEM,TC,P,PC,CNCH2S,CNCCO2,ZED,CMPG,JERR)
                 SUMP=P*DX(I)*DY(J)+SUMP
                 SUMPZ=P/ZED*DX(I)*DY(J)+SUMPZ
72                  CONTINUE
70              CONTINUE
                SUM=SUM*POROS/4.0D0/TDEL
                SUMP=SUMP/XCUM/YCUM
                SUMPZ=SUMPZ/XCUM/YCUM
                CALL ZANDC(TEM,TC,SUMP,PC,CNCH2S,CNCCO2,ZED,CMPG,
```

```
     A                JERR)
                SUMP=SUMP/ZED
                EMBL=TSC*POROS/PSC/(TEM+TEMRAK)*(SUMPZ-SUMOLD)
     A               /QSORMB/TDEL
                EMBG=TSC*POROS/PSC/(TEM+TEMRAK)*(SUMPZ-SUMINT)
     A               /QSORMB/TCUM
                SUMOLD=SUMPZ
                 IF(TCUM.EQ.TDEL) THEN
                     WRITE(10,*)'TCUM,(P/Z)B,PB/ZB,MBG,MGL'
                     WRITE(10,*)TCUM-TDEL,SUMINT,SUMINT,
     A                           EMBG-EMBG,EMBL-EMBL
                     WRITE(10,*)TCUM,SUMPZ,SUMP,EMBG,EMBL
                 ELSE
                     WRITE(10,*)TCUM,SUMPZ,SUMP,EMBG,EMBL
                 ENDIF
               ENDIF
            OGIP=POROS*XCUM*YCUM*PINIT*TSC/PSC/(TEM+TEMRAK)/ZIN/1000.0D0
            ZATOL=0.0001
            GPRO=QINPT*TCUM/24.0D0
            SUMPZA=SUMINT*(1-GPRO/OGIP)
            PAVGO=SUMPZA
            ZAVGO=1.0
91          CALL ZANDC(TEM,TC,PAVGO,PC,CNCH2S,CNCCO2,ZAVG,CMPGA,JERR)
            ZACH=ABS(ZAVGO-ZAVG)
            IF(ZACH.LE.ZATOL) THEN
            GOTO 90
            ELSE
            PAVGO=SUMPZA*ZAVG
            ZAVGO=ZAVG
            GOTO 91
            ENDIF
90          CONTINUE
            PAVG=SUMPZA*ZAVG
            CALL TABSEQ(PAVG,TABP,TABMP,NSTEP,PPAVG)
            CALL VISCY((TEM+TEMRAK)/TC,PAVG/PC,SPG,TEM,CNCH2S,CNCCO2
     A,CNCN2,VISGRA,VISGA,JERR)
                  IF (TCUM.EQ.TDEL) THEN
               WRITE(9,*)XCUM,YCUM
               WRITE(9,*)XG(IWELL),YG(JWELL)
               WRITE(9,*)SPG,CNCN2,CNCH2S,CNCCO2
               WRITE(9,*)PC
               WRITE(9,*)TC
               WRITE(9,*)VISIN
               WRITE(9,*)CGIN
               WRITE(9,*)ZIN
               WRITE(9,*)PERM
               WRITE(9,*)QINPT
               WRITE(9,*)TEM
               WRITE(9,*)POROS
               WRITE(9,*)RW
                     WRITE(9,*)'TCUM,TDEL,M(P),M(Pwf),P,RES,I,J'
                     WRITE(9,*)TCUM-TDEL,TDEL-TDEL,PPRESO(LWELL),
     A                          PPRESO(LWELL),PO,RESMAX-RESMAX,
     B                          IRESMX-IRESMX,JRESMX-JRESMX
                     WRITE(9,*)TCUM,TDEL,PPRESN(LWELL),PPWFN,PN,
     A                          RESMAX,IRESMX,JRESMX
                WRITE(12,*)ARWRAT
                WRITE(12,*)TDIMA,PPDIM
                WRITE(13,*)SUMPZA,PAVG,VISGA,CMPGA,PPAVG
               ELSE
```

```
                NTDEL=NTDEL+1
                WRITE(6,*) TCUM
                   WRITE(9,*)TCUM,TDEL,PPRESN(LWELL),PPWFN,PN,
     A                        RESMAX,IRESMX,JRESMX
                WRITE(12,*)TDIMA,PPDIM
                WRITE(13,*)SUMPZA,PAVG,VISGA,CMPGA,PPAVG
               ENDIF
               DO 82 I=1,MAXX
                   NORD=(I-1)*MAXY+JWELL
                   IF (I.EQ.1) THEN
                        WRITE(11,*)TCUM,PPRESN(NORD),XG(I)
                   ELSE
                        WRITE(11,*)'         ',PPRESN(NORD),
     A                      XG(I)
                   ENDIF
82             CONTINUE
               DO 84 J=1,MAXY
                   NORD=(IWELL-1)*MAXY+J
                   WRITE(11,*)'         ',PPRESN(NORD),YG(J)
84             CONTINUE
--        ENDIF
          GOTO 600
          ELSE
             DO 75 I=1,MAXX*MAXY
                PPRESI(I)=PPRESN(I)
75           CONTINUE
C
C         PERFORM M(P) - P - VIS*CG COMPUTATION
C         FOR NEXT ITERATION IF NOT CONVERGED
C
          DO 80 I=1,MAXX*MAXY
C            WRITE(6,*)I,PPRESN(I),'CALLING TABSEQ'
             CALL TABSEQ(PPRESN(I),TABMP,TABP,NSTEP,P)
C            WRITE(6,*)P,'CALLING VISCY'
             CALL VISCY((TEM+TEMRAK)/TC,P/PC,SPG,TEM,CNCH2S,
     A                  CNCCO2,CNCN2,VISGR,VISG,JERR)
C            WRITE(6,*)'CALLING ZANDC'
             CALL ZANDC(TEM,TC,P,PC,CNCH2S,CNCCO2,ZED,CMPG,JERR)
             VISCGN(I)=VISG*CMPG
80        CONTINUE
          ENDIF
          GOTO 300
          END


        SUBROUTINE INPUT(PCP,TCP,PERM,P,T,RW,PHI,SG,PDEL,OUTFIL,
     AMX,MY,NX,NY,XG,YG,FBUP,TFDD,TSLD,TCONS,TSI,TFBU,TSLB,QSOR)
          IMPLICIT REAL*8(A-H,O-Z)
          DIMENSION X(100),Y(100),XG(100),YG(100),YM(12),RD(5),SG(4),
     A    GM(12),PC(12),TC(12)
          LOGICAL FBUP
          CHARACTER*8 OUTFIL
          DATA GM /
     A28.013,34.076,44.010,16.043,30.070,44.097,58.124,58.124,
     B72.151,72.151,86.178,100.205 /
          DATA TC /
     A227.0,672.3,547.54,342.99,549.77,665.68,734.63,765.29,828.70
     B,845.28,913.32,972.36 /
          DATA PC /
     A493.,1306.,1072.,667.8,707.8,616.3,529.1,550.7,490.4,488.6,
```

```
     B436.9,396.8 /
        WRITE(6,*)'INPUT DATA FILE OUTPUT NAME'
        READ(5,*)OUTFIL
C
C       INPUTTING TYPE OF SIMULATION ANALYSIS - BUILD-UP OR DRAWDOWN
C
        WRITE(6,*)'TYPE OF SIMULATION ANALYSIS'
        WRITE(6,*)'1 - FOR BUILD-UP , 2 - FOR DRAWDOWN'
        READ(5,*)ITSA
         IF(ITSA.EQ.1) THEN
          FBUP=.TRUE.
         ELSE
          FBUP=.FALSE.
         ENDIF
C
C       INPUTTING TIMES FOR RESPECTIVE ANALYSIS
C
        WRITE(6,*)'INPUT FIRST TIME TO COMPUTE DRAWDOWN PRESSURE - HRS'
        READ(5,*)TFDD
        WRITE(6,*)'INPUT FINAL LOGARITHMIC TIME INCREMENT - HRS'
        READ(5,*)TSLD
        WRITE(6,*)'INPUT TIME CONSTANT INCREMENT FOR DRAWDOWN  - HRS'
        READ(5,*)TCONS
        WRITE(6,*)'INPUT TIME WELL SHUT-IN - HRS'
        READ(5,*)TSI
        IF(FBUP) THEN
        WRITE(6,*)'INPUT FIRST TIME TO COMPUTE BUILD-UP PRESSURE - HRS'
        READ(5,*)TFBU
        WRITE(6,*)'INPUT FINAL TIME TO COMPUTE BUILD-UP PRESSURE - HRS'
        READ(5,*)TSLB
        ENDIF
C
C       INPUTTING DELTA P (PSI) FOR P-M(P) TABLE
C
        WRITE(6,*)'INPUT DELTA P FOR P-M(P) TABLE - PSI'
        READ(5,*)PDEL
C
C       INPUTTING FLOWRATE TERM - QSOR
C
        WRITE(6,*)'INPUT FLOWRATE - MSCF/D'
        READ(5,*)QSOR
C
C       SUBROUTINE INPUT CONTAINS GAS PROPERTIES, RESERVOIR DATA,
C       RESERVOIR GRID SIZING, AND WELL LOCATION INFORMATION.
C
C       ARRAY DESCRIPTION
C
C               X , Y - block locations from well to respective x,y
C                       origins
C               XG,YG - grid block x,y locations from 0,0 at lower left
C                       corner
C               YM    - mole fracitons of gas analysis components
C               RD    - reservoir properties
C               SG    - gas SG and mole fractions of N2, H2S, CO2
C               GM    - molar mss of gas components
C               PC,TC - critical pressure, temperature of gas component
C
C
C       FILE DEFINITION  -  FILE        DESCRIPTION
C
```

```
C                          SGDAT        gas specific gravity and mole
C                                       fractions of N2, H2S, CO2.
C                          RDAT         reservoir properties
C                          FDAT         mole fractions of gas analysis
C                                       components
C                          SIMDAT       reservoir geometry data
C
      OPEN(UNIT=3,FILE='SGDAT')
      OPEN(UNIT=4,FILE='RDAT')
      OPEN(UNIT=7,FILE='FDAT')
      OPEN(UNIT=8,FILE='SIMDAT')
C
C     INPUTTING GAS PROPERTIES - BY EITHER GAS SG OR MOLE FRACTION
C
C             VARIABLE DESCRIPTION
C
C     VARIABLE       TYPE       DESCRIPTION
C
C     IGP             flag     identifies type of gas input, i.e. by
C                              mole fraction or specific gravity
C     ISGC            flag     identifies if new or old gas data to be
C                              used
C     YMC             real     sum. of mole fractions
C
      WRITE(6,*)'GAS PROPERTIES CALCULATIONS'
      WRITE(6,*)'BY MOLE FRACTIONS OR BY SPECIFIC GRAVITY ?'
      WRITE(6,*)'1 - FOR MOLE FRACTION, 0 - FOR SPECIFIC GRAVITY'
      READ(5,*)IGP
      IF(IGP.EQ.1) GOTO 7
              IF(IGP.EQ.0) THEN
              WRITE(6,*)'GAS ANALYSIS - INPUT NEW SPECIFIC GRAVITY ?'
              WRITE(6,*)'1 - FOR "YES", 0 - FOR "NO"'
              READ(5,*)ISGC
                      IF(ISGC.EQ.1) THEN
                      WRITE(6,*)'GAS SPECIFIC GRAVITY'
                      READ(5,*)SG(1)
                      WRITE(3,*)SG(1)
                      WRITE(6,*)'M. F. NITROGEN, N2 - Y'
                      READ(5,*)SG(2)
                      WRITE(3,*)SG(2)
                      WRITE(6,*)'M. F. HYDROGEN SULFIDE, H2S - Y'
                      READ(5,*)SG(3)
                      WRITE(3,*)SG(3)
                      WRITE(6,*)'M. F. CARBON DIOXIDE, CO2 - Y'
                      READ(5,*)SG(4)
                      WRITE(3,*)SG(4)
                      PCP=700.55-47.94*SG(1)
                      TCP=175.59+307.97*SG(1)
                      GOTO 3
                      ELSE
                       DO 9 I=1,4
                       READ(3,*)SG(I)
9                      CONTINUE
                      PCP=700.55-47.94*SG(1)
                      TCP=175.59+307.97*SG(1)
                      GOTO 3
                      ENDIF
              ENDIF
7     CONTINUE
        WRITE(6,*)'GAS ANALYSIS - INPUT NEW MOLE FRACTIONS ?'
```

```
      WRITE(6,*)'1 - FOR "YES", 0 - FOR "NO"'
      READ(5,*)ISGC
11    CONTINUE
            IF(ISGC.EQ.1) THEN
            WRITE(6,*)'INPUTTING GAS ANALYSIS MOLE FRACTIONS'
            WRITE(6,*)'NITROGEN, N2 - Y'
            READ(5,*)YM(1)
            WRITE(7,*)YM(1)
            WRITE(6,*)'HYDROGEN SULFIDE, H2S - Y'
            READ(5,*)YM(2)
            WRITE(7,*)YM(2)
            WRITE(6,*)'CARBON DIOXIDE, CO2 - Y'
            READ(5,*)YM(3)
            WRITE(7,*)YM(3)
            WRITE(6,*)'METHANE, CH4 - Y'
            READ(5,*)YM(4)
            WRITE(7,*)YM(4)
            WRITE(6,*)'ETHANE, C2H6 - Y'
            READ(5,*)YM(5)
            WRITE(7,*)YM(5)
            WRITE(6,*)'PROPANE, C3H8 - Y'
            READ(5,*)YM(6)
            WRITE(7,*)YM(6)
            WRITE(6,*)'ISO-BUTANE, i-C4H10 - Y'
            READ(5,*)YM(7)
            WRITE(7,*)YM(7)
            WRITE(6,*)'N-BUTANE, n-C4H10 - Y'
            READ(5,*)YM(8)
            WRITE(7,*)YM(8)
            WRITE(6,*)'ISO-PENTANE, i-C5H12 - Y'
            READ(5,*)YM(9)
            WRITE(7,*)YM(9)
            WRITE(6,*)'N-PENTANE, n-C5H12 - Y'
            READ(5,*)YM(10)
            WRITE(7,*)YM(10)
            WRITE(6,*)'HEXANES, C6 - Y'
            READ(5,*)YM(11)
            WRITE(7,*)YM(11)
            WRITE(6,*)'HEPTANES +, C7 - Y'
            READ(5,*)YM(12)
            WRITE(7,*)YM(12)
            ELSE
             DO 2 I=1,12
             READ(7,*)YM(I)
2             CONTINUE
            ENDIF
      YMC=0.
       DO 8 I=1,12
       YMC=YMC+YM(I)
8     CONTINUE
      YMC=1.-YMC
            IF(YMC.LE.0.000001) GOTO 22
      WRITE(*,*)YMC
      WRITE(6,*)'SUM. OF MOLE FRACTIONS NOT EQUAL TO 1.0'
      GOTO 11
22    CONTINUE
C
C     READING IN DATA FOR GAS MOLAR MASS & CRITICAL PROPERTIES
C     NOTE: IN OILFIELD UNITS
C
```

```
C                VARIABLE DESCRIPTION
C
C       VARIABLE        TYPE        DESCRIPTION
C
C       SGM              real     SG calculated from mole fractions
C       SGM1             real     increment SG of gas components
C       TCP              real     gas critical temperature
C       TC1              real     increment TC of gas components
C       PCP              real     gas critical pressure
C       PC1              real     increment PC of gas components
C
        SGM1=0.
        TC1=0.
        PC1=0.
         DO 21 I=1,12
         SGM=SGM1+(YM(I)*GM(I)/28.96)
         SGM1=SGM
         TCP=TC1+(YM(I)*TC(I))
         TC1=TCP
         PCP=PC1+(YM(I)*PC(I))
         PC1=PCP
21       CONTINUE
        SG(1)=SGM
        SG(2)=YM(1)
        SG(3)=YM(2)
        SG(4)=YM(3)
3       CONTINUE
C
C       INPUTTING RESERVOIR PROPERTY DATA
C
C               VARIABLE DESCRIPTION
C
C       VARIABLE        TYPE        DESCRIPTION
C
C       IRDC             flag     for input of old or new reservoir data
C       PERM             real     reservoir permeability (md)
C       P                real     reservoir pressure (psia)
C       T                real     reservoir temperature (R)
C       PHI              real     reservoir porositye (decimal)
C       RW               real     well radius (ft.)
C
        WRITE(6,*)'RESERVOIR DATA - INPUT NEW PROPERTIES ?'
        WRITE(6,*)'1 - FOR "YES", 0 - FOR "NO"'
        READ(5,*)IRDC
              IF(IRDC.EQ.0) GOTO 4
        WRITE(6,*)'INPUTTING RESERVOIR DATA'
        WRITE(6,*)'RESERVOIR PERMEABILITY - MD'
        READ(5,*)RD(1)
        WRITE(4,*)RD(1)
        WRITE(6,*)'RESERVOIR PRESSURE - PSIA'
        READ(5,*)RD(2)
        WRITE(4,*)RD(2)
        WRITE(6,*)'RESERVOIR TEMPERATURE - F'
        READ(5,*)RD(3)
        WRITE(4,*)RD(3)
        WRITE(6,*)'RESERVOIR POROSITY - (decimal)'
        READ(5,*)RD(4)
        WRITE(4,*)RD(4)
        WRITE(6,*)'WELL RADIUS - FT'
        READ(5,*)RD(5)
```

```
      WRITE(4,*)RD(5)
      GOTO 52
4           CONTINUE
       DO 51 J=1,5
       READ(4,*)RD(J)
51     CONTINUE
52    CONTINUE
      PERM=RD(1)
      P=RD(2)
      T=RD(3)
      PHI=RD(4)
      RW=RD(5)
C
C
C
C              RESERVOIR DIMENSIONS & GRID DEFINITION
C
C              VARIABLE DESCRIPTION
C
C     VARIABLE        TYPE        DESCRIPTION
C
C     XL(FT.)          real     reservoir length
C     YL(FT.)          real     reservoir width
C     XP(FT.)          real     well X location from 0.
C     YP(FT.)          real     well Y location from 0.
C     IG               flag     indicates grid spacing not fine enough
C                               for well location
C     XWB1(FT.)        real     wellblock AREA 1 grid spacing
C       XWB2(FT.)        real     wellblock AREA 2 grid spacing
C       XWB1F            real     wellblock AREA 1 fraction
C     XBM              real     X grid spacing multiplier
C     XYR              real     ratio XL/YL
C     YBM              real     Y grid spacing multiplier
C     XGM              real     multiplier defining grid sections
C     YGM              real     multiplier defining Y grid sections
C     XGM1             real     initial value of XGM
C     YGM1             real     initial value of YGM
C     XWB              real     X grid spacing around wellbore
C     YWB              real     Y grid spacing around wellbore
C     XSM,YSM          real     X,Y multipliers for adding half block
C                               lengths when changing block size
C     GMX,GMY          real     X,Y multipliers for changing the end
C                               grid point observed before changing
C                               block lengths
C     XEC,YEC          real     incremental length added when changing
C                               block lengths
C     XGC,YGC          real     grid sections identifier
C     GC,CC            real     dividers for calculating block lengths
C                               when changing block size
C     NX,NY   interger          well block X,Y location in XG,YG
C     XED,YED(FT.)     real     end X,Y locations before changing
C                               grid size
C     XE1,YE1          real     last XEC,YEC value
C     XCH,YCH          real     summ of XG,YG to ensure equal to XL,YL
C     MX,MY   interger          number of X,Y blocks in XG,YG
C
        WRITE(6,*)'RESERVOIR DIMENSIONS & GRID CONFIGURATION'
        WRITE(6,*)'INPUT NEW DATA ?'
        WRITE(6,*)'1 - FOR "YES" , 0 - FOR "NO"'
        READ(5,*)IRGC
```

```
            IF(IRGC.EQ.1) THEN
            CALL EMPTYF(8)
          WRITE(6,*)'Input reservoir length, xl'
          READ(5,*)XL
          WRITE(6,*)'Input reservoir width, yl'
          READ(5,*)YL
          WRITE(6,*)'Input well location, xp'
          READ(5,*)XP
          WRITE(6,*)'Input well location, yp'
          READ(5,*)YP
          IG=0
C
C         CHECK FOR PROPER GRID SET-UP
C
5         CONTINUE
                  IF(IG.EQ.1) THEN
                  WRITE(6,*)'1st block nonexistent-DECREASE GRID SPACING'
                  IG=0
                  ENDIF
          WRITE(6,*)'Input GRID SPACING AROUND WELL - AREA 1 (FT)'
          READ(5,*)XWB1
            WRITE(6,*)'INPUT AREA 1 GRID FRACTION - 0 TO 1.0 '
            READ(5,*)XWB1F
            WRITE(6,*)'INPUT GRID SPACING AROUND WELL - AREA 2 (FT)'
            READ(5,*)XWB2
            XWB1FI=XWB1F
6         CONTINUE
          WRITE(6,*)'Input GRID SPACING MULTIPLIER'
          READ(5,*)XBM
          XYR=XL/YL
          YBM=XBM/XYR
                  IF(YBM.LT.1.) YBM=1.
          X(1)=XP
          Y(1)=YP
          XGM1=1.
          YGM1=1.
          XWB=XWB1
          YWB=XWB1
          XGM=XGM1
          YGM=YGM1
          XSM=0.
          YSM=0.
          XECS=0.
          YECS=0.
          GMX=1.
          GMY=1.
          GC=2.
          CC=1.
           DO 10 I=2,100
           NX=I
           X(I)=X(I-1)-XWB/CC-XSM*XECS
                   IF(X(I).LE.0.) THEN
                   X(I)=(X(I-1)-XEC)/2.
                   GOTO 15
                   ENDIF
           XGC=XP-(XL/(2.*5.))*XGM*XWB1F
           XEC=(X(I-1)-X(I))/GC-XSM*XECS
           XSM=0.
           GC=2.
           CC=1.
```

```
          XGC=XGC+XEC
                IF(X(2).LE.0.) THEN
                IG=1
                GOTO 5
                ENDIF
         IF(X(I).LE.XGC) THEN
             IF(XWB1F.LT.1.) THEN
             XWB=XWB2
             XWB1F=1.
             ELSE
         XGM=XGM+2
         XWB=XWB*XBM
             ENDIF
         XSM=1.
         GC=1.
         CC=2.
         GMX=0.75
         XECS=XEC
         ENDIF
          XED=2.*XEC*GMX
         IF(X(I).LE.XED) THEN
         X(I)=(X(I-1)-XE1)/2.
         GOTO 15
         ENDIF
         XE1=XEC
10        CONTINUE
15      DO 20 J=1,NX
          XG(J)=X(I)
          I=I-1
20        CONTINUE
        XWB=XWB1
        XGM=XGM1
        XSM=0.
        GMX=1.
        GC=2.
        CC=1.
          XWB1F=XWB1FI
        DO 25 I=NX+1,100
        MX=I
        XG(I)=XG(I-1)+XWB/CC+XSM*XECS
        XBC=XL-XG(I)
        IF(XG(I).GE.XL) THEN
        XG(I)=(XL-(XG(I-1)+XEC))/2.+XG(I-1)+XEC
        GOTO 30
        ENDIF
        XGC=XP+(XL/(2.*5.))*XGM*XWB1F
        XEC=(XG(I)-XG(I-1))/GC-XSM*XECS
        XSM=0.
        GC=2.
        CC=1.
        XGC=XGC-XEC
        IF(XG(NX+1).GE.XL) THEN
        IG=1
        GOTO 5
        ENDIF
        IF(XG(I).GE.XGC) THEN
            IF(XWB1F.LT.1.) THEN
            XWB=XWB2
            XWB1F=1.
            ELSE
```

```
            XGM=XGM+2.
            XWB=XWB*XBM
                ENDIF
            XSM=1.
            GC=1.
            CC=2.
            GMX=0.75
            XECS=XEC
            ENDIF
            XED=2.*XEC*GMX
            IF(XBC.LE.XED) THEN
            XG(I)=(XL-(XG(I-1)+XE1))/2.+XG(I-1)+XE1
            GOTO 30
            ENDIF
            XE1=XEC
25          CONTINUE
30          CONTINUE
            GC=2.
            CC=1.
              XWB1F=XWB1FI
            DO 35 I=2,100
            NY=I
            Y(I)=Y(I-1)-YWB/CC-YSM*YECS
            IF(Y(I).LE.0.) THEN
            Y(I)=(Y(I-1)-YEC)/2.
            GOTO 40
            ENDIF
            YGC=YP-(YL/(2.*5.))*YGM*XWB1F
            YEC=(Y(I-1)-Y(I))/GC-YSM*YECS
            YSM=0.
            GC=2.
            CC=1.
            YGC=YGC+YEC
            IF(Y(2).LE.0.) THEN
            IG=1
            GOTO 5
            ENDIF
            IF(Y(I).LE.YGC) THEN
                IF(XWB1F.LT.1.) THEN
                YWB=XWB2
                XWB1F=1.
                ELSE
            YGM=YGM+2.
            YWB=YWB*YBM
                ENDIF
            YSM=1.
            GC=1.
            CC=2.
            GMY=0.75
            YECS=YEC
            ENDIF
            YED=2.*YEC*GMY
            IF(Y(I).LE.YED) THEN
            Y(I)=(Y(I-1)-YE1)/2.
            GOTO 40
            ENDIF
            YE1=YEC
35          CONTINUE
40        DO 45 J=1,NY
            YG(J)=Y(I)
```

```
          I=I-1
45        CONTINUE
          YWB=XWB1
          YGM=YGM1
          YSM=0
          GMY=1.0
          GC=2.
          CC=1.
            XWB1F=XWB1FI
          DO 50 I=NY+1,100
          MY=I
          YG(I)=YG(I-1)+YWB/CC+YSM*YECS
          YBC=YL-YG(I)
          IF(YG(I).LE.0.) THEN
          YG(I)=(YL-(YG(I-1)+YEC))/2.+YG(I-1)+YEC
          GOTO 55
          ENDIF
          YGC=YP+(YL/(2.*5.))*YGM*XWB1F
          YEC=(YG(I)-YG(I-1))/GC-YSM*YECS
          YSM=0
          GC=2.
          CC=1.
          YGC=YGC-YEC
          IF(YG(NY+1).GE.YL) THEN
          IG=1
          GOTO 5
          ENDIF
          IF(YG(I).GE.YGC) THEN
              IF(XWB1F.LT.1.) THEN
              YWB=XWB2
              XWB1F=1.
              ELSE
          YGM=YGM+2.
          YWB=YWB*YBM
              ENDIF
          YSM=1.
          GC=1.
          CC=2.
          GMY=0.75
          YECS=YEC
          ENDIF
          YED=2.*YEC*GMY
          IF(YBC.LE.YED) THEN
          YG(I)=(YL-(YG(I-1)+YE1))/2.+YG(I-1)+YE1
          GOTO 55
          ENDIF
          YE1=YEC
50        CONTINUE
55        CONTINUE
          WRITE(8,*)XL,YL
          WRITE(8,*)XP,YP
          WRITE(8,*)XWB1,XWB1FI,XWB2,XBM,YBM,XYR
          WRITE(8,*)MX,MY
          DO 60 I=1,MX
          WRITE(8,*)XG(I)
 60       CONTINUE
          DO 65 I=1,MY
          WRITE(8,*)YG(I)
 65        CONTINUE
          XCH=0.
```

```
      YCH=0.
      DO 70 I=2,MX
      XCH=XCH+XG(I)-XG(I-1)
70    CONTINUE
      DO 75 I=2,MY
      YCH=YCH+YG(I)-YG(I-1)
75    CONTINUE
      XCH=XCH+XG(1)+(XL-XG(MX))
      YCH=YCH+YG(1)+(YL-YG(MY))
      WRITE(8,*)XCH,YCH
      WRITE(8,*)XG(NX),NX
      WRITE(8,*)YG(NY),NY
         ELSE
          DO 110 I=1,3
           READ(8,*)DUMM
110       CONTINUE
          READ(8,*)MX,MY
           DO 111 I=1,MX
            READ(8,*)XG(I)
111         CONTINUE
           DO 112 J=1,MY
            READ(8,*)YG(J)
112         CONTINUE
          READ(8,*)DUMM
          READ(8,*)DUMM,NX
          READ(8,*)DUMM,NY
        ENDIF
        CLOSE(3)
      CLOSE(4)
      CLOSE(7)
      CLOSE(8)
      RETURN
      END
```

```
c          PROGRAM 2 - ANALYTICAL LIQUID SIMULATOR
c
c        PROGRAM TO CALCULATE PRESSURE RESPONSE IN
c        RECTANGULAR RESERVOIRS WITH COMBINATIONS
c        OF CLOSED AND CONSTANT PRESSURE OUTER
c        BOUNDARY CONDITIONS
c
c        NOTE: PROGRAM TIME INPUTS FROM SIMULATION DATA
c
c        NOTE: PROGRAM ALSO CALCULATES EI & EI' SOLUTIONS
c              FOR INTERFERENCE TEST DATA
c
c
c        INPUTTING TYPE OF TEST
c        1 - DRAWDOWN
c        2 - INTERFERENCE
c        3 - BUILDUP
c
c                VARIABLE LIST
c                ntd=number of dimensionless times based on simulation
c                td=dimensionless time based on area
c                tpd=dimensionless producing time based on area
c                xp,yp =observation point for interference test
c                xw,yw =well location
c                xl,yl =reservoir dimensions
c                xh,yh =xl/2, yl/2 - half reservoir dimensions
c                ar=reservoir area
c                rw=well radius
c
c                ARRAYS
c                x,y =point locations for well and image wells
c                w,z =flag indicating if wells are injectors or producers
c
        implicit real*8(a-h,o-z)
        dimension x(55),y(55),w(55),z(55),tdd(200)
          OPEN(UNIT=7,FILE='TDDAT')
        OPEN(UNIT=8,FILE='PD5OUT')
        OPEN(UNIT=9,FILE='PD5DAT')
        pi=2.*asin(1.)
        write(6,*)'Input type of analysis'
        write(6,*)'Enter 1 for DRAWDOWN'
        write(6,*)'Enter 2 for INTERFERENCE'
        write(6,*)'Enter 3 for BUILDUP'
        read(5,*)inp
c
          write(6,*)'Input number of time points for analysis'
        read(5,*)ntdt
        read(7,*)wrat
          do 2 i=1,ntdt
2         read(7,*)tdd(I)
c
c               INPUTTING GRID DIMENSIONS AND WELL LOCATIONS
c               Input grid lengths and well locations in absolute
c               dimensions from reference at bottom left of reservoir
c               grid.
c
        write(6,*)'Input length of X axis'
        read(5,*)xl
        write(6,*)'Input length of Y axis'
        read(5,*)yl
```

```
      xyrat=xl/yl
      xh=xl/2.0d00
      yh=yl/2.0d00
      n=1
c
c
      write(6,*)'Input well X coordinate'
      read(5,*)xw
      xw=xw-xh
      write(6,*)'Input well Y coordinate'
      read(5,*)yw
      yw=yw-yh
      if(inp.eq.1) then
      tpd=0.0
      xp=xw
      yp=yw
      endif
      if(inp.eq.2) then
      tpd=0.0
      write(6,*)'Input point X coordinate'
      read(5,*)xp
      xp=xp-xh
      write(6,*)'Input point Y coordinate'
      read(5,*)yp
      yp=yp-yh
      endif
      if(inp.eq.3) then
      write(6,*)'Input Dimensionless tp, tpd'
      read(5,*)tpd
      xp=xw
      yp=yw
      endif
      xd=xp-xw
      yd=yp-yw
      ar=xl*yl
      rw=(((ar**0.5d00))/wrat)
c
c     Inputting boundary conditions
c
      write(6,*)'Inputting boundary conditions'
      write(6,*)'bc#=...1 for constant press.,...0 for closed.'
      write(6,*)'bc1=?, for +Y axis'
      read(5,*)bc1
      write(6,*)'bc2=?, for -Y axis'
      read(5,*)bc2
      write(6,*)'bc3=?, for +X axis'
      read(5,*)bc3
      write(6,*)'bc4=?, for -X axis'
      read(5,*)bc4
c
c     Outputting test data
c
      if(inp.eq.1) then
      write(8,*) 'DRAWDOWN TEST'
      endif
      if(inp.eq.2) then
      write(8,*) 'INTERFERENCE TEST'
      endif
      if(inp.eq.3) then
      write(8,*) 'BUILDUP TEST'
```

```
      write(8,170)tpd
170   format(/,2x,'Producing time, tpda=',f8.4)
      endif
      write(8,169)wrat
169   format(/,2x,'FOR (A**0.5)/rw=',f10.0)
      write(8,171)
171   format(/,2x,'BOUNDARY CONDITIONS')
      if(bc1.eq.1.) then
      write(8,*) 'boundary 1 - Constant Pressure'
      else
      write(8,*) 'boundary 1 - Closed'
      endif
      if(bc2.eq.1.) then
      write(8,*) 'boundary 2 - Constant Pressure'
      else
      write(8,*) 'boundary 2 - Closed'
      endif
      if(bc3.eq.1.) then
      write(8,*) 'boundary 3 - Constant Pressure'
      else
      write(8,*) 'boundary 3 - Closed'
      endif
      if(bc4.eq.1.) then
      write(8,*) 'boundary 4 - Constant Pressure'
      else
      write(8,*) 'boundary 4 - Closed'
      endif
      write(8,172)
172   format(/,2x,'RECTANGULAR RESERVOIR DIMENSIONS')
      xlrat=xl/yl
      ylrat=1.
      write(8,173)xlrat,ylrat
173   format(4x,'X-axis length=',f8.4,4x,'Y-axis length=',f8.4)
      write(8,174)
174   format(/,2x,'WELL LOCATION')
      xwc=xw+xh
      ywc=yw+yh
      xwcr=xwc/xl
      ywcr=ywc/yl
      write(8,175)xwcr,ywcr
175   format(4x,'xw=',f8.4,4x,'yw=',f8.4)
      if(inp.eq.2) then
      write(8,176)
176   format(/,2x,'POINT LOCATION')
      xpc=xp+xh
      ypc=yp+yh
      xpcr=xpc/xl
      ypcr=ypc/yl
      write(8,177)xpcr,ypcr
177   format(4x,'xp=',f8.4,4x,'yp=',f8.4)
      endif
c
c     Setting boundary conditions constants.
c
      if(bc1.eq.0..and.bc2.eq.0..and.bc3.eq.0..and.bc4.eq.0.) then
      w(1)=1.
      w(2)=1.
      w(3)=1.
      w(4)=1.
      w(5)=1.
```

```
      wm=-1.
      z(1)=1.
      z(2)=1.
      z(3)=1.
      z(4)=1.
      z(5)=1.
      zm=-1.
      endif
c
      if(bc1.eq.0..and.bc2.eq.1..and.bc3.eq.0..and.bc4.eq.0.) then
      w(1)=1.
      w(2)=-1.
      w(3)=1.
      w(4)=-1.
      w(5)=-1.
      wm=1.
      z(1)=1.
      z(2)=1.
      z(3)=1.
      z(4)=1.
      z(5)=1.
      zm=-1.
      endif
c
      if(bc1.eq.1..and.bc2.eq.0..and.bc3.eq.0..and.bc4.eq.0.) then
      w(1)=1.
      w(2)=-1.
      w(3)=1.
      w(4)=-1.
      w(5)=-1.
      wm=1.
      z(1)=1.
      z(2)=1.
      z(3)=1.
      z(4)=1.
      z(5)=1.
      zm=-1.
      endif
c
      if(bc1.eq.1..and.bc2.eq.0..and.bc3.eq.1..and.bc4.eq.1.) then
      w(1)=1.
      w(2)=-1.
      w(3)=1.
      w(4)=-1.
      w(5)=-1.
      wm=1.
      z(1)=1.
      z(2)=-1.
      z(3)=-1.
      z(4)=1.
      z(5)=1.
      zm=-1.
      endif
c
      if(bc1.eq.1..and.bc2.eq.1..and.bc3.eq.0..and.bc4.eq.0.) then
      w(1)=1.
      w(2)=-1.
      w(3)=-1.
      w(4)=1.
      w(5)=1.
```

```
      wm=-1.
      z(1)=1.
      z(2)=1.
      z(3)=1.
      z(4)=1.
      z(5)=1.
      zm=-1.
      endif
c
      if(bc1.eq.1..and.bc2.eq.0..and.bc3.eq.1..and.bc4.eq.0.) then
      w(1)=1.
      w(2)=-1.
      w(3)=1.
      w(4)=-1.
      w(5)=-1.
      wm=1.
      z(1)=1.
      z(2)=-1.
      z(3)=1.
      z(4)=-1.
      z(5)=-1.
      zm=1.
      endif
c
      if(bc1.eq.1..and.bc2.eq.1..and.bc3.eq.0..and.bc4.eq.1.) then
      w(1)=1.
      w(2)=-1.
      w(3)=-1.
      w(4)=1.
      w(5)=1.
      wm=-1.
      z(1)=1.
      z(2)=1.
      z(3)=-1.
      z(4)=-1.
      z(5)=-1.
      zm=1.
      endif
c
      if(bc1.eq.1..and.bc2.eq.1..and.bc3.eq.1..and.bc4.eq.1.) then
      w(1)=1.
      w(2)=-1.
      w(3)=-1.
      w(4)=1.
      w(5)=1.
      wm=-1.
      z(1)=1.
      z(2)=-1.
      z(3)=-1.
      z(4)=1.
      z(5)=1.
      zm=-1.
      endif
c
c
c     Setting up points with Boundary Condition Constants
c
      x(1)=xd
      x(2)=2.0d00*(xh-xw)-xd
      x(3)=2.0d00*(xh+xw)+xd
```

```
      x(4)=x(3)+(2.0d00*(xh-xw))
      x(5)=x(2)+(2.0d00*(xh+xw))
      y(1)=yd
      y(2)=2.0d00*(yh-yw)-yd
      y(3)=2.0d00*(yh+yw)+yd
      y(4)=y(3)+(2.0d00*(yh-yw))
      y(5)=y(2)+(2.0d00*(yh+yw))
      do 11 i=6,50
      w(i)=w(i-4)*((-1.0d00)*wm)
      z(i)=z(i-4)*((-1.0d00)*zm)
11    continue
      do 15 i=6,50,4
      x(i)=x(i-1)+2.0d00*(xh-xw)
      x(i+1)=x(i-2)+2.0d00*(xh+xw)
      x(i+2)=x(i+1)+2.0d00*(xh-xw)
      x(i+3)=x(i)+2.0d00*(xh+xw)
      y(i)=y(i-1)+2.0d00*(yh-yw)
      y(i+1)=y(i-2)+2.0d00*(yh+yw)
      y(i+2)=y(i+1)+2.0d00*(yh-yw)
      y(i+3)=y(i)+2.0d00*(yh+yw)
15    continue
c     Calculating Dimensionless Pressure Data
c
c             VARIABLE LIST
c
c             td=dimensionless time based on area
c             sum=dimensionless pressure
c             sump=dimensionless pressure for buildup
c             sumd=dimensionless semi-log derivative
c             sumpd=dimensionless semi-log derivative for buildup
c             summ=dimensionless MBH pressure
c             sumw=EI solution at obs. point for interference test
c             sumwd=semi-log derivative of EI solution
c             a=length to image well
c
      write(8,149)
149   format(/,2x,'DATA POINTS',/)
      if(inp.eq.3) then
      write(8,150)
150   format(3x,'tda',11x,'pdmdh',11x,'dpd',13x,'pwds',11x,' pds',/)
      else
      if(inp.eq.2) then
      write(8,151)
151   format(3x,'tda',9x,'pd',14x,'dpd',10x,'Ei DATA',7x,'dEi DATA'/)
      else
      write(8,152)
152   format(3x,'tda',9x,'pd',14x,'dpd'/)
      endif
      endif
      ll=0
        ntd=1
1     continue
        td=tdd(ntd)
      sum1=0.0
      sum1d=0.0
      sump1=0.0
      sump1d=0.0
      sumps1=0.0
      l=0
      ll=ll+1
```

```
      xch=0.
      ych=0.
      do 25 k=1,50
      do 30 j=1,50
      l=l+1
      if(xd.eq.0..and.yd.eq.0..and.j.eq.1.and.k.eq.1) then
      a=(rw/((ar)**0.5d00))**2.0d00
      else
      a=(((abs(x(j))**2.0d00)+(abs(y(k))**2.0d00))/ar)
      endif
      if(j.eq.1.and.k.eq.1) then
      aw=a
      vw=((-1.0d00)*aw)/(4.0d00*td)
      vw1=dei(vw)
      vw1d=dexp(vw)
      vw2=-0.5d00*vw1
      vw2d=0.5d00*vw1d/td
      sumw=vw2
      sumwd=vw2d
      endif
      v=((-1.0d00)*a)/(4.0d00*td)
      v1=dei(v)
      v1d=dexp(v)
      v2=-0.5d00*v1*w(j)*z(k)
      v2d=0.5d00*v1d*w(j)*z(k)/td
      sum=sum1+v2
      sumd=sum1d+v2d
      sum1=sum
      sum1d=sumd
      l=l+1
      if(inp.eq.3) then
      vp=((-1.0d00)*a)/(4.0d00*(td+tpd))
      vp1=dei(vp)
      vp1d=dexp(vp)
      vp2=-0.5d00*vp1*w(j)*z(k)
      vp2d=0.5d00*vp1d*w(j)*z(k)/(td+tpd)
      sump=sump1+vp2
      sumpd=sump1d+vp2d
      sump1=sump
      sump1d=sumpd
      endif
      if(inp.eq.3.and.ll.eq.1) then
      vps=((-1.0d00)*a)/(4.0d00*tpd)
      vps1=dei(vps)
      vps2=-0.5d00*vps1*w(j)*z(k)
      sumps=sumps1+vps2
      sumps1=sumps
      endif
      if(dabs(v2).le.10.d-10.and.dabs(vp2).le.10.d-10) then
      xch=x(j+1)-x(j)
      if(xch.ge.0.) goto 40
      endif
30    continue
40    continue
     if(dabs(v2).le.10.d-10.and.dabs(vp2).le.10.d-10.and.
    cj.eq.1) then
      ych=y(k+1)-y(k)
      if(ych.ge.0.) goto 21
      endif
25    continue
```

```
21      continue
        sumd=sumd*td
        sumwd=sumwd*td
        if(inp.eq.3) then
        sum=sump-sum
        sumpd=sumpd*td
        sumd=sumd-sumpd
        endif
        if(inp.eq.3.and.bc1.eq.0..and.bc2.eq.0..and.bc3.eq.0..and.
     cbc4.eq.0.) then
        sums1=sum
        sums2=sum
        sum=sum-(2.*pi*tpd)
        else
        sums1=sum
        sums2=sum
        endif
c
c       Output results
c
c
        a1=ar/(rw*rw)
        sums=sumps-sums1
        summ=(4.0d00*pi*td)-2.0d00*sum+dlog(td)+dlog(a1)+0.80907
        if(inp.eq.3) then
        write(8,105) td,sum,sumd,sums,sums2
105     format(1x,f8.5,1x,f14.6,1x,f15.6,1x,f15.6,1x,f15.6)
        else
        if(inp.eq.2) then
        write(8,106) td,sum,sumd,sumw,sumwd,j,k,l
106     format(1x,f8.5,1x,f12.6,2x,f13.6,3x,f13.6,2x,f13.6,i5,i5,i5)
        write(9,706) td,sum,sumd,sumw,sumwd
706     format(1x,f7.4,1x,f12.6,2x,f13.6,3x,f13.6,2x,f13.6)
        else
      write(9,*)td,sum,sumd
        write(8,107) td,sum,sumd
107     format(1x,f9.6,1x,f12.6,2x,f13.6)
        endif
        endif
c
c       Adding other td values
c
        ntd=ntd+1
        if(inp.ne.3) then
        goto 109
        endif
        if(sum.le.1.0d-10) then
        goto 110
        else
        goto 109
        endif
109     continue
        if(ntd.gt.ntdt) then
        goto 110
        else
        goto 1
        endif
110   continue
        end
```